Published in final edited form as:
J Ultrasound Med. 2000 February ; 19(2): 120–168.

Section 6—Mechanical Bioeffects in the Presence of Gas-Carrier Ultrasound Contrast Agents

Abstract

This review addresses the issue of mechanical ultrasound-induced bioeffects in the presence of gas carrier contrast agents (GCAs). Here, the term “contrast agent” refers to those agents that provide ultrasound contrast by being composed of microbubbles, encapsulated or not, containing one or more gases. Provided in this section are summaries on how contrast agents work, some of their current uses, and the potential for bio-effects associated with their presence in an ultrasonic field.

6.1 Introduction

Enhanced sonographic contrast is desirable in many imaging applications, e.g., detection of tumors and myocardial ischemia. In recent years, a number of gas carrier contrast agents (GCAs) have been developed or are in development. Some are now in clinical use in the United States or Europe and have demonstrated their utility and limitations. An extensive primary literature exists on the physical and clinical properties of GCAs, as well as several reviews (e.g., Ophir and Parker, 1989;Schlief et al, 1993;Goldberg, 1993a;Balen et al, 1994;Burns, 1994a;Goldberg et al, 1994;Winkelmann et al, 1994). However, the minutiae of clinical experience with GCAs are not dealt with here.

GCAs have been available for bioeffect research for only a short time. Consequently, the literature pertaining to mechanical bioeffects in the presence of GCAs is sparse, and thus our knowledge of such phenomena is limited. However, this topic is the subject of current research in several laboratories. Most of the mechanical bioeffects arising from insonation of cells or tissues with GCAs present can be attributed to the occurrence of inertial cavitation.

Subsection 6.2 provides an overview of GCAs in use or under development and discusses briefly some clinical GCA applications. These discussions are not exhaustive but offer an overview of GCAs: what they are, their general properties, and how they have been applied. In subsection 6.3, some clinical applications of GCAs are reviewed. Subsection 6.4 summarizes the literature pertaining to mechanical ultrasound bioeffects in the presence of GCAs.

6.2 Overview of GCAS in Use or Under Development

6.2.1 General Properties of Contrast Agents

Most GCAs comprise micrometer-diameter gas bodies, variously referred to as microbubbles or microspheres, that may or may not be surrounded by a shell of material that stabilizes the gas against diffusion. These are intended for intravascular or intraluminal injection.

A major problem in the development of GCAs has been obtaining a satisfactory size distribution. For imaging applications following intravenous injection of the agent, the microbubbles must be smaller than ~8 μm in diameter to pass through capillaries, thus allowing passage through the pulmonary circulation. The GCA must be tolerated by patients, should be stable with respect to rapid dissolution in the blood, and should be tolerant of hydrostatic pressures produced by the heart. A variety of engineering solutions to these problems has been attempted.

Microbubbles composed of atmospheric gases that are not stabilized in some way dissolve rapidly in aqueous media because of the pressure exerted on the gas by surface tension at the microbubble surface and outward diffusion of the gas (Porter and Xie, 1995a). Stability against dissolution can be provided by a shell of material around the gas or by using relatively insoluble gases. Various stabilizing shell materials have been used, including lipids (Unger et al, 1992;Simon et al, 1992b,1993;D'Arrigo and Imae, 1992;Barbarese et al, 1995;Schneider et al, 1995), albumin (Bleeker et al, 1990b), dextrose-albumin (Porter et al, 1995a,1995b,1995c, 1995d), sugars (Schurmann and Schlief, 1994;Cennamo et al, 1994), gelatin (Prat et al, 1993), and polymers (Schneider et al, 1992). Various gases also have been used, ranging from relatively soluble gases, e.g., air (Bleeker et al, 1990b), nitrogen (Unger et al, 1992), and carbon dioxide (Kudo et al, 1994;Veltri et al, 1994), to gases with relatively low solubility or slow diffusion rates, such as helium (Porter and Xie, 1995a), sulfur hexafluoride (Porter and Xie, 1995a;Schneider et al, 1995), perfluoropropane (Porter et al, 1995d), and dodecafluoropentane (Quay, 1994).

6.2.2 Acoustic Properties of Contrast Agents

The ultrasonic beam generated by a transducer or array is fairly complicated (Shung and Zipparo, 1996;Zagzebski, 1996). However, for the sake of simplicity, here a plane wave is assumed. As an ultrasonic plane wave penetrates a distribution of scatterers, in the present case microbubbles, assuming that the nonlinear effects caused by these bubbles can be neglected, the sound velocity in the medium, c, is given by

$$c = \sqrt{\frac{1}{\rho G}} \tag{6-1}$$

where ρ and G are the effective density and compressibility of the medium, respectively. In general, if the volume concentration V of the bubbles is small, the mixture relationships, which are represented by

$$\rho = \rho_b V + \rho_m (1 - V) \tag{6-2}$$

$$G = G_b V + G_m (1 - V) \tag{6-3}$$

where subscripts *b* and *m* stand for bubble and surrounding medium, are valid (Ophir and Parker, 1989;Mobley et al, 1998). Since sound velocity in a gas is lower than in fluids, the sound velocity in a liquid containing a GCA is lower than that of the liquid alone. Figure 6-1 shows that the sound velocity in Albunex decreases as the Albunex concentration increases at 7.5 MHz (Bleeker, 1990a). Recent studies (Wu et al, 1995;Mobley et al, 1998) indicate that the sound velocity in a distribution of microbubbles is a function of frequency and of bubble concentration, and may be affected by the nonlinear resonance behavior of the bubbles at frequencies near the resonance frequencies of the bubbles.

As the wave penetrates the medium, the pressure amplitude, P_z, and intensity, I_z, decrease according to the following equations (Shung et al, 1992;Zagzebski, 1996):

$$I_z = I_0 e^{-2\beta z} \tag{6-4}$$

$$P_z = P_0 e^{-\beta z} \tag{6-5}$$

where z = distance traveled, I_0 = intensity at z = 0, P_0 = pressure at z = 0, and β= pressure attenuation coefficient in np/cm (1 np = 8.686 dB) of the medium.

For a distribution of low bubble concentration, the attenuation coefficient is given by

$$\beta = \frac{n\sigma_e}{2} \tag{6-6}$$

where n = the number of bubbles per unit volume, and σe = the extinction cross section (Ishimaru, 1978;de Jong et al, 1992). The extinction cross section, σe, with dimensions of cm^2, is frequency dependent and represents the total energy loss for an ultrasonic wave resulting from the presence of one scatterer in a unit volume; e.g., per cm^3. It is the sum of the absorption cross section, σa, and the scattering cross section, σs (Ishimaru, 1978;de Jong et al, 1992)

$$\sigma e = \sigma a + \sigma s \tag{6-7}$$

Both σa and σs have the dimension of cm^2 and represent the energy absorbed and scattered by one scatterer in a unit volume, respectively. The question that often arises is the relative contribution of each of these terms to the total attenuation. The attenuation, if estimated accurately, can sometimes give information about the properties of the scatterer but, in general, attenuation is not desirable in diagnostic applications, especially its absorption component. To achieve optimal ultrasonic contrast, the absorption of the contrast agent should be made as low as possible to avoid losing energy and shadowing biological structures, while the scattering is maximized.

The scattering properties of biological tissues and blood have been investigated intensively because these signals are used to form ultrasonic images (Shung and Thieme, 1993). Several investigators have also studied the acoustic properties of liquids containing gas bubbles (Devin, 1959;Medwin, 1977;Anderson and Hampton, 1980). The total scattering cross section of a single bubble can be expressed as follows (Medwin, 1977):

$$\sigma_s = \frac{4\pi R^2}{\left(\frac{f_r^2}{f^2} - 1\right)^2 + \delta^2} \tag{6-8}$$

where R = bubble radius, f_r = bubble resonance frequency, f = frequency of the incident ultrasonic wave, and δ = total damping constant, caused by the surrounding liquid medium and consisting of terms due to re-radiation, thermal conductivity, and shear viscosity (Devin, 1959).

The resonance frequency of a bubble can be determined assuming the following: the wavelength of the ultrasonic wave is much larger than the bubble diameter, the radial displacement of the bubble is small relative to its radius; and the surrounding fluid is incompressible. The first two conditions are fulfilled by the majority of GCAs and the third by water and blood, which are virtually incompressible.

The simplest equation of resonance frequency for a bubble in water is

$$f_r = \frac{1}{2\pi R}\sqrt{\frac{3\gamma P_0}{\rho_m}} \tag{6-9}$$

which can be modified to

$$f_r = \frac{1}{2\pi}\sqrt{\frac{S_a}{m}} \tag{6-10}$$

where γ = ratio of specific heats of the gas (~1.4), P0 = ambient hydrostatic pressure (= 1.103 × 10^6 dyne/cm), ρm = density of the surrounding fluid (=1.03 g/cm^3), S_a = adiabatic stiffness (=12πγP_0R), and m = effective mass of the system (=4πR^3ρm). Here an adiabatic equation of state is assumed. However, for bubbles of small radii, surface tension becomes a significant additional restoring force and must be considered. The oscillation in this case is closer to an isothermal process. When these points are considered the equation for resonance frequency changes. P_0 in Equation 6.10 is replaced by the average *interior* pressure including surface tension, ξP_0, and γ is replaced by the *effective* ratio of specific heats in the presence of thermal conductivity, γb (Medwin, 1977;de Jong et al, 1992;de Jong, 1996)

$$f_r = \frac{1}{2\pi R}\sqrt{\frac{3\gamma_b \zeta P_0}{\rho_m}} \tag{6-11}$$

where

$$b = (1 + B^2)^{-1}\left[1 + \frac{3(\gamma - 1)}{X}\left(\frac{\sinh X - \sin X}{\cosh X - \cos X}\right)\right]^{-1} \tag{6-12}$$

$$B = 3(\gamma - 1)\left[\frac{X(\sinh X + \sin X) - 2(\cosh X - \cos X)}{X^2(\cosh X - \cos X) + 3(\gamma - 1)X(\sinh X - \sin X)}\right] \tag{6-13}$$

$$\zeta = 1 + \frac{2\sigma}{P_0 R}\left(1 - \frac{1}{3\gamma_b}\right) \tag{6-14}$$

$$X = R\left(\frac{2\omega\rho_a C_{pg}}{K_g}\right)^{\frac{1}{2}} \tag{6-15}$$

In these equations, Kg= thermal conductivity of gas (=5.6 × 10^{-5} cal/cm-s-°C); ρa = density of free gas at sea level (=1.29 × 10^{-3} g/cm^3); σ = surface tension (=75 dyne/cm); C_{pg} = specific heat at constant pressure for air (=0.24 cal/g), λ = ratio of specific heats and ω = angular frequency.

The parameters b and ζ are functions of the bubble radius. Equation 6.11 is plotted in Figure 6-2, which shows the bubble resonance frequency as a function of the bubble size. Note here that smaller bubbles yield higher resonance frequencies. Figure 6-3 shows the scattering cross section of a bubble of 1.7 μm radius at an ambient pressure of 1 atm calculated using the numerical values of parameters given above. Measured data are in reasonable agreement with the calculated curve (de Jong et al, 1992;Chang et al, 1993).

The portion of the energy absorbed or converted into heat by a scatterer from an ultrasonic wave is referred as the absorption cross section, and it is related to scattering cross section as follows (Medwin, 1977;de Jong et al, 1992):

$$\sigma_a = \sigma_s\left(\frac{\delta}{\delta_r} - 1\right) \tag{6-16}$$

where the damping constant δ is the sum of three components (Devin, 1959):

$$\delta = \delta_r + \delta_t + \delta_v \tag{6-17}$$

and where δ_r = kR = damping constant due to re-radiation, k = wave number, $\delta_t = B(fr/f)^2$ = damping constant due to thermal conductivity, $\delta_v = 4\eta/(\rho\omega R^2)$ = damping constant due to shear viscosity and η is the shear viscosity of the surrounding liquid (= 0.01 g/cm-s).

6.2.2.1 Bubbles with an Elastic Shell—The discussion above applies only to a free bubble. However, most GCAs used today have some form of a shell. Unfortunately, there has been very little study on encapsulated microbubbles. An early work by Fox and Herzfield (1954) discussed the issue that gas bubbles acting as cavitation nuclei are stabilized by an organic monomolecular skin that would act as an elastic shell and as a mechanical barrier to diffusion. The skin provides rigidity and, therefore, would increase the resonance frequency of the microbubbles. Microbubble stabilization by an organic skin is essential for GCAs composed of soluble gases in order to increase their persistence in the blood stream. A theoretical model describing ultrasonic propagation in a distribution of shelled microbubbles was made by de Jong et al (1992), who considered the shell surrounding Albunex microbubbles as layers of elastic solids. Recently, Church (1995) treated the surface layers by including numerical values for such parameters as the modulus of elasticity, density, viscosity and thickness.

de Jong et al (1992) hypothesized that the shell introduced an additional restoring force to the system, which would increase the resonance frequency and decrease the scattering cross section. The contribution of the shell to the bubble stiffness is given by

$$S_{shell} = 8\pi \frac{Et}{1-v} = 8\pi S_p \tag{6-18}$$

where E = shell elasticity, t = wall thickness, v = Poisson ratio, and $S_p = Et/(1-v)$ = the shell parameter given in dynes/cm. Although the shell elasticity, wall thickness, and Poisson ratio are unknown, the shell parameter can be estimated by matching the measured attenuation coefficient to the theory. The model has shown better agreement for large microbubbles (lower resonance frequencies) than for small ones. To improve the agreement between theory and measurements, de Jong and Hoff (1993) added an additional damping term referred to as the shell friction parameter, S_f, which accounted for the internal friction or viscosity within the shell. The damping coefficient due to the shell friction introduces an additional term to the total damping coefficient,

$$\delta_{tot} = \delta_r + \delta_t + \delta_v + \delta_f \tag{6-19}$$

where

$$\delta_f = \frac{S_f}{m\omega} \tag{6-20}$$

The modified resonance frequency, taking the shell stiffness into account, is given by

$$f_{rs} = \frac{1}{2\pi}\sqrt{\frac{S_a b\zeta + S_{shell}}{m}} \tag{6-21}$$

6.2.2.2 Cloud of Bubbles—The dynamics of individual microbubbles is of limited importance when considering the response of GCAs to an acoustic wave. A method for determining the effects of a cloud of microbubbles is needed. When the scatterer concentration is low, the scattered power is proportional to the scatterer concentration (Ishimaru, 1978). For a distribution of microbubbles of different sizes, the mean attenuation or scattering property at a single frequency, <φ>, can be calculated by considering the contribution of each microbubble divided by the total concentration:

$$\langle \phi(f) \rangle = \frac{\int_0^\infty \phi(R, f) n(R) dR}{N} \tag{6-22}$$

where R = radius of the scatterer, f = ultrasound frequency, n(R)dR = number of bubbles of radius between R and R + dR per unit volume of scattering medium, φ(R,f) = the attenuation or scattering property of a scatterer with radius R, and N = total concentration of scatterers.

6.2.2.3 Attenuation Coefficient of Albunex—Figure 6-4 shows measured results of the attenuation coefficient of Albunex as a function of the ultrasound frequency (Chang and Shung, 1993). Experimental results obtained using a broadband approach (Bleeker et al, 1990b;de Jong et al, 1992;Chang et al, 1995,1996) agree well with the theory developed for encapsulated microbubbles discussed above, especially in the vicinity of microbubble resonance. The size distribution of Albunex shown in Figure 6-5 was used to calculate the theoretical curve. The attenuation coefficient peaks at 2.1 and the values of S_p and S_f were assumed to be 5,500 dyne/cm and 0.004 g/s, respectively. The attenuation coefficient of Albunex at different concentrations has also been measured (Marsh et al, 1997).

6.2.3 Some Specific Contrast Agents

The first GCAs used for research and clinical purposes were handmade materials produced immediately before administration. Many different materials were tried; e.g., agitated saline, x-ray contrast media, or combinations of the two (Tei et al, 1983;Kaul et al, 1984). These procedures trapped air in suspension, but the microbubbles were unstable, often varied dramatically from batch to batch, had wide size distributions, and failed to cross the pulmonary circulation after intravenous injection. More sophisticated methods of making GCAs evolved that led to commercially prepared products (Keller et al, 1986;Feinstein et al, 1989). These GCAs are easier to use than the “handmade” materials, demonstrate less lot-to-lot variability, provide an excellent pharmacological safety profile and, after intravenous injection, consistently produce contrast in the left ventricle and enhance the Doppler signals from the arterial circulation. Many different GCAs are either on the market or are in development as of this writing.

Echovist (SHU 454; Schering AG, Berlin, Germany) was the first commercially available GCA. This material starts as a powder of desiccated galactose microparticles <12 μm in diameter (3.5 μm median diameter; Fritzsch et al, 1988) that are suspended or dissolved in an aqueous galactose solution. Air attached to or trapped within the particles produces microbubbles with a median diameter of 3 μm, 97% of which are <7 μm in diameter. Echovist microbubbles do not cross the pulmonary circulation after intravenous administration and thus are limited to use in right heart or intralumenal studies; e.g., in evaluation of fallopian tube patency (Smith MD et al, 1984;Venezia and Zangara, 1991). A closely related product is Levovist [SHU 508 (A), Schering AG], which starts as desiccated microparticles of galactose and 0.01% palmitic acid (Fritzsch et al, 1990;Schwarz et al, 1994). The surfactant activity of the fatty acid stabilizes the microbubbles and facilitates their passage through the pulmonary circulation (Smith MD et al, 1989). Intravenous injection of Levovist increases the backscatter of the blood pool, opacifies the left ventricle of the heart, and enhances Doppler ultrasound signals from abdominal organs (Schlief et al, 1990;Goldberg et al, 1993b). Levovist is approved for use in Europe.

Albunex (Molecular Biosystems, Inc., San Diego, CA) is the first GCA approved by the Food and Drug Administration (FDA) for use in the United States. Controlled sonication of 5% human serum albumin produces stable, air-filled microbubbles (Barnhart et al, 1990). The preparation possesses a microbubble concentration of $3–5 \times 10^8$/mL, with a mean microbubble diameter of 3–5 μm, more than 95% of which are <10 μm in diameter. These possess a denatured albumin shell ~15 nm thick (Christiansen et al, 1994). Intravenously injected Albunex traverses pulmonary capillaries, increases left ventricular contrast, and enhances arterial Doppler signals (Keller et al, 1987;Jakobsen et al, 1996). Left ventricular opacification

by Albunex improves endocardial border definition in echocardiograms and thus facilitates evaluation of wall motion and estimation of ejection fraction (Feinstein et al, 1990;Crouse et al, 1993).

A GCA undergoing clinical trials in Europe is BY963 (Bracco-Byk Gulden, Konstanz, Germany). Air bubbles are surrounded by a phospholipid (3-SN-phosphatidyl-D,L-glycero-disteroyl-Na [DSPG-Na]; Solleder et al, 1996). The lyophilized material is rehydrated and then passed back and forth several times through a small chamber to induce microbubble formation. This agent possesses a gas volume of 40 μL/mL and 1.7×10^8 microbubbles/mL. The mean microbubble diameter is 3.8 μm, with 95% of the microbubbles smaller than 8 μm. Intravenous administration of BY963 in humans opacifies the left ventricle and enhances the Doppler signal during transcranial color Doppler imaging (Belz et al, 1994;Kaps et al, 1995).

The commercial materials discussed thus far might be considered to be “first generation” GCAs. All use air as the active agent. However, because of an inherent unsaturation of the air-gases in blood, the air contained within these GCAs readily diffuses out of the microbubbles when injected into the body (Van Liew and Burkard, 1995a).

GCAs are unstable under sonication by diagnostic ultrasound; the problem may be severe at high intensity (Mor-Avi et al, 1994;Porter et al, 1996a;Uhlendorf and Scholle, 1996). This significantly reduces the GCA effectiveness in ultrasonic imaging. A significant fraction of GCA microbubbles may be destroyed by several minutes of exposure to diagnostic ultrasound *in vitro*, resulting from structural alteration of the microbubble shell, leading to gas loss by diffusion and the formation of microbubble clusters due to the attractive force among nearby microbubbles in an ultrasound field (Wu and Tong, 1998a). With loss of air, the GCAs lose the ability to produce ultrasonic contrast. The next advancement made in GCAs (i.e., the second generation) was the use of gases having lower solubility and diffusivity. These GCAs retain their gas for longer periods, thus increasing the duration of contrast and Doppler enhancement from several seconds, as with first generation agents, to several minutes (Van Liew and Burkard, 1995b).

Molecular Biosystems’ second generation GCA is Optison (FS069), consisting of a proteinaceous shell surrounding a perfluoropropane bubble (Meza et al, 1996). This relatively insoluble gas is inert and is eliminated from the body via normal gas exchange. Optison is produced by controlled sonication of 1% human serum albumin in the presence of perfluoropropane. The microbubble concentration is $6.3–9.0 \times 10^8$/mL and the mean microbubble diameter is 2.0–4.5 μm (Dittrich et al, 1995a). Optison opacifies the cardiac ventricular chambers at smaller doses than required for Albunex (0.2 mL versus 15–20 mL, respectively). The duration of contrast produced by Optison dramatically exceeds that of Albunex (>5 min versus 30–45 s, respectively). After intravenous administration, Optison enhances Doppler signals from abdominal and peripheral organs (Dittrich et al, 1994;Brown et al, 1996), enhances two-dimensional ultrasound reflectivity from the heart, demonstrates myocardial perfusion (Dittrich et al, 1995a,1995b;Meza et al, 1996), and increases the echogenicity of the parenchyma from other organs (Nada et al, 1995;Aronson et al, 1996). At dose volumes much larger than those required to achieve parenchymal enhancement, Optison causes no changes in hemodynamic or blood gas measurements in anesthetized dogs (Dittrich et al, 1994,1995a;Meza et al, 1996). Phase One human trial results demonstrate an excellent margin of pharmacological safety (Dittrich et al, 1995b). Optison is approved by the FDA for use in the United States.

Another perfluoropropane-based GCA is Aerosomes (MRX115; ImaRx Pharmaceutical, Tuscon, AZ). These microbubbles are stabilized by a phospholipid coating <10 nm thick (Unger, 1995a). The microbubble concentration is $\sim 8 \times 10^8$/mL, with a mean microbubble

diameter of ~2.5 μm (Unger, 1995b). Intravenous administration of Aerosomes at dose volumes of 0.01–0.05 mL/kg provides myocardial enhancement in subhuman primates (Grauer et al, 1996). Small doses also opacify the left ventricle and enhance Doppler signals from the peripheral vasculature for prolonged periods (Unger, 1995b;Metzger-Rose et al, 1996). In anesthetized monkeys, Aerosomes produce no significant hemodynamic or blood gas changes at dose volumes of 0.05–0.10 mL/kg (Grauer et al, 1995). As of this writing, the agent is undergoing clinical trials to evaluate safety and efficacy in humans.

Imagent US (AFO150; Alliance Pharmaceutical Corp., San Diego, CA) is another GCA that utilizes a perfluorocarbon to increase stability *in vivo*. It is composed of surfactants, phosphate buffers, NaCl, and a blend of perfluorohexane vapors and nitrogen (Mulvagh et al, 1996). The materials start as a powder and gas mixture that is reconstituted with water (20 mg/mL). This preparation results in microbubbles with a median diameter of 6.0 μm and a concentration of ~5.0×10^8 microbubbles/mL. Intravenous administration (0.5 to 2.0 mL) produces homogeneous left ventricle opacification and enhancement of the myocardial tissue in anesthetized dogs. In rabbits, Imagent (0.007 to 0.2 mL/kg) dramatically enhances color Doppler signals from the kidney for extended periods; e.g., from ~300 to >1,000 ss, depending on the dose (Taylor et al, 1996). At dose volumes of 0.2 mL/kg, Imagent produces a modest gray scale enhancement in the renal cortex. At doses up to 40 mL in a dog, Imagent caused no changes in hemodynamic parameters (Mulvagh et al, 1996). Clinical evaluations of this agent are under way as of this writing.

Sonovue (BR1; Bracco Research SA, Geneva, Switzerland) is composed of phospholipids (distearoylphosphatidylcholine and dipalmitoylphosphatidylglycerol), ethylene glycol 4000 and sulfur hexafluoride gas (Schneider et al, 1995). This lyophilized material is dispersed in saline, resulting in a suspension of 2×10^8 microbubbles/mL and a mean microbubble diameter of 2.5 μm, with >90% smaller than 8 μm. The preparation has a gas volume of 2–10 μL/mL. After intravenous administration, Sonovue opacifies the right and left ventricles of the heart. Doses of Sonovue above 0.025 mL/kg cause no further increase in contrast intensity but prolong the duration of contrast in the ventricles, from 27 ± 23 s to 104 ± 35 s at a dose of 0.2 mL/kg (Rovai et al, 1995). Sonovue also enhances the Doppler signals from the vasculature of abdominal organs (Schneider et al, 1996). As of this writing, Sonovue is undergoing clinical evaluation.

A unique second generation GCA is the perfluoropentane emulsion EchoGen (SONUS Pharmaceuticals, Bothell, WA). EchoGen is formulated as a liquid-liquid aqueous emulsion. Dodecafluoropentane, the active ingredient in EchoGen, undergoes a phase change as it warms from room temperature to body temperature (Quay, 1994). EchoGen emulsion contains 2% dodecafluoropentane in stabilized droplets with a diameter of ~0.3 μm and a concentration of 10^{12} droplets/mL (Correas and Quay, 1996); as these warm, the liquid boils (at 28°C) to form microbubbles with a calculated final mean diameter of 2–5 μm. When injected at small doses and without preactivation (see below), EchoGen produces contrast in the ventricular chambers of the heart and enhances Doppler signals from the abdominal organ vasculature (Grayburn et al, 1995;Forsberg et al, 1995). At higher doses, EchoGen enhances the echogenicity of the myocardium and parenchyma of peripheral organs (Sehgal et al, 1995). Activated prior to injection by either sonication or hypobaric manipulation, EchoGen enhances the myocardium and parenchyma of the liver and kidneys at dose volumes one fourth and one tenth those used previously (Cotter et al, 1995;Forsberg et al, 1996). With preactivation and the use of smaller dose volumes, EchoGen causes no hemodynamic or blood gas alterations. As of this writing, EchoGen is under FDA review and is undergoing clinical trial evaluations.

The second generation GCAs discussed above are the ones that are the furthest along in their journey toward clinical utility. Other GCAs are also being developed by several companies. Their development status, physical characteristics, and imaging profiles are less well known.

6.3 Clinical Applications of Contrast Agents

6.3.1 Harmonic and Transient Mode Imaging

6.3.1.1 Harmonic Mode Imaging—Ultrasound imaging is based on the pulse-echo method of the fundamental frequency (*f*). An ultrasonic transducer transmits repeated ultrasonic pulses (the center frequency is *f*) to a target, and the echoes received by the transducer have the same center frequency. The brightness of the pixels on a monitor corresponding to the image of the target is proportional to the echo amplitude. GCAs significantly enhance the backscattered echo signals of the fundamental frequency, as the acoustic impedance of the gas-filled encapsulated microbubbles is quite different from that of soft tissue.

It is well known that a bubbly liquid is highly nonlinear. The second order nonlinearity parameter, B/A, characterizes the nonlinearity in the relationship between acoustic pressure and density. The magnitude of the equivalent nonlinearity parameter B/A of a bubbly liquid can be four orders greater than that of most soft tissue (Wu et al, 1995). Direct experimental measurements (Schrope et al, 1992;Wu and Tong, 1998b) indicated that B/A for Albunex and Levovist solutions can reach 3–4 digits; in contrast, the B/A for most soft tissues is only in the single digits. The highly nonlinear property of GCAs has been used to create a new ultrasonic imaging mode; *viz.*, harmonic imaging. Harmonic imaging is realized by transmitting ultrasonic pulses with a center frequency *f*, but receiving the echoes at *nf*, where *n* is an integer greater or equal to 2 (Schrope et al, 1992;Chang et al, 1995,1996). Since B/A of soft tissue is much smaller than that of GCAs, the contrast of the backscattered signals at the harmonic frequencies is greatly enhanced relative to the contrast obtained at the fundamental frequency. Using this technique, it is possible to detect and measure slow and small volume blood flow. This is not possible by using the current fundamental frequency imaging technique, as the echo from more prevalent tissue at the fundamental frequency dominates the echo from the blood (Burns et al, 1994b). Additionally, since the wavelength and beam width of the nth harmonic frequency are smaller than those of the fundamental by nearly a factor of 1/*n* (Ward et al, 1997), the axial and lateral spatial resolutions of the image are improved.

6.3.1.2 Transient Mode Imaging—Although newer generation GCAs improve the amount of myocardial contrast produced from an intravenous injection of contrast agent, the doses required to produce this contrast are very large and cause acoustic shadowing of myocardium in the near field of insonation (Carstensen et al, 1992;Villanueva et al, 1992;Porter et al, 1995b). Harmonic imaging significantly improves the signal to noise ratio by taking advantage of the nonlinear reflective characteristics of microbubbles (Villanueva et al, 1993;Schrope and Newhouse, 1993; see also subsection 6.3.1.1. above).

A second method of improving myocardial contrast from an intravenous administration of microbubbles is by reducing their exposure to ultrasound. The peak negative acoustic pressures produced by diagnostic ultrasound transducers, which range from 0.5 to 3 MPa (de Jong et al, 1991;Patton et al, 1994), can destroy air-filled as well as fluorocarbon-filled microbubbles (Wray et al, 1992;Mor-Avi et al, 1994;Vandenberg and Melton, 1994). GCA destruction by ultrasound can involve inertial cavitation (Crum et al, 1992;Everbach et al, 1996b); indeed, the rapidity of microbubble destruction (and decrease in video intensity) is related directly to the magnitude of the peak negative pressure (Vandenberg and Melton, 1994). Less frequent exposure (i.e., lower frame rates) has been shown to reduce microbubble destruction rates (Porter et al, 1997).

Transient mode imaging was first observed in animal studies when the imaging ultrasound was frozen for 30–60 s after an intravenous injection of perfluorocarbon-exposed sonicated dextrose albumin microbubbles. Even when using conventional (i.e., >30 Hz) frame rates, a marked increase in myocardial contrast was observed in the first few frames after turning the freeze button off. Often, this increase in contrast was so transient that the only means to observe it was to search the analogue videotape and view each individual frame obtained after turning the freeze button off. Because of the short duration of contrast obtained when using conventional imaging frame rates, this type of imaging was initially termed “transient response” (or “transient mode”) imaging. An equivalent increase in myocardial contrast can be observed by transmitting ultrasound at only one point triggered to every one (or several) cardiac cycles after the intravenous GCA administration.

Even with a high diagnostic peak negative pressure (e.g., 1.1 MPa), a reduced frame rate (e.g., 1 Hz) destroys significantly fewer microbubbles than a conventional frame rate (Porter et al, 1996b,1997). Some of the myocardial contrast improvement obtained with transient mode imaging is actually due to the enhancement of cavitation activity produced under these conditions (Porter et al, 1998a). Upon initial exposure to diagnostic ultrasound pressures, perfluorocarbon-exposed microbubbles have exhibited cavitation activity (Everbach et al, 1996b). The magnitude of this activity varies as a function of both the ultrasound pulse repetition frequency and pulse duration. Interestingly, the greatest initial cavitation activity occurs in response to the lowest pulse repetition frequencies, presumably because of less rapid depletion of gas nuclei. Inertial cavitation activity upon initial exposure to diagnostic ultrasound pressures has also been observed with sonicated albumin-coated microbubbles (Crum et al, 1992). The duration of this transient growth and collapse of the latter microbubbles was even shorter than that observed with perfluorocarbon exposed microbubbles. However, transient mode imaging results in sufficient enhancement of myocardial contrast to allow the use of relatively low acoustic pressures. Porter et al (1997) have shown that the threshold for producing an increase in contrast with transient mode imaging is well below commonly used diagnostic ultrasound acoustic pressures. Even at 0.4–0.5 MPa, contrast increases can be observed with triggered imaging. However, this lower peak negative pressure is not nearly as destructive of the microbubbles as is 0.7–0.8 MPa when using frame rates of 10–15 Hz (Porter et al, 1997), and the operator can still see increased myocardial contrast at frame rates that permit simultaneous assessment of wall thickening (Porter et al, 1998b).

The dramatic impact this has on the amount of contrast produced from intravenously injected microbubbles is demonstrated in Figure 6-6. The image on the left is from a patient during a continuous infusion of perfluorocarbon-exposed sonicated dextrose albumin microbubbles during standard, conventional imaging at 30–40 frames/s. The right side of Figure 6-6 is an image from the same patient during the same continuous infusion of microbubbles, but in this case the frame rate had been reduced to one frame in every two cardiac cycles. The large increase in contrast within the myocardium is obvious.

6.3.2 Cardiovascular Applications

The contrast echocardiography effect was described by Gramiak and Shah (1968), who observed a “cloud” of echoes during injection of indocyanin green dye for performance of a dye curve in a catheterization laboratory. Contrast echocardiography has since been used for structure identification, identification of intracardiac and intrapulmonary shunts, valvular regurgitation, Doppler enhancement, and myocardial perfusion imaging (Jayaweera et al, 1994;Grayburn et al, 1995;Porter et al, 1995a,1995c). Early developments in contrast echocardiography are reviewed elsewhere (Meltzer and Roelandt, 1982a;Meerbaum and Meltzer, 1989).

One of the original uses of contrast echocardiography was for the detection of intracardiac and intra-pulmonary shunts, which remains the most common use for contrast; e.g., quantitation of shunts in atrial septal defect (Okura et al, 1995). For such investigations, agitated saline or dextrose is usually adequate as the GCA, and an intravenous injection is made to search for right-to-left shunting. Contrast echocardiography is particularly important in pediatric cardiology.

Myocardial perfusion imaging by contrast echocardiography was demonstrated in animals in 1982 (Armstrong et al, 1982;Meltzer et al, 1982b) and in humans in 1985 (Santoso et al, 1985). At first, investigators noted the “geographic” extent of contrast distribution in the myocardium and related this to the coronary distribution area. Many subsequent studies of myocardial contrast focused on the “kinetics” of contrast wash-in and wash-out from the myocardium or in the cardiac chambers. These video density curves (or sometimes integrated backscatter curves) are similar to more traditional indicator dilution curves. However, “geographic” studies of contrast distribution within the myocardium are more promising than those from many myocardial “kinetic” contrast studies. Myocardial contrast echocardiography can help delineate areas at risk within coronary territories; i.e., the area likely to infarct related to the occlusion of a coronary artery in experimental animal models. It can be used to delineate the extent of myocardium that has an effective collateral circulation (Sabia et al, 1992a, 1992b); i.e., the area of myocardium opacified by each of two separate injections—one into the right and one into the left coronary artery—is presumably functionally perfused by flow from both coronary arteries. Such myocardium is less likely to infarct and more likely to be viable after an infarction than myocardium not perfused by dual circulation (Galiuto et al, 1994;Camarano et al, 1995). Another important effect of microvascular physiology on gross left ventricular function relates to the “no reflow” phenomenon seen after reperfusion in the setting of acute myocardial infarction (Ito et al, 1992).

Contrast echocardiography is also used to enhance endocardial border definition during stress echocardiography and in technically difficult cases. It can enhance Doppler signals as well as improve two-dimensional (2D) and M-mode imaging. Contrast material can opacify the left ventricle (Sonne et al, 1995) and has been used to enhance weak color Doppler signals, such as those in diastole and in the left ventricular apex. GCAs may prove to be useful for the measurement of ejection fraction.

The ultimate market for contrast echocardiography is still unclear, but new applications and contrast agents designed for these applications will likely continue to evolve; e.g., second and third generation agents that may allow myocardial perfusion imaging after intravenous injections. There is also an exciting possibility that GCAs may enhance therapeutic ultrasound applications involving acoustic cavitation, such as accelerating thrombolysis and perhaps ultrasound angioplasty (Meltzer et al, 1986,1991;Kornowski et al, 1994;Makin et al, 1995).

6.3.3 Obstetric and Gynecologic Applications

Although GCAs are gaining increased acceptance in abdominal or cardiac applications, their use in obstetrics and gynecology is still limited (Abramowicz, 1997). The reason for this is obvious in obstetrics: GCA manufacturers have not attempted to obtain FDA approval for use of their products in pregnancy. Nonetheless, GCAs offer advantages in placental imaging. In experimental settings, two GCAs, iodipamide ethyl ester and Albunex, improved placental imaging and visualization of maternal and fetal placental blood flow (Panigel et al, 1996;Abramowicz et al, 1996). The GCAs permitted color demonstration of flow in fetal capillaries otherwise not resolved by gray-scale, color, or Doppler ultrasound. This could be used to better delineate placental function, e.g., in cases of restricted fetal growth. *In vivo*, conventional ultrasound does not differentiate between areas of adequate or reduced perfusion. In the future, GCAs may allow this type of analysis of placental physiopathology.

As of this writing, the only published report on the use of GCA in obstetrics is a case report of twins with unclear chorionicity. Levovist was injected into the circulation of one twin and observed appearing in the second twin, thus confirming monochorionicity (Denbow et al, 1997).

In gynecology, the situation is very different. Adequate visualization of the uterus and ovaries is possible by gray-scale ultrasound, particularly via the transvaginal approach. However, demonstration of the fallopian tubes is possible only in the presence of peritoneal-abdominal fluid, and then only with difficulty. Intrauterine cavity pathologies are also difficult to discern because there is apposition of the uterine cavity walls, except in pregnancy or during menses when blood is present. Furthermore, the uterus is a solid tissue and so are anomalies of the uterine wall (myometrium) or uterine cavity lining (endometrium). Since tissue differentiation by ultrasound is still less than ideal, the addition of a GCA may improve diagnostic capabilities.

Use of a contrast medium in the uterine cavity was first reported by Richman et al (1984). A 32% solution of Dextran 70 was used to distend the uterus under abdominal ultrasound for tubal patency investigation. This medium was used in another study in which 10 anomalies that had been missed by conventional gray-scale ultrasound were detected in 21 “normal” uteri (Van Roessel et al, 1987). A logical approach would be to inject a clear, neutral, non-irritant material. Normal saline is the natural choice, described originally in 1988 in a study of 30 patients with sterility problems, menstrual irregularities, or suspected tumors (Deichert et al, 1988). The procedure has since been extensively studied under different names: contrast ultrasonography or echography (Crequat et al, 1993), hystero-contrast-sonography or Hy-Co-Sy (Deichert et al, 1989;Campbell et al, 1994), hysterosalpingosonography (Bonilla-Musoles et al, 1992), or sonohysterography, echo-hysterosalpingography (Venezia and Zangara, 1991), or hydro-gynecography (Maroulis et al, 1992). The diagnostic accuracy is excellent (Bonilla-Musoles et al, 1992;Parsons and Lense, 1993;Gaucherand et al, 1995;Goldstein, 1996). Evaluation of the postmenopausal uterus with its usually atrophic endometrium is facilitated by introduction of saline (Achiron et al, 1995). Although transvaginal ultrasound is the usual scanning method, abdominal ultrasound (with the addition of saline) has also yielded good results (Cicinelli et al, 1994,1995). Refinements of these methods include modification of saline by the addition of air bubbles (Allahbadia, 1992) and the use of actual GCAs.

Saline or a contrast medium can be injected into the uterine cavity to study anomalies of the uterus (Fujiwaki et al, 1995). Sonographic examination of the fallopian tubes is facilitated by natural fluid collections in the fallopian tubes and peritoneal cavity (Tufecki et al, 1992;Yarali et al, 1994;Degenhardt et al, 1995). The diagnostic accuracy is comparable to that of hysterosalpingography (Mitri et al, 1991). More sophisticated sonographic technology can also be used for further delineation of the anatomy or pathology; e.g., 2D or color Doppler for detection of fluid flow through the fallopian tubes (Deichert et al, 1989;Peters and Coulam, 1991), as well as three-dimensional (3D) ultrasound.

A recent report described the following additional potential for GCAs in gynecology: After injection of Levovist, blood flow was demonstrated in small vessels of ovarian tumors (Suren et al, 1994). Flow velocity is extremely low in these vessels and, therefore, beyond the limit of resolution of conventional color or Doppler imaging.

The application of ultrasound contrast media in obstetrics and gynecology is a recent phenomenon, but an extensive literature already exists on gynecologic applications of contrast, including detailed descriptions of methodology and an atlas of anatomical and pathological findings (Cullinan et al, 1995;Parsons et al, 1996). It seems that the use of ultrasound contrast media in gynecology (and perhaps in obstetrics) can only expand in the future.

6.3.4 Other Applications

GCAs have been used to enhance sonographic contrast in a variety of other applications. A few recent examples are listed here. In urogynecology, Echovist was instilled into the bladder, leading to improved imaging of the bladder neck. Known pathology present in 39 patients was demonstrated in 38 of these patients when examined using GCA-enhanced ultrasound, but in only 19 of the same patients when similarly examined without GCA (Schaer et al, 1995). In breast ultrasound, Doppler signals were enhanced after injection of GCA. Transit of the GCA was prolonged in malignant lesions as compared with benign masses. Detected vessel number and "tortuosity" indications were also increased. This resulted in 100% sensitivity and specificity in 34 patients (Kedar et al, 1996). GCAs have been used to enhance the detection of brain gliomas (Simon et al, 1992b), cancerous liver growths (Kudo et al, 1992a,1992b, 1994;Nomura et al, 1993), and ophthalmic (Cennamo et al, 1994) and renal tumors (Forsberg et al, 1995). Contrast has been used to guide peri-cardiocentesis (Chiang and Lin, 1993), to visualize renal perfusion (Porter et al, 1995b), for the detection of venous thrombosis (Coley et al, 1994), for the enhancement of Doppler signals from large and small blood vessels (Goldberg et al, 1993b), and blood flowmetry (Shung and Flenniken, 1995).

GCAs have been used in limited therapeutic applications for the intentional enrichment of tumors with gas nuclei followed by the induction of cavitation and resultant tissue destruction (Prat et al, 1993; Simon et al, 1993), and in accelerating thrombolysis, apparently via a cavitation-related mechanism (see, e.g., Tachibana and Tachibana, 1995;Porter et al, 1996c). These are discussed in subsection 6.4.

6.4 Bioeffects

6.4.1 Introduction

Acoustic cavitation is defined as "any interaction between an ultrasound field and any gaseous inclusion in the medium" (Miller DL and Thomas, 1995b), and they note that by this definition, "cavitation occurs … whenever bubble-based contrast agents are exposed to ultrasound." The pulsations of air-filled (Schrope et al, 1992;Chang et al, 1995) and perfluorocarbon-enhanced (Chang et al, 1996;Krishna and Newhouse, 1997) GCAs in an ultrasonic field have nonlinear characteristics, including the generation of scattered signals at harmonic frequencies relative to the applied ultrasound field; the second harmonic is exploited in Doppler ultrasound imaging. As will be developed, GCAs or the derivative microbubbles formed upon their ultrasonic modification can also nucleate inertial cavitation, which can increase the signal strength for imaging (Uhlendorf and Hoffmann, 1994), but can also produce biological damage. In many of the studies discussed here, the acoustic pressures used were sufficiently large to ascribe the observed bioeffects to inertial cavitation. In others, the involvement of inertial cavitation is indicated by physical measures of cavitation activity (see, e.g., Miller DL and Bao, 1998a). Bioeffects associated with inertial cavitation can result from the mechanical forces generated by bubble collapse, shock waves generated by bubble rebound, or sonochemical activity.

6.4.2 Effect of Contrast Agents on Cavitation Nucleation and Cavitation Thresholds

Holland and Apfel (1990) explored the effect of Albunex on the threshold for inertial cavitation. Highly filtered water was used as a host fluid and control; filtration removes many of the endogenous gas nuclei. A passive cavitation detector, based on broad-band scattering of acoustic energy from cavitation microbubbles, was used. With 10 μs pulses of ~0.8–2.3 MHz ultrasound, the threshold for inertial cavitation in filtered water ranged from 1.94–2.43 MPa. A small amount of Albunex reduced the threshold for inertial cavitation at 0.757 MHz to 0.52–0.64 MPa; i.e., by a factor of ~1/3. The threshold for inertial cavitation in control preparations containing filtered, 5% human albumin was similar to that of filtered water. Miller and Thomas (1995a) also studied the ability of GCAs to nucleate inertial cavitation. Sonochemical

production of H_2O_2 (a product of inertial cavitation) was the endpoint. Filtered saline with or without either Levovist or Albunex were exposed for 5 min to pulsed 2.17 MHz ultrasound, followed by assay for accumulated H_2O_2. At 0.82 MPa, no measurable H_2O_2 was produced in the filtered saline. With either Levovist or Albunex present, detectable H_2O_2 production was associated with a pressure amplitude of ~0.4 MPa. At higher ultrasound frequencies, the threshold for inertial cavitation was greater than at lower frequencies for filtered saline and filtered saline containing either Albunex or Levovist. At 2.95 MHz, the threshold for H_2O_2 production in the fluids containing GCA was about 0.6 MPa, and at 2.17 MHz, the threshold was about 0.4 MPa, as noted above. In whole human blood exposed to 2.5 MHz ultrasound, the pressure threshold for actively detected inertial cavitation activity is on the order of 4–5 MPa (Deng et al, 1996); with GCAs present, the pressure threshold for hemolysis in whole blood is on the order of 0.5 MPa (see below).

These results make it clear that GCAs significantly lower the threshold acoustic pressures required for the inception of inertial cavitation and may increase the extent of such activity relative to non-nucleated or poorly nucleated fluids. These findings have potentially important consequences to the occurrence of mechanical, ultrasound-induced bioeffects. As discussed below, mechanical bioeffects of ultrasound exposure may be potentiated by GCAs. However, a recent microscopic study of Albunex microbubbles adherent to a petri dish and exposed to the 5 MHz output of a Hewlett Packard Sonos 500 medical imager indicates that at maximum output power, the microbubbles slowly diminished in size, but did not appear to undergo inertial collapse (Klibanov et al, 1998).

6.4.3 Potentially Undesirable Bioeffects

6.4.3.1 Simple Model Systems—As of this writing, most of the research on the enhancement of mechanical ultrasound-induced bioeffects by GCAs has been conducted using *in vitro* systems. Because the results obtained in these experiments often depend critically on the methods used (e.g., the use of stationary versus rotating exposure vessels), the inclusion of some significant experimental detail in this subsection is unavoidable.

The published report of which we are aware concerning a GCA-enhanced bioeffect is that of Williams et al (1991). Dilute suspensions of human erythrocytes in plasma were used to explore the hemolytic effect of ultrasound exposure in the presence of Echovist. Most samples were exposed for 5 min to continuous wave, 0.75 MHz ultrasound in a rotating vessel, although some were exposed in stationary vessels. Echovist was added to experimental samples at concentrations ranging from 5–10 mg/mL. The volume fraction of red cells in suspension was also varied. In very dilute cell suspensions (0.5% volume fraction or hematocrit) exposed with vessel rotation to a spatial average, temporal average intensity (SATA) of 0.5 W/cm^2, ~33% of the cells lysed in the absence of Echovist. With 8 mg Echovist/mL present, hemolysis increased to ~60%. In other dilute suspensions, there appeared to be a dose:response relationship between Echovist concentration and percent hemolysis. Below ~5 mg/mL, the fraction of cells lysed in the presence of Echovist was comparable to that in the controls, while at Echovist concentrations of ≥8 mg/mL, hemolysis was ~twofold greater. Exposure vessel rotation was found to be an important variable in determining the extent of hemolysis, which was greater with than without rotation, both with and without GCA present. However, the relative enhancement of hemolysis by the GCA was much greater in the stationary than in the rotated vessels.

Williams et al (1991) observed that with or without GCA, the fraction of cells lysed by the ultrasound decreased as the hematocrit of red cells in suspension increased. No lysis was detectable in most samples having hematocrits >5%. In canine red cell suspensions prepared with variable hematocrits and Albunex concentrations and exposed to 2.25 MHz ultrasound (1.6 MPa, 1 s continuous wave), hemolysis increased monotonically with increasing hematocrit

at constant concentration, and with increasing concentration at constant hematocrit (Miller DL et al, 1997). No hemolysis was observed without added Albunex. The observation that the extent of cell lysis appears to decline to immeasurably low levels with increasing cell concentration has often been noted (Veress and Vincze, 1977;Saad, 1983;Williams, 1983;Ellwart et al, 1988;Brayman et al, 1992;Carstensen et al, 1993;Miller MW et al, 1995), suggesting that high cell concentrations either inhibit or eliminate inertial cavitation activity, and that ultrasonic hemolysis *in vivo* is unlikely. However, Miller et al (Miller MW et al, 1995) noted that while the *percentage* of erythrocytes lysed by sonication in the presence of Albunex decreased with increasing cell concentration, the *number* of cells lysed per sample remained more or less constant. Similar results were obtained in a study of cell lysis produced by stable microbubble pulsations (Miller DL, 1988). A subsequent analysis (Brayman et al, 1996b) indicates that *in vitro* sonolysis of cells at high cell concentrations is limited by the number of microbubbles available, or by the number of cells a microbubble may encounter before being “inactivated” by cell aggregation around pulsating microbubbles, but that hemolysis might be produced by sonication of dense cell suspensions supplemented with GCAs. Although Williams et al (1991) reported that hemolysis in blood cell suspensions declined to undetectable levels as hematocrit increased, regardless of the presence or absence of a GCA, the results of other studies conducted with GCAs and human erythrocyte suspensions of high hematocrit indicate that readily detectable hemolysis can be produced by sonication of whole blood with GCA present.

Miller et al (Miller MW et al, 1995) studied ultrasonic hemolysis of human erythrocytes of 1%–20% hematocrit using Albunex at concentrations of 0–41 μL/mL. Cell suspensions were exposed or sham-exposed to CW ultrasound (1 MHz with a spatial peak, temporal peak intensity (I_{SPTP}) of 1–5 W/cm^2 (SPTP intensity) for 60–120 s. Exposure vessel rotation was also explored as an experimental variable. Most experiments used samples prepared from a stock suspension of red cells that had been anticoagulated with CPDA (citrate-phosphate-dextrose-adenine) and stored under refrigeration, although some experiments were conducted using freshly collected heparinized blood. In 1% hematocrit cell suspensions prepared from stored blood and insonated with vessel rotation, sonication alone (5 W/cm^2, 60 s) produced 28% hemolysis, versus 1% hemolysis in sham-exposed controls. The addition of Albunex to insonated samples increased the level of hemolysis to ~50%. There was no apparent dose:response relationship between Albunex concentration (1.3–41 μL/mL) and hemolytic yield. There was a dose:response relationship between ultrasound intensity (0–5 W/cm^2) and hemolysis. A significant elevation of hemolysis, relative to sham-insonated controls, was produced in samples insonated at intensities of ≥ 1 W/cm^2, regardless of the presence or absence of Albunex, but significantly greater levels of hemolysis were produced with GCA present.

The hematocrit of stored blood samples affected cell lysis, with or without Albunex present; percent hemolysis decreased generally as hematocrit increased over the range of 1%–20%. When samples were rotated during exposure, significantly greater levels of hemolysis were produced with Albunex than without Albunex at all hematocrits <10%; at 20% hematocrit, the difference was nominal. Similar results were obtained using stationary exposure vessels, although the levels of hemolysis produced in the stationary vessels were less than in rotating vessels. Quite different results were obtained when freshly drawn blood was used. Whereas exposure of 20% hematocrit suspensions of stored blood cells to 5 W/cm^2 ultrasound with vessel rotation lysed ~10% (without Albunex) to ~20% (with Albunex) of the cells, when fresh blood was used, comparable exposures produced very low levels of hemolysis (~0.5%) that did not differ significantly among cells exposed with or without Albunex or sham-exposed to ultrasound. It seems probable that the disparity of results obtained with stored or fresh blood relates to the level of sample aeration. Sample oxygenation increases cavitation activity in “normal” media (Kondo and Kano, 1987,1988b;Inoue et al, 1990;Riesz and Kondo, 1992;Brayman et al, 1992;Carstensen et al, 1993), but the samples used in these experiments

were not intentionally oxygenated. The enhancement of ultrasonic hemolysis by Albunex was later shown to depend strongly on the oxygenation state of the sample (Azadniv et al, 1995). Interestingly, Williams et al (1991) had noted that the ability of Echovist to nucleate cavitation activity was abolished when the agent was added to degassed plasma. Presumably, these effects arise by dissolution of the microbubbles in undersaturated fluids.

Brayman et al (1995) further explored the issue of ultrasonic hemolysis in the presence of 35 μL/mL Albunex. Human erythrocyte suspensions were prepared in autologous plasma to hematocrits of 1%–40% using refrigerated stock suspensions. Samples were exposed for 60 s to pulsed 1.1 MHz ultrasound (1 ms pulse duration, 20 Hz pulse repetition frequency). The peak acoustic pressures of the pulses were 4.7 MPa (peak positive) and 2.7 MPa (peak negative), corresponding to an I_{SPPA} of ~420 W/cm^2. Without Albunex, statistically significant levels of ultrasound-induced hemolysis, relative to sham-exposed controls, were observed only at the lowest tested hematocrit (1%), while significant levels of hemolysis were observed at all tested hematocrits when Albunex was present in exposed samples. With Albunex, percent hemolysis declined as sample hematocrit increased, but the total number of cells lysed per sample remained approximately constant over the 5%–40% range of hematocrits. At 40% hematocrit (equivalent to whole blood), the background level of hemolysis in sham-exposed samples was 2.4 ± 0.4%. The level of hemolysis in samples insonated with or without Albunex were 6.7 ± 1.3 *versus* 2.8 ± 0.4%, respectively. For these samples, hemolysis in the presence of Albunex was significantly greater than in either the sham-exposed control or the insonated, Albunex-free preparations. Hemolysis in the shams and the Albunex-free, insonated samples were statistically indistinguishable. Thus, there was a twofold increase in hemolysis associated with insonation in the presence of Albunex.

A subsequent study (Brayman et al, 1996b) examined the acoustic pressure and pulse duration dependence of hemolysis produced by ultrasound in the presence of Albunex. Freshly collected, oxygenated human blood containing 3.6 V% Albunex was exposed to pulsed 1 MHz ultrasound with sample rotation. Acoustic pressures ranged from 0 to 7.4 MPa (peak positive), 4.0 MPa (peak negative); I_{SPTP} ranged from 0 to ~1080 W/cm^2. The duty factor was 0.01, and pulse durations varied between 5 μs–1,000 μs. Statistically significant levels of background-corrected hemolysis were observed in all insonated samples, including those exposed to the lowest acoustic pressure or intensity at the shortest pulse duration tested (0.5 MPa, 5 μs pulses). At constant pulse duration, there was a dose:response relationship between ultrasound intensity and hemolysis. At constant intensity, hemolysis increased generally with increasing pulse duration, but at relatively high intensities, this trend was not monotonic. The hemolysis data for relatively brief pulses (5–30 μs) were analyzed in relation to the MI values associated with the various exposures. Although statistically significant levels of hemolysis were produced at an MI of 0.5 for each of these pulse durations, the level of hemolysis was generally low (~0.5%–1.0%). Hemolysis increased slowly with increasing MI up to a value of ~2, and then increased sharply. The point at which this sharp inflection appeared to increase as pulse duration decreased. Since most diagnostic pulses are on the order of 1 μs in duration, this observation is encouraging from the perspective of the potential for diagnostic ultrasound exposures in the presence of GCAs to produce little or no hemolysis *in vivo*.

The frequency dependence of hemolysis produced by pulsed ultrasound exposure in the presence of 3.5 V% Albunex was investigated using erythrocyte suspensions prepared as described above (Brayman et al, 1997b). Peak negative acoustic pressures ranged from 0.0 to ~3.0 MPa, the ultrasound frequencies were 1.0, 2.2, or 3.5 MHz, pulse durations were 20 (see Figure 6-7) or 200 μs, the duty factor was 0.01, and total treatment time was 60 s. Hemolysis increased with increasing acoustic pressure at each frequency and depended weakly on pulse duration. At low peak negative acoustic pressures, the frequency dependence of ultrasonic hemolysis was relatively weak, but it was very strong at high pressures (e.g., at 0.5 MPa, the

data appear to follow a P–/$f^{0.5}$ relationship, whereas at 3 MPa, the data appear to follow a P–/f^3 or P–/f^4 relationship, where P– is the peak negative acoustic pressure and f is the ultrasound frequency). Because most diagnostic ultrasound equipment emits ultrasound in the 2–7 MHz range and inertial cavitation-related hemolysis *in vitro* (and *in vivo*; see below) declines very rapidly with ultrasound frequency at constant acoustic pressure, it therefore appears that large-scale ultrasound-induced hemolysis *in vivo* is unlikely under diagnostic examination conditions. However, Brayman et al (1997b) estimate that under worst case conditions during an echocardiographic examination in the presence of Albunex, it might be possible to lyse ~1% of the systemic erythrocyte population in the body. Dalecki et al (1997d) have demonstrated with an animal model that ultrasound exposures with GCA present in the vasculature can produce systemic levels of hemolysis on the order of 1% (see subsection 6.4.3.2). Killam et al (1998) detected no hemolysis *in vivo* due to diagnostic insonation of rabbit hearts following administration of Optison. However, the exposure conditions were such that hemolysis would probably not be expected to occur (see subsection 6.4.3.2).

Miller and Thomas (Miller DL and Thomas, 1996a) studied the effect of Albunex on hemolysis in whole canine blood of ~50% hematocrit. A lithotripter (peak positive pressure ~24 MPa, peak negative pressure ~5 MPa) and a focused 1.3 MHz ultrasound source were used. The focused ultrasound was applied in continuous or burst mode, with burst durations of 20, 100, or 1,000 μs, and with pressure amplitudes ranging from 1 to ~18 MPa. Albunex was added to some samples at final concentrations of 0.1, 1, or 10 V%. The presence of Albunex in samples exposed to the lithotripter shocks decreased the number of shocks required to observe greater hemolysis than in the shams. Without Albunex, 500 shocks were necessary; with 1% or 10% Albunex, 200 and 100 shocks, respectively, were required. However, while there was a nominal twofold increase in hemolysis associated with the presence of 10% Albunex in the shock-exposed samples, this difference was not statistically significant, leading the authors to conclude that the shock waves were capable of reliably nucleating inertial cavitation without the need for exogenous nuclei. With continuous 1.3 MHz ultrasound, the presence or absence of Albunex markedly affected hemolysis. The threshold acoustic pressure required for significant hemolysis varied with exposure duration and the presence or absence of Albunex. For example, without Albunex, the threshold pressure was > 17.8 MPa when the exposure duration was 1 ms, 17.8 MPa at 100 ms, and 10 MPa with 10 s exposure. With 1% Albunex present, the threshold acoustic pressure was ~10 MPa with 100 and 1,000 ms exposures, and 3.2 MPa with 10 s exposure. Thus, 1% Albunex reduced the apparent threshold for hemolysis by a factor of two or more. With 100 ms exposures, the threshold pressure with 0.1% Albunex was the same as for the Albunex-free control (*viz.*, ~18 MPa); with 1% or 10% Albunex, the threshold pressures were 10 MPa. Thus, the 0.1% Albunex was not effective in reducing the threshold pressure for hemolysis relative to control blood, and 10% Albunex was no more effective in reducing the threshold pressure than was the 1% concentration. Additional experiments were conducted using 1.3 MHz ultrasound applied in burst mode, with a total “on” time of 100 ms and a constant duty factor of 0.01. The threshold acoustic pressures were similar to those noted above for the continuous wave exposures; as before, 0.1% Albunex had no effect on the threshold pressure for hemolysis, while 1% and 10% Albunex were equivalently effective in lowering the threshold to ~10 MPa. At very high acoustic pressures (e.g., ~18 MPa), hemolysis occurred in all insonated samples, regardless of the presence or absence of Albunex, with the exception of those exposed to 20 μs bursts without Albunex, in which there was none. Hemolysis increased with increasing burst length (20, 100, or 1,000 μs), and was greater with Albunex than without at suprathreshold acoustic pressures.

Albumin-stabilized microbubbles are acoustically labile (subsection 6.3), and there is evidence that ultrasonic modification of these GCAs creates “derivative” gas bodies capable of nucleating inertial cavitation. With highly concentrated Albunex, different levels of hemolysis are produced by pulsed or continuous wave, 2.25 MHz ultrasound exposures of constant total

"on" time, with greater hemolysis produced by the continuous wave exposures (Miller DL et al, 1997). At 1.6 MHz, continuous wave bursts of 0.001–100 s produced statistically significant levels of hemolysis relative to shams. With pulsed exposures of 1 s total "on" time but variable duty factors, hemolysis declined rapidly as duty factor decreased. These results suggest that (1) ultrasound modifies the GCA, producing free microbubbles that then serve as cavitation nuclei; (2) with continuous wave exposure, the biological effect is expressed quickly; and (3) without continuous exposure to replenish the nuclei via sustained inertial cavitation activity (i.e., with pulsed exposures), the free microbubbles dissolve rapidly, thus producing a smaller biological effect than continuous wave exposures of the same total duration. Albunex microbubbles can nucleate inertial cavitation *in vitro* after the bulk of the microbubbles has been destroyed by ultrasound (Brayman and Miller, 1997a); because free microbubbles generated by the acoustic destruction of Albunex are expected to dissolve rapidly, this result suggests that a small number of the Albunex microbubbles escaped initial ultrasonic destruction, and that these can nucleate significant cavitation activity. For a dramatic example of the latter point, see Dalecki et al (1997e).

Everbach et al (1997) used a passive, 20 MHz acoustic detector to measure inertial cavitation activity in dilute human erythrocyte suspensions, and demonstrated that sonolysis induced in the presence of 3.5 V% Albunex is correlated with inertial cavitation activity occurring in the sample. Samples were exposed or sham-exposed to 1 MHz ultrasound (peak positive and peak negative pressures of 5.0 and 2.8 MPa, respectively) of various pulse durations for 60 s. Inertial cavitation activity within the samples was monitored throughout the exposure period and hemolysis assessed subsequently. At a 20 Hz pulse repetition frequency, both inertial cavitation activity and hemolysis increased in parallel with increasing pulse duration when samples contained Albunex; these correlations were statistically significant at the $p<0.0001$ level. Therefore, this study provides direct physical evidence in support of the assumption usually made in GCA bioeffect studies; *viz.*, that the effect arises via an inertial cavitation mechanism.

Perfluorocarbon-based GCAs, by virtue of their greater persistence in an ultrasonic field, appear to have a greater potential for enhancing mechanical bioeffects than do air-based GCAs. Miller and Geis (Miller DL and Geis, 1998b) studied *in vitro* hemolysis in relation to the presence of different GCAs or filtered buffered saline solution. Two perfluoropentane-based GCAs (FSO69 and MRX-130) and two air-based GCAs (Albunex and Levovist) were used. The different agents were used at comparable volume fractions in the experimental mixtures, but differ somewhat in microbubble concentration in the stock material (Albunex: 0.3–0.9 × 10^9/mL; FS069: 0.6–0.9 × 10^9/mL; MRX–130: ~1 × 10^9/mL; Levovist: unquantified. (See Miller DL and Geis, 1998b, subsection 6.2.3, and Figure 6-5). In 50:50 mixtures of whole canine blood and GCA exposed (stationary) for 1 s to continuous wave, 2.4 MHz ultrasound, the pressure thresholds for hemolysis were similar (0.2–0.4 MPa) for Albunex, FS069 and MRX-130; the threshold for Levovist treatment could not be determined. However, at suprathreshold acoustic pressures, the hemolytic yield was consistently greater for the perfluoropentane-based agents than for Albunex; e.g., at 1.6 MPa, hemolysis was 8, 24, and 48% for Albunex, MRX-130, and FS069 addition treatments, respectively. With pulsed ultrasound exposure (10 μs pulse duration, 0.01 duty factor) of the same total "on" time used in the continuous wave experiments, hemolysis was generally lower than produced by continuous wave exposures at comparable acoustic pressures. The general trends observed in the continuous wave experiments were again observed, and at acoustic pressures within the range of diagnostic ultrasound, levels of hemolysis were considerable. At a pressure amplitude of 3.2 MPa, insonation produced ~60 or ~10% hemolysis with FS069 or MRX-130 present, respectively, as compared with ~2%–5% hemolysis with Albunex or Levovist present. Hemolysis produced in the presence of the perfluorocarbon-based GCAs had a marked dependence of GCA concentration. Pulse duration was not a strong determinant of hemolysis. Most of the difference in the ability of the different GCAs to promote ultrasonic hemolysis

appears to be related to the ability of the perfluorocarbon gases to persist in the cell suspension during insonation. A comparison of hemolysis produced with Albunex or FSO69 present and application of either 1, 10, 100, 1,000, or 10,000 pulses (10 μs, 1 ms pulse repetition period) of 2.4 MHz ultrasound indicated that for low numbers of pulses (up to 100), the enhancement of hemolysis produced by these two GCAs were equivalent. However, with 1,000 or 10,000 pulses, the levels of hemolysis produced in the presence of FSO69 were sixfold to eightfold greater than produced with Albunex. This factor is far greater than the expected differences in microbubble concentration in the samples (see above).

Erythrocytes are neither the sole corpuscular element of blood, nor are they the only blood cell type susceptible to ultrasonic damage. At comparable concentrations, human erythrocytes and lymphocytes are lysed in similar numbers by ultrasound exposures, the white cells being somewhat more sensitive than the red cells (Miller MW and Brayman, 1997). Platelets are also susceptible to inertial cavitation-induced membrane damage. Everbach et al (1996a) studied ultrasound-induced platelet lysis and membrane permeability changes (pre-loaded ^{51}Cr leakage) in relation to inertial cavitation activity, and the effect of Albunex on these endpoints. Cavitation activity was assessed using a passive detector. Platelets were exposed to pulsed 1 MHz ultrasound with either 0 or 3.5 V% Albunex present. With Albunex, lysis increased with increasing pulse duration; without Albunex, lysis remained at control levels. Platelet lysis in samples containing Albunex was highly correlated with measures of inertial cavitation occurring in the sample. The assay for sublytic damage also showed that the number of cells damaged increased with increasing pulse duration, but this endpoint was not well correlated with inertial cavitation activity.

Monolayers of CHO cells grown on Mylar membranes undergo membrane damage, as evidenced by ATP release, when insonated at 3.3 MHz in the presence of 5% Albunex (Miller DL and Bao, 1998a). The effect is dependent on the applied acoustic pressure and exposure mode, with a threshold of ~0.3 MPa for 1 s of continuous exposure and ~0.6 MPa for pulsed exposures (10 μs pulses, 0.01 duty factor, 1 s “on” time). ATP release was highly correlated with the strength of subharmonic signals emitted by the microbubbles, indicating that cavitation was involved. The cell populated surface orientation was an important determinant of the amount of membrane damage observed, with much greater ATP release obtained when the populated surface was at the site of ultrasound entry into the exposure vessel than when at the site of exit. However, the harmonic signals were unaffected by vessel orientation. Qualitatively similar results have been obtained by Brayman (unpublished; work in progress). Data obtained using confluent V79 fibroblasts on Mylar membranes and exposed to pulsed 1.0, 2.2, or 3.5 MHz ultrasound indicate that (1) 3% Albunex reduces the pressure threshold for an erosive effect of insonation on the monolayer relative to that when Albunex is absent, (2) without Albunex, cell populated surfaces at the site of ultrasound exit from the exposure vessel are more susceptible to erosion than are those at the site of entry, but that this differential disappears when Albunex is present, and (3) the effect is frequency and pressure dependent. Because these studies involve diagnostically realistic ultrasound frequencies, acoustic pressures and pulse durations, these results suggest that the use of GCAs during vascular ultrasound imaging may damage the endothelial cells of blood vessels.

6.4.3.2 Laboratory Animals—Since tissues that contain gas bodies naturally are susceptible to damage from exposure to diagnostic levels of ultrasound (see Section 5), and because of the evidence from *in vitro* studies that GCAs enhance ultrasound-induced bioeffects, it is reasonable to hypothesize that GCAs will increase the likelihood of ultrasound-induced bioeffects *in vivo*. Dalecki et al (1997d) studied ultrasound-induced hemolysis *in vivo* when Albunex was present in the blood. Murine hearts were exposed for 5 min to 1.2 or 2.4 MHz pulsed ultrasound (10 μs pulse duration, 100 Hz PRF) at pressure amplitudes ranging from 0–10 MPa. At evenly spaced intervals during the exposure period, four ~25 μL boluses of Albunex

were injected into a tail vein. Two studies, using different strains of mice, were performed at 1.2 MHz to determine the threshold for hemolysis. At 2.4 MHz, animals were exposed to only the highest pressure amplitude (10 MPa). Control animals were exposed at 1.2 MHz with a peak amplitude of 10 MPa and were injected with four boluses of saline. Following exposure, the animals were killed, the blood collected and the blood assayed for hemolysis. Figure 6-7 presents the percent hemolysis as a function of exposure amplitude for all experiments in this investigation. Analyses of the data at 1.2 MHz for the C3H and CD1 strains of mice indicated that the threshold values did not differ significantly. The threshold for detectable hemolysis *in vivo* at 1.2 MHz was 3.5 MPa peak positive pressure, 2 MPa peak negative pressure and ~200 W/cm^2 SPPA intensity at the surface of the animal. After correcting for the chest wall attenuation, the threshold at the surface of the heart at 1.2 MHz was 3.0 MPa peak positive pressure, 1.9 MPa peak negative pressure, corresponding to an MI of 1.8 and an SPPA intensity ~180 W/cm^2. Hemolysis in mice injected with Albunex and exposed at 2.4 MHz with the highest exposure amplitude (10 MPa) was only 0.46%, and was comparable to that in sham exposed mice receiving Albunex (~0.4% hemolysis) and in control mice receiving saline injections and exposed at 10 MPa (~0.4% hemolysis). This strong frequency dependence of hemolysis was also observed in whole blood *in vitro* (Brayman et al, 1997b) and is similar to the frequency dependence of the threshold for ultrasound-induced hemorrhage in the intestine (Dalecki et al, 1995b). These results indicate that when GCAs are present in the blood, ultrasonically induced hemolysis can occur *in vivo* at diagnostically relevant pulse durations and pulse repetition frequencies. The relatively high threshold for detectable hemolysis at 1.2 MHz combined with the strong dependence of the threshold on frequency suggest there is little likelihood of extensive (i.e., more than ~1% of the systemic red cell pool) ultrasound-induced hemolysis under most current diagnostic imaging procedures. Killam et al (1998) detected no hemolysis in rabbits injected with Optison and exposed *in vivo* to 5 MHz pulsed ultrasound. A Hewlett Packard Sonos 500 with a 5 MHz phased array transducer was used at maximum output power (MI ~0.5) (A. Killam, personal communication). The pressure amplitude was therefore ~1 MPa). Blood samples were collected from the carotid and femoral arteries at baseline, and at 0, 3, and 6 min after infusion of 0.6 mL/kg Optison. Analysis of blood samples showed no increase in serum free hemoglobin or serum lactate dehydrogenase, both markers for hemolysis. However, at the acoustic frequency and pressure used in this study (i.e., 5 MHz, ~1 MPa), the available *in vitro* and *in vivo* data indicate that little or no hemolysis would be likely to arise (see, e.g., Fig. 6-8). These data indicate that under conditions of “conventional” B-mode imaging, the administration of Optison did not produce detectable lysis of red blood cells.

Rupture of microvessels in exteriorized rat spino-trapezius muscle following injection of modified Optison microbubbles and exposure of the muscle to single sweeps of 2.3 MHz diagnostic ultrasound has been reported (Skyba et al, 1998). The numbers of ruptured capillaries and killed nucleated cells scaled with increasing MI value over the range of 0.4–1.0 as indicated by the output display. However, because the muscle was exteriorized and bathed in Ringer’s solution (which has a much lower attenuation coefficient than assumed for tissue), the tissues were exposed to greater acoustic pressures than indicated by the on-screen MI values. Capillaries smaller than ~7 μm in diameter were affected. The mean number of ruptured vessels per g fresh tissue weight increased monotonically with increasing MI value, from ~320 at an MI of ~0.4 to ~2,400 at MI ~1.0. Microscopic observation during the exposure allowed direct visualization of ultrasonic microbubble destruction *in vivo*.

Ultrasound-induced lung hemorrhage under diagnostically relevant exposure conditions is well documented (Section 4) and depends on the presence of gas in the tissue (Hartman et al, 1990). If cavitation in the lung vasculature were the mechanism for lung hemorrhage, then the addition of GCAs to the blood should increase the extent of ultrasound-induced lung hemorrhage. This was tested by Raeman et al (1997). Murine lungs were exposed to pulsed

ultrasound (1.2 MHz, 10 μs pulse duration, 100 Hz PRF, 2 MPa peak positive pressure, 5 min). During exposure, four 25 μL boluses of Albunex were injected into a tail vein. The mean area of ultrasound-induced lung hemorrhage in Albunex-injected mice was not statistically different from that in saline-injected or uninjected mice. For several echocardiographic procedures, using current diagnostic imaging systems, the acoustic pressure amplitude at the surface of the lung may approach the threshold for lung hemorrhage (Carstensen et al, 1992). This study indicates that the presence of Albunex in the lung vasculature does not increase the extent of ultrasound-induced lung hemorrhage.

Miller and Geis (1998b) investigated the effects of the presence of GCAs in the vasculature on ultrasound-induced intestinal hemorrhage in mice. For exposure to continuous wave ultrasound at 1 MHz (0.75 MPa peak positive pressure), the extent of hyperemia, petechiae, and hemorrhages increased in comparison with control animals injected with a blank agent. For pulsed ultrasound exposures at 1 MHz (10 μs pulse duration, 0.01 duty cycle), Albunex injection greatly increased the number of ultrasound-induced petechiae; e.g., for exposures at 2.8 MPa, there was a thirtyfold increase in petechia in the mice with Albunex compared with Albunex-free control animals. The number of petechiae produced increased linearly with increasing Albunex dosage.

Tissue damage resulting from lithotripsy is often attributed to inertial cavitation. Prat et al (1991b) investigated whether the presence of GCAs increases the tissue damage produced by exposure to lithotripter fields at amplitudes typically used clinically to treat kidney stones. Three treatment groups of rabbits were used: Group 1 received 500 lithotripter shocks focused on the right hepatic lobe, Group 2 received an infusion of microbubbles (Plasmion; Roger Bellon, Neuillysur-Seine, France), and Group 3 received 500 shocks and microbubbles during the exposure period. Animals in Group 1 exhibited a few, small subcapsular and intraparenchymal hematomas, while animals in Group 2 showed only moderate liver congestion. Animals exposed to lithotripter fields in the presence of microbubbles (Group 3) showed numerous subcapsular and intraparenchymal hematomas of significantly larger size than those observed in Group 1 animals. Hence, infusion of microbubbles during lithotripsy greatly increased hepatic tissue damage. Tissue damage is enhanced by the intravascular presence of GCAs during lithotripsy treatment even for relatively low pressure amplitude exposures (Dalecki et al, 1997e). In uninjected mice exposed abdominally to 200 piezoelectric lithotripter pulses (2 MPa peak pressure amplitude), there was only minimal damage to the intestine and lung tissue. In similarly exposed animals who received four 25 μL injections of Albunex during exposure there were extensive hemorrhages in the muscle, fat, mesentery, intestine, kidneys, stomach, bladder, and seminal vesicles.

Although Albunex is effective as a diagnostic contrast agent for only a few minutes, Albunex continues to supply cavitation nuclei *in vivo* for long periods of time after injection (Dalecki et al, 1997e). Mice were given a single injection of Albunex prior to exposure to 200 lithotripter pulses at times ranging from 5 min to 24 hr following the injection. For many tissues, such as intestine, mesentery and bladder, Albunex continued to enhance hemorrhage from exposure to lithotripter fields at amplitudes of 2 MPa for up to 4 hr after injection. For exposures at clinical amplitudes, Albunex continued to enhance hemorrhage in the bladder, muscle and seminal vesicles when exposures were performed up to 6 hr after injection. These studies suggest that great caution should be practiced in the use of GCAs before or during lithotripsy procedures.

6.4.4 Potentially Useful Bioeffects

6.4.4.1 Tumor Disruption and Enhancement of Chemotherapy—A number of papers have been published in which ultrasound was reported to enhance the effectiveness of certain anticancer drugs, apparently *via* nonthermal mechanisms (see, e.g., Yumita et al, 1989,

1990;Saad and Hahn, 1989;Loverock et al, 1990;Umemura et al, 1990;Harrison et al, 1991;Kessel et al, 1994). However, most of the published reports dealing with this topic have used “normal” media; i.e., media not supplemented with exogenous gas bodies, and will, therefore, not be considered here.

As therapeutic tools for tumor treatment, GCAs have been employed thus far for three general uses: (1) as a means of disrupting tissues via direct mechanical effects resulting from inertial cavitation; (2) as an adjunct to ultrasound:drug interactions in which inertial cavitation enhances anticancer drug effectiveness, apparently via a sonochemical effect, and (3) as a site-specific drug carrier that releases a drug in the neighborhood of the target tissue when the microbubbles are destroyed by insonation of the tissue. The use of GCAs or similar preparations to deliberately nucleate inertial cavitation for these purposes is a relatively recent development.

6.4.4.1.1 Mechanical Tumor Disruption by Microbubble-Enhanced Inertial Cavitation Lipid-coated microbubbles accumulate in tumor tissue to a much greater extent than in surrounding tissues (Simon et al, 1992b,1993), thus presenting the possibility of therapeutic intervention by the induction of inertial cavitation in microbubble-enriched tumor tissues (Simon et al, 1993). Simon et al (1993) tested this idea using Walker-256 tumors implanted subcutaneously in rats. There was one control group (no ultrasound, no microbubbles), and two ultrasound-exposed groups, one of which received lipid-coated microbubbles via tail vein injection prior to insonation. Tumors were located using 7.5 MHz ultrasound scans. In the ultrasound-exposed groups, this was followed by exposure to continuous wave, 4.5 MHz ultrasound (I_{SATA} = 250 mW/cm^2) for 8 min. Insonation did not demonstrably affect tissue temperature. Animals were sacrificed at 0–72 hr post-insonation and scored blindly for hemorrhage and tumor necrosis. A consistent elevation of tumor necrosis was associated with microbubble and ultrasound treatment relative to either the controls or the ultrasound-only treatment group. The authors, while not entirely ruling out possible tissue heating effects, interpret their results in terms of inertial cavitation activity. That insonation of microbubble-enriched tumor tissue may enhance tumor necrosis is exciting, but caution is warranted because of the potential for metastasis (see subsection 6.4.4.1.4).

6.4.4.1.2 Increased Tumoricidal Drug Activity with Microbubble-Enhanced Inertial Cavitation Prat et al (1993) explored the combined effects of shock wave–induced, microbubble-enhanced cavitation and an anticancer drug *in vivo*. Tumors were implanted in the abdomens of rats, and an electrohydraulic lithotripter (250–500 shocks, peak positive pressure ~60 MPa) used to induce inertial cavitation while the abdomens were being infused with air-filled, gelatin-encapsulated microbubbles with or without co-treatment with the drug fluorouracil. At a relatively high dose, the drug alone cured 100% of the animals, but produced signs of liver compromise. Low dosages of the drug cured none of the animals when used alone. Treatment with shock waves and microbubbles without the drug cured about half of the animals. However, treatment of the rats with shock waves and microbubbles, in combination with a low dose of fluorouracil, was as effective as the high dose of the drug alone.

Jeffers et al (1995) also explored ultrasound-induced inertial collapse of stabilized microbubbles, combined with drug therapy, as a potential tool for tumor destruction. The goal was to enhance the membrane-damaging effect of the polar solvent and tumoricidal drug *N*,*N*-dimethylforamide by ultrasound in a localized tissue volume, such that systemic drug doses might be reduced while still producing tumoricidal activity. The related drugs monomethylforamide and dimethylsulfoxide were also tested. *In vitro* suspensions of HL-60 human promyelocytic leukemia cells were used; membrane damage was assessed by released lactate dehydrogenase activity. The GCAs used in this study were “homemade” albumin stabilized microbubbles having a median diameter of 3.2 μm. Controls (i.e., no bubbles) were prepared by adding an equivalent volume of 5% albumin solution. Cells were exposed or sham-

exposed to 1 MHz ultrasound (continuous wave, 15 s) at 0, 0.6, 1.0, 1.9 or 2.5 W/cm^2 SPTA intensity, which did not result in bulk heating of the suspensions. Subharmonic emissions from the sample were monitored simultaneously as a measure of cavitation activity within the samples. Without microbubbles, neither ultrasound + albumin nor ultrasound + albumin + *N*,*N*-dimethylforamide increased levels of membrane damage at any of the tested intensities. In contrast, membrane damage produced by the ultrasound + microbubble treatment increased with increasing ultrasound intensity, reaching ~35% at the highest exposure level. Membrane damage produced by the ultrasound + *N*,*N*-dimethylforamide + microbubble treatment also increased with ultrasound intensity, but was significantly greater than that produced by the ultrasound + microbubbles treatment at all nonzero ultrasound intensities. Qualitatively similar results were obtained with the other drugs tested. Cell membrane damage in the ultrasound + *N*,*N*-dimethylforamide + microbubble and the ultrasound + microbubble treatments was correlated strongly with the subharmonic emission amplitude measured during sample insonation, indicating that cavitation was involved in the effect. At comparable “levels” of cavitation activity, membrane damage was greater in samples containing *N*,*N*-dimethylforamide than in those lacking it. Separate assessments for sonochemical effects failed to detect any significant effect on membrane damage, suggesting that any effective sonochemicals produced by the insonation were short-lived. Other assessments indicated that the presence of *N*,*N*-dimethylforamide did not increase cavitation activity relative to *N*,*N*-dimethylforamide-free controls, nor did *N*,*N*-dimethylforamide sensitize the cells to damage by shear forces applied to the cells by non-acoustic means. When taken together, the observations that (1) there was no bulk heating of the insonated suspensions, (2) enhancement of *N*,*N*-dimethylforamide cytotoxicity was proportional to subharmonic emission, and (3) the *N*,*N*-dimethylforamide did not affect the occurrence of subharmonic emission or the susceptibility of the cells to rupture by mechanical shear forces, suggest that cavitation is responsible for the effect.

The study of Yumita et al (1997) did not involve the use of exogenous microbubbles, but it is relevant to this discussion because the insonation method used (*viz.*, superposition of a 1 MHz ultrasound field and its 500 kHz subharmonic) was designed specifically to promote the occurrence of cavitation. Colon 26 carcinoma tumors were transplanted into the kidneys of mice. A gallium-porphyrin compound (ATX-70) was administered intravenously. Neither ATX-70 treatment alone nor sonication alone produced tumor necrosis; however, combined ultrasound + ATX-70 treatment produced extensive tumor necrosis. The ultrasound SPTP intensities (~30 W/cm^2 at both 500 kHz and 1 MHz) produced significant tissue heating (3–8°C), but because ultrasound treatment alone was ineffective, the effect of combined ultrasound + ATX-70 treatment was not ascribed to thermal mechanisms. The authors speculate that active oxygen species are generated by sonodynamically activated (i.e., inertial cavitation-activated) porphyrin, and that these oxygen species then destroy the tissue. Miyoshi et al (1997) further explored this issue, using suspension cultured HL-525 human leukemia cells with ATX-70 treatment. Cavitation activity was generated in the cell suspensions with a 50 kHz commercial sonicator. Sonication alone lysed ~20% of the cells, while ATX-70 alone had no effect. Ultrasound + ATX-70 treatment produced a large increase in cytotoxicity. Accumulation of the ATX-70 in the cells was demonstrated, but only extracellular ATX-70 was effective as a sonosensitizer; cells with incorporated ATX-70 sonicated in ATX-70 free medium were no more sensitive to killing than control cells. Sonication of ATX-70 solutions followed by incubation of cells in the fluid was ineffective, suggesting the involvement of short-lived sonochemical products. However, the presence of free radicals could not be demonstrated by electron paramagnetic resonance (EPR) spin trapping, nor was the cytotoxic effect of simultaneous ultrasound + ATX-70 treatment overcome by inclusion of spin traps (which can remove radical intermediates) in the suspension fluid. Thus, the mechanism by which the enhanced ATX-70 activity arises remains unclear.

Prat et al (1994) explored the combined effect of 5-fluorouracil and inertial cavitation on cancer cell killing and other endpoints. They had previously demonstrated (Prat et al, 1993) that cancer cells *in vitro* and *in vivo* can be perturbed by exposure to lithotripter shock waves with microbubbles present. Among their findings was that exposure to shock waves + microbubbles resulted in a greater immediate cell kill and an increase in delayed mortality relative to cells exposed to shock waves alone. Prat et al (1994) facilitated inertial cavitation occurrence by the use of a lithotripter (peak positive pressure ~60 MPa) and by supplementing the cell preparations with gelatin-stabilized, air-filled microbubbles (10–100 μm diameter). HT-29 human colon cancer cells were exposed to shock waves + microbubbles followed by a 12 hr incubation period of the surviving cells. Various concentrations of 5-fluorouracil were then added and the cells allowed to incubate in the presence of the drug for up to 72 hr. The drug was then removed and clonogenic growth assessed. Other shock + microbubble treated cells were subcultured after shock treatment for 24 or 48 hr, followed by assessment of the rate of [^{3}H]deoxuridine incorporation into DNA. In the absence of 5-fluorouracil, cells that survived the initial exposure to shock + microbubble treatment had decreased clonogenic growth, as did cells exposed to 5-fluorouracil only. The effect of shock + microbubble pretreatment decreased the dose of 5-fluorouracil needed to kill 50% of the cells and reduced the rate of deoxuridine incorporation relative to untreated control cells. 5-Fluorouracil treatment alone suppressed deoxuridine incorporation after 24 or 48 hr of subculture, but shock + microbubble pretreatment reduced by fourfold to tenfold the concentration of 5-fluorouracil needed to inhibit deoxuridine incorporation by 50% relative to cells treated with 5-fluorouracil only. Thus, the shock + microbubble treatment sensitized the cells to the toxic effects of the drug despite the passage of many hours between shock treatment and drug application. The mechanism by which this arises is not yet certain.

6.4.4.1.3 Microbubbles as a Local Drug Delivery System Porter et al (1996a) report the results of an interesting “proof-of-concept” study in which microbubbles were used as a vehicle to carry drugs to a target tissue, with release of the drug *in situ* produced by insonation of the microbubbles and target tissue, presumably via microbubble destruction. A synthetic antisense oligodeoxyribonucleotide, phosphorothiolate oligonucleotide, was found to bind to the albumin coating of perfluorocarbon-exposed sonicated dextrose albumin (PESDA) microbubbles. To test the ability of PESDA microbubbles to deliver and release the drug in a target tissue, microbubbles bearing bound phosphorothiolate oligonucleotide were injected intravenously into three dogs. The left kidney of each was insonated using a diagnostic ultrasound transducer (peak negative pressure = 1.1 MPa, 30 Hz frame rate, 2.0–2.5 MHz frequency) after the injection; the PESDA microbubbles were visualized simultaneously as sonographic contrast. The right kidney received no ultrasound. The dogs were killed 4 hr later, and the kidneys sampled and assayed for phosphorothiolate oligonucleotide. In two of the three dogs, there was a substantial increase in accumulated phosphorothiolate oligonucleotide in the insonated kidney (ninefold and threefold greater than in the matched control kidneys), while in the third dog, there was no difference. The mean relative increase was ~fourfold; however, possibly because of the small number of subjects, this difference was not statistically significant. Nonetheless, the result indicates that the general technique is worthy of further exploration.

6.4.4.1.4 Inertial Cavitation-Related Metastasis The foregoing discussion indicates that the intentional induction of cavitation *in vivo* may have therapeutic value in the treatment of tumors. In this regard, an issue of considerable concern is whether the treatment may increase the potential for metastasis. Only a few studies have addressed this issue, and while most of these have been negative (see, e.g., Geldhof et al, 1989;Oosterhof et al, 1990;Hoshi et al, 1991), a recent positive report by Oosterhof et al (1996) is noteworthy. Although this study was conducted with high pressure lithotripter shocks, it is somewhat unsettling because these effects presumably arise via inertial cavitation and, as discussed, inertial cavitation activity

sufficient to disrupt the microcirculation may arise in tissues during ultrasonic imaging with GCA present (see subsection 6.4.3.2).

6.4.4.2 Ultrasound-Enhanced Thrombolysis with GCAs—Ultrasound can enhance the dissolution of thrombi (Hong et al, 1990;Ariani et al, 1991;Francis et al, 1992;Lauer et al, 1992;Tachibana, 1992;Blinc et al, 1993;Harpaz et al, 1993;Luo et al, 1993;Sehgal et al, 1993;Olsson et al, 1994). The bulk of the evidence indicates that this occurs via nonthermal mechanisms, presumably by increasing the permeance of fibrolytic agents into the thrombi. Tachibana and Tachibana (1995) postulated that inertial cavitation contributes to the process, and that increasing inertial cavitation activity by nucleating thrombus-containing fluids with GCAs would further increase ultrasound-enhanced thrombolysis. Artificial thrombi formed from whole blood were placed in ultrasound exposure vessels into which test fluids could be circulated (urokinase or albumin solutions, Albunex or various combinations). These were exposed or sham-exposed for 3 min (170 kHz, 2 s bursts, duty factor = 0.33, SPTP intensity = 0.5 W/cm^2) followed by an incubation period. Fibrinolysis was assessed by the loss of thrombus dry weight relative to untreated control thrombi. After 120 min of posttreatment incubation, neither albumin, microbubbles, ultrasound + albumin, nor ultrasound + microbubbles significantly enhanced thrombolysis in the absence of urokinase (~1%–3% fibrinolysis). Without ultrasound treatment, urokinase increased fibrinolysis to ~50% in the presence of either albumin or microbubbles. With ultrasound treatment, fibrinolysis with urokinase + albumin was significantly enhanced (from 51% to 58%; $p \ll 0.005$) and enhanced further with urokinase + microbubbles (from 48% to 72%; $p \ll 0.005$). Tachibana and Tachibana (1995) attributed the increased level of thrombolysis associated with simultaneous treatment with urokinase, ultrasound, and Albunex to the occurrence of inertial cavitation in the fluid surrounding the thrombus, and speculated that the mechanism involves cavitation-induced microstreaming that increases urokinase penetration into the thrombus.

Porter et al (1996c) compared the efficacy of PESDA and room air exposed sonicated dextrose albumin (RASDA) microbubbles in ultrasound-enhanced thrombolysis. Artificial thrombi formed from whole blood were insonated or sham-insonated (20 kHz, 0.85 MPa peak negative pressure, 2 min) in a variety of test solutions. Sonication in saline solution increased thrombolysis relative to simple incubation in saline solution (from 7% to 23%). Saline + ultrasound treatment was about as effective as urokinase treatment alone (23% versus 17%, respectively). Ultrasound + urokinase treatment produced 48% thrombolysis. PESDA alone had no effect on thrombolysis, and PESDA + urokinase was no more effective than urokinase alone. However, treatment of the thrombi with ultrasound + PESDA, in the absence of urokinase, produced a large increase in thrombolysis [*c.f.* ultrasound + Albunex treatment by Tachibana and Tachibana (1995), described above, and results obtained with RASDA, described below]. The ultrasound + urokinase + PESDA treatment was the most effective, producing 60% thrombolysis. RASDA microbubbles were less effective than PESDA microbubbles. Ultrasound + RASDA treatment, without urokinase, was no more effective than ultrasound treatment of thrombi in saline solution; however, when urokinase was present, the level of thrombolysis produced with RASDA microbubbles present was about the same as that produced by treatment with ultrasound + PESDA without urokinase. Porter et al (1996c) attribute the microbubble enhancement of ultrasound-accelerated thrombolysis to cavitation. They suggest that the difference in the responses to PESDA and RASDA may relate to the number of cavitation nuclei present, because of a fivefold greater microbubble concentration in the PESDA preparations, and because the PESDA microbubbles are more stable and persist longer.

Nishioka et al (1997) conducted a study of the thrombolytic effectiveness of ultrasound with or without perfluorocarbon-based GCAs in the absence of thrombolytic drugs. Dodecafluoropentane emulsion or saline solution was tested for thrombolytic effectiveness

with or without ultrasound. Human thrombi *in vitro* and rabbit ileofemoral arterial thrombi *in vivo* were the model systems. The former were exposed/sham-exposed for 3 min to 25 kHz ultrasound at an intensity of 2.9 W/cm^2. The latter were insonated transcutaneously (20 kHz, *in situ* intensity ~1.5 W/cm^2). *In vitro* clot dissolution was significantly enhanced by ultrasound treatment alone (no ultrasound + saline: 10%; ultrasound + saline: 72%). The GCA without ultrasound had no effect on thrombolysis, while GCA + ultrasound produced 98% thrombolysis. The maximum diameter of clot debris particles formed by insonation with or without dodecafluoropentane was ~4 μm in both cases. The *in vivo* study produced somewhat different results. Ultrasound treatment alone produced reperfusion in none of six rabbits. Reperfusion was observed in 1 of 11 rabbits (9%) treated with dodecafluoropentane treatment alone, but in 14 of 17 rabbits (82%) treated with ultrasound + dodecafluoropentane. Thermal effects may have played a role, because histological examination of insonated tissues revealed evidence of coagulative necrosis and focal hemorrhage.

A potential problem with the therapeutic use of GCAs to improve ultrasound-enhanced thrombolysis *in vivo* is that often the thrombus occludes the blood vessel to the extent that blood flow is minimal and, therefore, the GCA may have limited access to the thrombus. Lanza et al (1996) described a method that may help to overcome this problem. Their interest was in site-specific image enhancement rather than production of a therapeutic bioeffect such as thrombolysis, but their approach may hold promise for cavitation-related thrombolysis and tumor necrosis. Their approach was to use ligand-specific binding and accumulation of a nongaseous, lipid-encapsulated perfluorocarbon emulsion (perfluorodichlorooctane). The lipid shell was biotinylated by incorporating biotinylated phosphatidlyethanolamine. The basic idea is as follows: the blood clot (or other target) is treated with a biotinylated monoclonal antibody specific to the target of interest (e.g., a fibrin domain in the case of thrombi). The biotinylated monoclonal antibody binds to the surface of the target. A biotin-binding molecule, avidin, is then administered and conjugates and cross-links the bound biotinylated monoclonal antibody on the target surface. Finally, the biotinylated, lipid-coated perfluorocarbon emulsion is administered. These microparticles bind, via unoccupied biotin binding sites on the immobilized avidin molecules, to the surface of the target. Lanza et al (1996) demonstrated site-specific accumulation of their preparation *in vivo* using a canine femoral artery thrombus model; image enhancement was marked. If it is possible to similarly biotinylate the lipid shell of a stable gaseous contrast agent, it may be possible to accumulate large numbers of microbubbles directly on the surface of the target structure. Because of their immediate proximity to the target, ultrasound induced inertial cavitation might then be quite effective in disrupting the target. However, because of the potential for this treatment to facilitate metastasis, this possible approach to tumor therapy must necessarily be approached with caution.

6.4.4.3 Enhancement of Sonoporation by GCAs—Enhancement of sonoporation (i.e., transient permeabilization) of mammalian cells by GCAs has been reported. Bao et al (1997) reported that plasmid transfection of CHO cells *in vitro* exposed to 2.25 MHz ultrasound occurred at a very low level without the inclusion of 10% Albunex and without exposure vessel rotation during insonation; with rotation and 10% Albunex present, the threshold pressure for transfection was ~ 0.3 MPa. Kim et al (1996) report the results of extensive *in vitro* experiments on ultrasonically induced transfection of mammalian cells in the absence of GCAs. However, the report also describes preliminary efforts to ultrasonically induce transfection *in vivo* by injection of Albunex and plasmid suspensions into rat knee joints prior to insonation or sham insonation. There was evidence of three successful transfections in four exposed knees, and none in the sham-exposed knees.

References

Abramowicz JS. Ultrasound contrast media and their use in obstetrics and gynecology. Ultrasound Med Biol 1997;23:1287. [PubMed: 9428126]

Abramowicz JS, Phillips DB, Jessee LN, et al. Enhanced blood flow visualization in the perfused human placenta by Albunex®, an ultrasound contrast medium. Placenta 1996;17:A.21.

Achiron R, Lipitz S, Sivan E, et al. Sonohysterography for ultrasonographic evaluation of tamoxifen-associated cystic thickened endometrium. J Ultrasound Med 1995;14:685. [PubMed: 7500435]

Allahbadia GN. Fallopian tubes and ultrasonography: The Sion experience. Fertil Steril 1992;58:901. [PubMed: 1426374]

AIUM American Insitute of Ultrasound in Medicine Bioeffects Committee. Bioeffects and Safety of Diagnostic Ultrasound. Laurel, MD: American Institute of Ultrasound in Medicine; 1993.

AIUM/NEMA: American Institute of Ultrasound in Medicine/National Electrical Manufacturers Association. Acoustic Output Measurement and Labeling Standard for Diagnostic Ultrasound Equipment. Laurel, MD: American Institute of Ultrasound in Medicine; 1992a.

AIUM/NEMA: American Institute of Ultrasound in Medicine/National Electrical Manufacturers Association. Acoustic Output Measurement Standard for Diagnostic Ultrasound Equipment. Laurel, MD: American Institute of Ultrasound in Medicine; 1998.

AIUM/NEMA: American Insitute of Ultrasound in Medicine/National Electrical Manufacturers Association. Standard for the Real-Time Display of Thermal and Mechanical Acoustic Output Indices on Diagnostic Ultrasound Equipment. Laurel, MD: American Institute of Ultrasound in Medicine; 1992b. rev 1996

Anderson AL, Hampton LD. Acoustics of gas-bearing sediments: I. Background. J Acoust Soc Am 1980;67:1865.

Apfel RE. Acoustic cavitation: A possible consequence of biomedical uses of ultrasound. Br J Cancer 1982;45:140. [PubMed: 7059457]

Apfel RE. Acoustic cavitation prediction. J Acoust Soc Am 1981;69:1624.

Apfel RE. Possibility of microcavitation from diagnostic ultrasound. IEEE Trans Ultrasonics, Ferroelectrics, and Frequency Control 1986;32:19.

Apfel RE. The role of the impurities in the cavitation-threshold determination. J Acoust Soc Am 1970;48:1179.

Apfel RE, Holland CK. Gauging the likelihood of cavitation from short pulse, low duty cycle diagnostic ultrasound. Ultrasound Med Biol 1991;17:179. [PubMed: 2053214]

Ariani M, Fishbein MC, Chae IS, et al. Dissolution of peripheral arterial thrombi by ultrasound. Circulation 1991;84:1680. [PubMed: 1914107]

Aris A, Solanes H, Camara ML, et al. Arterial line filtration during cardiopulmonary bypass. J Thorac Cardiovasc Surg 1986;91:526. [PubMed: 3959571]

Armour EL, Corry PM. Cytotoxic effects of ultrasound *in vitro*: Dependence on gas content, frequency, radical scavengers, and attachment. Radiat Res 1982;89:369. [PubMed: 7063619]

Armstrong WF, Mueller TM, Kinney EL, et al. Assessment of myocardial perfusion abnormalities with contrast-enhanced two-dimensional echocardiography. Circulation 1982;66:166. [PubMed: 7083503]

Aronson S, Roth R, Fernandez A, et al. Assessment of regional renal blood flow in the dog with FS069, a novel intravenous ultrasound contrast agent. Anesth Analg 1996;82:510.

Atchley AA, Frizzell LA, Apfel RE, et al. Thresholds for cavitation produced in water by pulsed ultrasound. Ultrasonics 1988;26:280. [PubMed: 3407017]

Atchley AA, Prosperetri A. The crevice model of bubble nucleation. J Acoust Soc Am 1989;86:1065.

Averkiou, M. Nonlinear propagation modeling with KZK equation and comparison with measurements. In: Edmonds, P., editor. American Institute of Ultrasound in Medicine Workshop on Effects of Nonlinear Propagation on Output Display Indices (TI and MI), Abstracts and Handouts, Boston, March 20, 1998. Laurel, MD: American Institute of Ultrasound in Medicine; 1998. Chair

Ayme EJ, Carstensen EL. Cavitation induced by asymmetric, distorted pulses of ultrasound: A biological test. Ultrasound Med Biol 1989;15:61. [PubMed: 2922882]

Azadniv M, Doida Y, Miller MW, et al. Temporality in ultrasound-induced cell lysis *in vitro*. Echocardiography 1995;13:45. [PubMed: 11442902]

Baggs R, Penney DP, Cox C, et al. Thresholds for ultrasonically induced lung hemorrhage in neonatal swine. Ultrasound Med Biol 1996;22:119. [PubMed: 8928309]

Bailey MR, Blackstock DT, Cleveland RO, et al. Comparison of electrohydraulic lithotripters with rigid and pressure-release ellipsoidal reflectors: I. Acoustic fields. J Acoust Soc Am 1998;104:2517. [PubMed: 10491712]

Bailey MR, Dalecki D, Child SZ, et al. Bioeffects of positive and negative acoustic pressures *in vivo*. J Acoust Soc Am 1996;100:3941. [PubMed: 8969491]

Balen FG, Allen CM, Lees WR. Ultrasound contrast agents. Clin Radiol 1994;49:77. [PubMed: 7907285]

Bao S, Thrall BD, Miller DL. Transfection of a reporter plasmid into cultured cells by sonoporation *in vitro*. Ultrasound Med Biol 1997;23:953. [PubMed: 9300999]

Barbarese E, Ho SY, D'Arrigo JS, et al. Internalization of microbubbles by tumor cells *in vivo* and *in vitro*. J Neurooncol 1995;26:25. [PubMed: 8583242]

Barnett SB, Miller MW, Cox C, et al. Increased sister chromatid exchanges in Chinese hamster ovary cells exposed to high intensity pulsed ultrasound. Ultrasound Med Biol 1988;14:397. [PubMed: 3176185]

Barnhart J, Levene H, Villanando E, et al. Air-filled albumin microspheres for echocardiography contrast enhancement. Invest Radiol 1990;25:S162. [PubMed: 2126533]

Bell E. The action of ultrasound on mouse liver. Journal of Cellular and Comparative Physiology 1957;50:83.

Belz GG, Breithaupt K, Butzer R, et al. Image quality and safety following intravenous BY963, a new transpulmonary echo contrast media in man. J Am Coll Cardiol 1994;23:A24.

Bender LF, Janes JM, Herrick JF. Histologic studies following exposure of bone to ultrasound. Arch Phys Med Rehabil 1954;35:555. [PubMed: 13189637]

Beranek, LL. Acoustical Measurements. New York, NY: American Institute of Physics; 1988. p. 33

Blackshear, PL.; Blackshear, GL. Mechanical hemolysis. In: Shalak, R.; Chien, S., editors. Handbook of Bioengineering. New York, NY: McGraw-Hill; 1987. p. 15.1-15.9.

Bleeker, H. Master of Science thesis in bioengineering. University Park, PA: Pennsylvania State University; 1990a. Physical and Ultrasonic Characterization of Ultrasonic Contrast Agents.

Bleeker HJ, Shung KK, Barnhart JL. Ultrasonic characterization of Albunex®, a new contrast agent. J Acoust Soc Am 1990b;87:1792.

Blinc A, Francis CW, Trudnowski JL, et al. Characterization of ultrasound-potentiated fibrinolysis *in vitro*. Blood 1993;81:2636. [PubMed: 8490172]

Bonilla-Musoles F, Simon C, Serra V, et al. An assessment of hysterosalpingosonography (HSSG) as a diagnostic tool for uterine cavity defects and tubal patency. J Clin Ultrasound 1992;20:175. [PubMed: 1313831]

Boussuges A, Abdellaoui S, Gardette B, et al. Circulating bubbles and breath-hold underwater fishing divers: A two-dimensional echocardiography and continuous wave Doppler study. Undersea Hyperb Med 1997;24:309. [PubMed: 9444062]

Boussuges A, Carturan D, Ambrosi P, et al. Decompression induced venous gas emboli in sport diving: Detection with 2D echocardiography and pulsed Doppler. Int J Sports Med 1998;19:7. [PubMed: 9506792]

Brand RP, Nyborg WL. Parametrically excited surface waves. J Acoust Soc Am 1965;37:509.

Brayman AA, Azadniv M, Cox C, et al. Hemolysis of Albunex®-supplemented, 40% hematocrit human erythrocytes *in vitro* by 1 MHz pulsed ultrasound: Acoustic pressure and pulse length dependence. Ultrasound Med Biol 1996a;22:927. [PubMed: 8923711]

Brayman AA, Azadniv M, Makin IRS, et al. Effect of a stabilized microbubble contrast agent on hemolysis of human erythrocytes exposed to high-intensity pulsed ultrasound. Echocardiography 1995;12:13.

Brayman AA, Church CC, Miller MW. Re-evaluation of the concept that high cell concentrations "protect" cells *in vitro* from ultrasonically-induced lysis. Ultrasound Med Biol 1996b;22:497. [PubMed: 8795177]

Brayman AA, Doida Y, Miller MW. Apparent contribution of respiratory gas exchange to the *in vitro* "cell density effect" in ultrasonic cell lysis. Ultrasound Med Biol 1992;18:701. [PubMed: 1440991]

Brayman AA, Miller MW. Acoustic cavitation nuclei survive the apparent ultrasonic destruction of Albunex® microspheres. Ultrasound Med Biol 1997a;23:793. [PubMed: 9253828]

Brayman AA, Miller MW. Ultrasonic cell lysis *in vitro* upon fractional, discontinuous exposure vessel rotation. J Acoust Soc Am 1994;95:3666. [PubMed: 8046155]

Brayman AA, Strickler PS, Luan H, et al. Hemolysis of 40% hematocrit, Albunex®-supplemented human erythrocyte suspensions by intense pulsed ultrasound: Frequency, duty factor, pulse length and sample rotation dependence. Ultrasound Med Biol 1997b;23:1237. [PubMed: 9372572]

Brown J, Alderman J, Quedens-Case C, et al. Enhancement demonstration of neovascularity in a VX2 carcinoma by ultrasonic contrast (FS069, MBI, Inc). J Ultrasound Med 1996;15:518.

Burns PN. Ultrasound contrast agents in radiological diagnosis. Radiol Med 1994a;87:71.

Burns PN, Powers JE, Hope-Simpson D, et al. Harmonic power mode Doppler using microbubble contrast agents: An improved method for small vessel flow imaging. Proc IEEE Ultrasononics Symp 1994b; 3:1547.

Camarano G, Ragosta M, Gimple W, et al. Identification of viable myocardium with contrast echocardiography in patients with poor left ventricular systolic function caused by recent or remote myocardial infarction. Am J Cardiol 1995;75:215. [PubMed: 7832125]

Campbell S, Bourne TH, Tan SL. Hysterosalpingo contrast sonography (HyCoSy) and its future role within the investigation of infertility in Europe. Ultrasound Obstet Gynecol 1994;4:245. [PubMed: 12797192]

Carmichael AJ, Mossoba MM, Riesz P, et al. Free radical production in aqueous solutions exposed to simulated ultrasonic diagnostic conditions. IEEE Trans Ultrasonics, Ferroelectrics, and Frequency Control 1986;33:148.

Carstensen EL, Campbell DS, Hoffman D, et al. Killing of Drosophila larvae by the fields of an electrohydraulic Iithotripter. Ultrasound Med Biol 1990a;16:687. [PubMed: 2126407]

Carstensen, EL.; Dalecki, D.; Gracewski, S., et al. Nonlinear propagation and the mechanical index scanners. In: Edmonds, P., editor. American Institute of Ultrasound in Medicine Abstracts and Handouts: Workshop on Effects of Nonlinear Propagation on Output Display Indices (TI and MI), Boston, March 20, 1998. Laurel, MD: American Institute of Ultrasound in Medicine; 1998. Chair

Carstensen EL, Duck FA, Meltzer RS, et al. Bioeffects in echocardiography. Echocardiography 1992;6:605. [PubMed: 10147799]

Carstensen EL, Hartman C, Child SZ, et al. Test for kidney hemorrhage following exposure to intense, pulsed ultrasound. Ultrasound Med Biol 1990b;16:681. [PubMed: 2281557]

Carstensen EL, Kelly P, Church C, et al. Lysis of erythrocytes by exposure to CW ultrasound. Ultrasound Med Biol 1993;19:147. [PubMed: 8516961]

Cennamo G, Rosa N, Vallone GF, et al. First experience with a new echographic contrast agent. Br J Ophthalmol 1994;78:823. [PubMed: 7848976]

Chang PH, Shung KK. Attenuation and backscatter measurements on Albunex®. Proc IEEE Ultrasonics Symp 1993;2:913.

Chang PH, Shung KK, Levene HB. Quantitative measurements of second harmonic Doppler using ultrasound contrast agents. Ultrasound Med Biol 1996;22:1205. [PubMed: 9123645]

Chang PH, Shung KK, Levene HB. Second harmonic imaging and harmonic Doppler measurements with Albunex®. IEEE Trans Ultrasonics, Ferroelectrics, and Frequency Control 1995;42:1020.

Chapelon JY, Dupenloup F, Cohen H, et al. Reduction of cavitation using pseudorandom signals. IEEE Trans Ultrasonics, Ferroelectrics, and Frequency Control 1996;43:623.

Chaussy, C. Extracorporeal Shock Wave Lithotripsy: New Aspects in the Treatment of Kidney Stone Disease. Basel; Karger: 1982.

Chaussy C, Brendel W, Schmiedt E. Extracorporeally induced destruction of kidney stones by shock waves. Lancet 1980;2:1265. [PubMed: 6108446]

Chiang HT, Lin M. Pericardiocentesis guided by two-dimensional contrast echocardiography. Echocardiography 1993;10:465. [PubMed: 10146322]

Child SZ, Hartman CL, Schery LA, et al. Lung damage from exposure to pulsed ultrasound. Ultrasound Med Biol 1990;16:817. [PubMed: 2095012]

Christenson HK, Claesson PM. Cavitation and the interaction between macroscopic hydrophobic surfaces. Science 1988;236:390. [PubMed: 17836871]

Christiansen C, Kryvi H, Sontum PC, et al. Physical and biochemical characterization of Albunex®, a new ultrasound contrast agent consisting of air-filled albumin microspheres suspended in a solution of human albumin. Appl Biochern Biotechnol 1994;19:307.

Christopher, T. A hopefully complete nonlinear model for predictiong *in vivo* fields of clinical scanners. In: Edmonds, P., editor. American Institute of Ultrasound in Medicine Abstracts and Handouts: Workshop on Effects of Nonlinear Propagation on Output Display Indices (TI and MI), Boston, March 20, 1998. Laurel, MD: American Institute of Ultrasound in Medicine; 1998. Chair

Church CC. The effects of an elastic solid surface layer on the radial pulsations of gas bubbles. J Acoust Soc Am 1995;97:1510.

Church CC, Flynn HG, Miller MW, et al. The exposure vessel as a factor in uttrasonically induced mammalian cell lysis II. Ultrasound Med Biol 1982;8:299. [PubMed: 7101578]

Ciaravino V, Brulfert A, Miller MW, et al. Diagnostic ultrasound and sister chromatid exchanges: Failure to reproduce positive results. Science 1985;227:1349. [PubMed: 3883487]

Ciaravino V, Miller MW, Carstensen EL. Sister chromatid exchanges in human lymphocytes exposed *in vitro* to therapeutic ultrasound. Mutat Res 1986;172:185. [PubMed: 3762575]

Ciaravino V, Miller MW, Kaufman GE. The effect of 1 MHz ultrasound on the proliferation of synchronized Chinese hamster V-79 cells. Ultrasound Med Biol 1981;7:175. [PubMed: 7256977]

Cicinelli E, Romano F, Anastasio PS, et al. Sonohysterography versus hysteroscopy in the diagnosis of endouterine polyps. Gynecol Obstet Invest 1994;38:266. [PubMed: 7851813]

Cicinelli E, Romano F, Anastasio PS, et al. Transabdominal sonohysterography, transvaginal sonography and hysteroscopy in the evaluation of submucous myomas. Obstet Gynecol 1995;85:42. [PubMed: 7800322]

Clarke PR, Hill CR. Physical and chemical aspects of ultrasonic disruption of cells. J Acoust Soc Am 1970;47:649. [PubMed: 5439664]

Coakley WT. Acoustical detection of single cavitation events in a focused field in water at 1 MHz. J Acoust Soc Am 1970;49:792.

Coakley, WT.; Nyborg, WL. Cavitation; dynamics of gas bubbles; applications. In: Fry, FJ., editor. Ultrasound: Its Application in Medicine and Biology. New York, NY: Elsevier; 1978. p. 77-159.

Cohen, J. Statistical Power Analysis for the Behavioral Sciences. Revised. New York, NY: Academic Press; 1977.

Coleman AJ, Chio MJ, Saunders JE, et al. Acoustic emission and sonoluminescence due to cavitation at the beam focus of an electrohydraulic shockwave lithotripter. Ultrasound Med Biol 1992;18:267. [PubMed: 1595133]

Coleman AJ, Chio MJ, Saunders JE, et al. Detection of acoustic cavitation in tissue during clinical extracorporeal lithotripsy. Ultrasound Med Biol 1996;22:1079. [PubMed: 9004432]

Coleman AJ, Saunders JE. A review of the physical properties and biological effects of the high amplitude acoustic fields used in extracorporeal lithotripsy. Ultrasonics 1993;31:75. [PubMed: 8438532]

Coleman AJ, Saunders JE, Crum LA, et al. Acoustic cavitation generated by an extracorporeal shock-wave lithotripter. Ultrasound Med Biol 1987;13:69. [PubMed: 3590362]

Coley BD, Trambert MA, Mattrey RF. Perfluorocarbon-enhanced sonography: Value in detecting acute venous thrombosis in rabbits. Am J Roentgenol 1994;163:961. [PubMed: 8092043]

Correas JM, Quay SA. EchoGen™ emulsion: A new ultrasound contrast agent based on phase shift colloids. Clin Radiol 1996;51(S1):11. [PubMed: 8605764]

Cotter B, Keramati S, Kwan OL, et al. Myocardial opacification with low dose activated EchoGen™ in patients: Initial experience. Circulation 1995;92:1. [PubMed: 7788902]

Cowden JW, Abell MR. Some effects of ultrasonic radiation on normal tissues. Exp Mol Pathol 1963;2:367. [PubMed: 14061854]

Crequat J, Pennehouat G, Cornier E, et al. Evaluation of intra-uterine pathology and tubal patency by contrast echography. Contraception, Fertilite, Sexualite (French) 1993;21:861.

Crosfill ML, Widdicombe JG. Physical characteristics of the chest and lungs and the work of breathing in different mammalian species. J Physiol (London) 1961;158:1. [PubMed: 13696595]

Crouch, EC.; Parks, WC. Comparative biochemistry and molecular biology of pulmonary connective tissues. In: Parent, RA., editor. Comparative Biology of the Normal Lung. Boca Raton, FL: CRC Press; 1992. p. 451

Crouse LJ, Cheirif J, Hanly DE, et al. Opacification and border delineation improvement in patients with suboptimal endocardial border definition in routine echocardiography: Results of the Phase III Albunex® Multicenter Trial. J Am Coll Cardiol 1993;22:1494. [PubMed: 8227810]

Crum LA. Tensile strength of water. Nature 1979;278:148.

Crum LA, Fowlkes JB. Acoustic cavitation generated by microsecond pulses of ultrasound. Nature 1986;319:52.

Crum LA, Roy RA, Dino MA, et al. Acoustic cavitation produced by microsecond pulses of ultrasound: A discussion of some selected results. J Acoust Soc Am 1992;91:1113. [PubMed: 1556312]

Cullinan JA, Fleischer AC, Kepple DM, et al. Sonohysterography: A technique for endometrial evaluation. Radiographics 1995;15:501. [PubMed: 7624559]

Curtis, JC. Action of intense ultrasound on the intact mouse liver. In: Kelly, E., editor. Ultrasonic Energy. Champaign-Urbana, IL: University of Illinois Press; 1965. p. 85

Dalecki D, Carstensen EL, Parker KJ, et al. Absorption of finite amplitude focused ultrasound. J Acoust Soc Am 1991;89:2435. [PubMed: 1861004]

Dalecki D, Child SZ, Raeman CH, et al. Age dependence of ultrasonically induced lung hemorrhage in mice. Ultrasound Med Biol 1997a;23:767. [PubMed: 9253825]

Dalecki D, Child SZ, Raeman CH, et al. Tactile perception of ultrasound. J Acoust Soc Am 1995a; 97:3165. [PubMed: 7759656]

Dalecki D, Child SZ, Raeman CH, et al. Thresholds for fetal hemorrhages produced by a piezoelectric lithotriper. Ultrasound Med Biol 1997b;23:287. [PubMed: 9140185]

Dalecki D, Child SZ, Raeman CH, et al. Ultrasonically induced lung hemorrhage in young swine. Ultrasound Med Biol 1997c;23:777. [PubMed: 9253826]

Dalecki D, Keller BB, Raeman CH, et al. Effects of pulsed ultrasound on the frog heart: I. Thresholds for changes in cardiac rhythm and aortic pressure. Ultrasound Med Biol 1993a;19:385. [PubMed: 8356782]

Dalecki D, Raeman CH, Carstensen EL. Effects of pulsed ultrasound on the frog heart: II. An investigation of heating as a potential mechanism. Ultrasound Med Biol 1993b;19:391. [PubMed: 8356783]

Dalecki D, Raeman CH, Child SZ, et al. A test for cavitation as a mechanism for intestinal hemorrhage in mice exposed to a piezoelectric lithotripter. Ultrasound Med Biol 1996;22:493. [PubMed: 8795176]

Dalecki D, Raeman CH, Child SZ, et al. Hemolysis *in vivo* from exposure to pulsed ultrasound. Ultrasound Med Biol 1997d;23:301.

Dalecki D, Raeman CH, Child SZ, et al. Intestinal hemorrhage from exposure to pulsed ultrasound. Ultrasound Med Biol 1995b;21:1067. [PubMed: 8553501]

Dalecki D, Raeman CH, Child SZ, et al. Remnants of Albunex® nucleate acoustic cavitation. Ultrasound Med Biol 1997e;23:1405. [PubMed: 9428139]

Dalecki D, Raeman CH, Child SZ, et al. The influence of contrast agents on hemorrhage produced by lithotripter fields. Ultrasound Med Biol 1997f;23:1435. [PubMed: 9428143]

Dalecki D, Raeman CH, Child SZ, et al. Effects of pulsed ultrasound on the frog heart: III. The radiation force mechanism. Ultrasound Med Biol 1997g;23:275. [PubMed: 9140184]

Dalecki D, Raeman CH, Child SZ, et al. Thresholds for intestinal hemorrhage in mice exposed to a piezo-electric lithotripter. Ultrasound Med Biol 1995c;21:1239. [PubMed: 8849838]

D'Arrigo JS, Imae T. Physical characteristics of ultra-stable lipid-coated microbubbles. J Colloid Interface Sci 1992;149:592.

Degenhardt E, Jibril S, Gohde M, et al. Ambulatory contrast hysterosonography as a possibility for assessing tubal patency. (German) Geburtshilfe Frauenheilkd 1995;55:143.

Deichert V, Schlief R, van de Sandt M, et al. Transvaginal hystero-contrast-sonography (Hy-Co-Sy) compared with conventional tubal diagnostics. Hum Reprod 1989;4:418. [PubMed: 2526153]

Deichert V, van de Sandt M, Lauth G, et al. Transvaginal hysterosonography. A new diagnostic procedure for differentiating intrauterine and myometrial findings. Geburstshilfe Frauenheilkd 1988;48:835.

de Jong N. Improvements in ultrasound contrast agents. IEEE Eng Med Biol Mag 1996;15:72.

de Jong N, Hoff L, Skotland T, et al. Absorption and scatter of encapsulated gas filled microspheres: Theoretical considerations and some measurements. Ultrasonics 1992;30:95. [PubMed: 1557838]

de Jong N, Hoff L. Ultrasound scattering properties of Albunex® microspheres. Ultrasonics 1993;31:175. [PubMed: 8484195]

de Jong N, Ten Cate FJ, Lancee CT, et al. Principles and recent developments in ultrasound contrast agents. Ultrasonics 1991;29:324. [PubMed: 2058051]

Delius M, Brendel W, Heine G. A mechanism of gall-stone destruction by extracorporeal shock wave. Naturwissenschaften 1988a;75:200. [PubMed: 3398924]

Delius M, Denk R, Berding C, et al. Biological effects of shock waves: Cavitation by shock waves in piglet liver. Ultrasound Med Biol 1990;16:467. [PubMed: 2238253]

Delius M, Draenert K, Aldiek Y, et al. Biological effects of shock-waves—*In vivo* effects of high-energy pulses on rabbit bone. Ultrasound Med Biol 1995;21:1219. [PubMed: 8849836]

Delius M, Enders G, Xuan Z, et al. Biological effects of shock waves: Kidney damage by shock waves in dogs—dose dependence. Ultrasound Med Biol 1988b;14:117. [PubMed: 3347964]

Delius M, Hoffman E, Steinbeck G, et al. Biological effects of shock waves—Induction of arrhythmia in piglet hearts. Ultrasound Med Biol 1994;20:279. [PubMed: 8059489]

Delius M, Jordan M, Eizenhoefer H, et al. Biological effects of shock waves: Kidney hemorrhage by shock waves in dogs—administration rate dependence. Ultrasound Med Biol 1988c;14:689. [PubMed: 3212839]

Denbow ML, Blomley MJK, Cosgrove DO, et al. Ultrasound microbubble contrast angiography in monochorionic twins. Lancet 1997;349:773. [PubMed: 9074579]

Deng CX, Xu Q, Apfel RE, et al. *In vitro* measurements of inertial cavitation thresholds in human blood. Ultrasound Med Biol 1996;22:939. [PubMed: 8923712]

Devin C. Survey of thermal, radiation, and viscous damping of pulsating air bubbles in water. J Acoust Soc Am 1959;31:1654.

Dittrich HC, Bales GL, Hunt RM, et al. Multiple organ tissue perfusion by intravenously (IV) administered novel ultrasound contrast agents in dogs. J Ultrasound Med 1994;13:S9.

Dittrich HC, Bales GL, Kuvelas T, et al. Myocardial contrast echocardiography in experimental coronary artery occlusion with a new intravenously administered contrast agent. J Am Soc Echocardiogr 1995a;8:465. [PubMed: 7546782]

Dittrich HC, Kuvelas T, Dadd K, et al. Safety and efficacy of the ultrasound contrast agent FS069 in normal humans: Results of a phase one trial. Circulation 1995b;92:1.

Doida Y, Miller MW. Failure to confirm an increase in unscheduled DNA synthesis in sonicated mammalian cells *in vitro*. Ultrasonics 1992;30:35. [PubMed: 1729774]

Doida Y, Miller MW, Cox C, et al. Confirmation of an ultrasound-induced mutation in two *in vitro* mammalian cell lines. Ultrasound Med Biol 1990;16:699. [PubMed: 2281558]

Dooley DA, Sacks PG, Miller MW. Production of thymine base damage in ultrasound exposed EMT6 mouse mammary sarcoma cells. Radiat Res 1984;97:71. [PubMed: 6695045]

Duarte LR. The stimulation of bone growth by ultrasound. Arch Orthop Trauma Surg 1989;101:153. [PubMed: 6870502]

Duck, F. Estimating *in situ* exposure in the presence of acoustic nonlinearities. In: Edmonds, P., editor. American Institute of Ultrasound in Medicine Workshop on Effects of Nonlinear Propagation on Output Display Indices (TI and MI), Abstracts and Handouts, Boston, March 20, 1998. Laurel, MD: American Institute of Ultrasound in Medicine; 1998. Chair

Duck FA, Martin K. Trends in diagnostic ultrasound exposure. Phys Med Biol 1991;36:1423. [PubMed: 1754612]

Duck FA, Starritt HC, Aindow JD, et al. The output of pulse-echo ultrasound equipment: A survey of powers, pressures and intensities. Br J Radiol 1985;58:989. [PubMed: 3916078]

Duck FA, Starritt HC, Anderson SP. A survey of the acoustic output of ultrasonic, Doppler equipment. Clinical Physics and Physiological Measurement 1987;8:39. [PubMed: 3555969]

Dújic Z, Eterovic D, Denoble P, et al. Effect of a single air dive on pulmonary diffusing capacity in professional divers. J Appl Physiol 1993;74:55. [PubMed: 8444735]

Dunnill MS. Postnatal growth of the lung. Thorax 1962;17:329.

Dyson M, Brookes M. Stimulation of bone repair by ultrasound. Ultrasound: 1982 Proceedings of the Third Meeting of the World Federation of Ultrasound in Medicine and Biology, Brighton England, July 1982. Ultrasound Med Biol 1982;8(Supplement 1):50.

Dyson M, Woodward B, Pond JB. Flow of red blood cells stopped by ultrasound. Nature (London) 1971;232:572. [PubMed: 4937504]

Eckenhoff RG, Olstad CS, Carrod G. Human dose-response relationship for decompression and endogenous bubble formation. J Appl Physiol 1990;69:914. [PubMed: 2246178]

Edmonds, P. American Institute of Ultrasound in Medicine Workshop on Effects of Nonlinear Propagation on Output Display Indices (TI and MI), Abstracts and Handouts, Boston, March 20, 1998. Laurel, MD: American Institute of Ultrasound in Medicine; 1998. Chair

Eisenmenger W. Dynamic properties of the surface tension of water and aqueous solutions of surface active agents with standing capillary waves in the frequency range from 10 kc/s to 1.5 Mc/s. Acustica 1959;9:327.

Ellwart JW, Brettel H, Kober LO. Cell membrane damage by ultrasound at different cell concentrations. Ultrasound Med Biol 1988;14:43. [PubMed: 3347962]

Endl E, Steinbach P, Hofstadter F. Flow cytometric analysis of cell suspensions exposed to shock waves in the presence of the radical sensitve dye hydroethidine. Ultrasound Med Biol 1995;21:569. [PubMed: 7571150]

Everbach EC, Makin IRS, Azadniv M, et al. Correlation of ultrasound-induced hemolysis with cavitation detector output *in vitro*. Ultrasound Med Biol 1997;23:619. [PubMed: 9232771]

Everbach EC, Makin IRS, Francis C, et al. Effect of acoustic cavitation on platelets in the presence of an echo-contrast agent. Ultrasound Med Biol 1996a;24:125.

Everbach EC, Makin IRS, Porter TR, et al. Acoustic emissions of a fluorocarbon echo-contrast agent undergoing inertial cavitation. Circulation 1996b;94:1.

Feinstein SB, Cheirif J, Ten Cate FJ, et al. Safety and efficacy of a new transpulmonary ultrasound contrast agent: Initial multicenter clinical results. J Am Coll Cardiol 1990;16:316. [PubMed: 2197312]

Feinstein SB, Keller MW, Kerber RE, et al. Sonicated echocardiographic contrast agents: Reproducibility studies. J Am Soc Echocardiogr 1989;2:125. [PubMed: 2629861]

Fischer JE, Acuff-Smith K-D, Schilling MA, et al. Teratologic evaluation of rats prenatally exposed to pulsed-wave ultrasound. Teratology 1994;49:150. [PubMed: 8016746]

Flynn HG. Cavitation dynamics, I. A mathematical formulation. J Acoust Soc Am 1975;57:1379.

Flynn HG. Generation of transient cavities in liquids by microsecond pulses of ultrasound. J Acoust Soc Am 1982;72:1926.

Flynn, HG. Physics of acoustic cavitation in liquids. In: Mason, WP., editor. Physical Acoustics. 1B. New York, New York: Academic Press; 1964. p. 57

Flynn H, Church CC. Transient pulsations of small gas bubbles in water. J Acoust Soc Am 1988;84:985.

Food and Drug Administration. Diagnostic Ultrasound Guidance for 1993 [February 17, 1993, Revised 510(k)]. Rockville, MD: Center for Devices and Radiological Health, Food and Drug Administration, US Department of Health and Human Services; 1993.

Food and Drug Administration. Use of Mechanical Index in Place of Spatial Peak, Pulse Average Intensity in Determining Substantial Equivalence. Rockville, MD: Center for Devices and Radiological Health, Food and Drug Administration, US Department of Health and Human Services; 1994.

Forsberg F, Liu JB, Merton DA, et al. Contrast injection with and without hypobaric activation. J Ultrasound Med 1996;15:S19.

Forsberg F, Liu JB, Merton DA, et al. Parenchymal enhancement and tumor visualization using a new sonographic contrast agent. J Ultrasound Med 1995;14:949. [PubMed: 8583531]

Fowlkes JB, Crum LA. Cavitation threshold measurements for microsecond pulses of ultrasound. J Acoust Soc Am 1988;83:2190. [PubMed: 3411016]

Fox FE, Herzfield KF. Gas bubbles with organic skin as cavitation nuclei. J Acoust Soc Am 1954;26:984.

Francis CW, Önundarson PT, Carstensen EL, et al. Enhancement of fibrinolysis *in vitro* by ultrasound. J Clin Invest 1992;90:2063. [PubMed: 1430229]

Fritzsch T, Hilmann J, Kämpfe M, et al. SHU 508, a transpulmonary echocontrast agent. Invest Radiol 1990;25:S160. [PubMed: 2283240]

Fritzsch T, Schartl M, Siegert J. Preclinical and clinical results with an ultrasonic contrast agent. Invest Radiol 1988;23:S302. [PubMed: 3058634]

Frizzell LA. Threshold dosages for damage to mammalian liver by high intensity focused ultrasound. IEEE Trans Ultrasonics, Ferroelectrics, and Frequency Control 1988;35:578.

Frizzell LA, Carstensen EL, Dyro J. Shear properties of mammalian tissues at low megaHertz frequencies. J Acoust Soc Am 1976;60:1409. [PubMed: 1010892]

Frizzell LA, Chen E, Lee C. Effects of pulsed ultrasound on the mouse neonate: Hind limb paralysis and lung hemorrhage. Ultrasound Med Biol 1994;20:53. [PubMed: 8197627]

Frizzell LA, Lee CS, Aschenbach PD, et al. Involvement of ultrasonically induced cavitation in the production of hind limb paralysis of the mouse neonate. J Acoust Soc Am 1983;74:1062. [PubMed: 6630721]

Fry FJ, Kossof G, Eggleton RC, et al. Threshold ultrasonic dosages for structural changes in mammalian brain. J Acoust Soc Am 1970;48:1413. [PubMed: 5489906]

Fry WJ. Action of ultrasound on nerve tissue—A review. J Acoust Soc Am 1953;25:1.

Fu Y-K, Kaufman GE, Miller MW, et al. Modification by cysteamine of ultrasound lethality to Chinese hamster V-79 cells. Radiat Res 1979;80:575. [PubMed: 515353]

Fu Y-K, Miller MW, Griffiths TD, et al. Ultrasound lethality to synchronous and asynchronous Chinese hamster V-79 cells. Ultrasound Med Biol 1980;6:39. [PubMed: 6989076]

Fujiwaki S, Saito J, Horikoshi H, et al. Diagnosis of intrauterine disorders by sonohysterography. (Japanese) Acta Obstet Gynaecol Jpn 1995;47:437.

Galiuto L, Marchese A, Cavallari D, et al. Evaluation of postinfarction viable myocardium at jeopardy by dobutamine echocardiography and myocardial contrast echocardiography. Echocardiography 1994;11:337.

Ganong, WF., editor. Review of Medical Physiology. Los Altos, CA: Lange Medical Publications; 1967. Respiration; p. 514

Gaucherand P, Piacenza JM, Salle B, et al. Sonohysterography of the uterine cavity: Preliminary investigations. J Clin Ultrasound 1995;23:339. [PubMed: 7673449]

Gavrilov LR, Tsirulnikov EM, Davies I. Application of focused ultrasound for the stimulation of neural structures. Ultrasound Med Biol 1996;22:179. [PubMed: 8735528]

Geldhof AA, DeVoogt HJ, Rao BR. High energy shock waves do not affect either primary tumor growth or metastasis of prostate carcinoma, R-3327-MatLyLu. Urol Res 1989;17:9. [PubMed: 2922893]

Georgiadis D, Baumgartner RW, Karatschai R, et al. Further evidence of gaseous embolic material in patients with artificial heart valves. J Thorac Cardiovasc Surg 1998;115:808. [PubMed: 9576214]

Glen SK, Georgiadis D, Grosset DG, et al. Transcranial Doppler ultrasound in commercial air divers: A field study including cases with right-to-left shunting. Undersea Hyperb Med 1995;22:129. [PubMed: 7633274]

Goldberg BB. Ultrasound contrast agents. Clin Diagn Ultrasound 1993a;28:35. [PubMed: 8476645]

Goldberg BB, Liu JB, Burns PN, et al. Galactose-based intravenous sonographic contrast agent: Experimental studies. J Ultrasound Med 1993b;12:463. [PubMed: 8411330]

Goldberg BB, Liu JB, Forsberg F. Ultrasound contrast agents: A review. Ultrasound Med Biol 1994;20:319. [PubMed: 8085289]

Goldstein SR. Saline infusion sonohysterography. Clin Obstet Gynaecol 1996;39:248.

Gramiak R, Shah PM. Echocardiography of the aortic root. Invest Radiol 1968;3:356. [PubMed: 5688346]

Grauer SE, Xu J, Gong Z, et al. Aerosomes™ MRX115 produces myocardial opacification without hemodynamic effects after intravenous injections in primates. Circulation 1995;92:1. [PubMed: 7788902]

Grauer SE, Xu J, Pantely GA, et al. MRX 115, an echocardiographic contrast agent, produces myocardial opacification after intravenous injection in primates: Studies before and after occlusion of the left anterior descending coronary artery. Acad Radiol 1996;3:S405. [PubMed: 8796615]

Grayburn PA, Erickson JM, Escobar J, et al. Peripheral intravenous myocardial contrast echocardiography using a 2% dodecafluoropentane emulsion: Identification of myocardial risk area and infarct size in the canine model of ischemia. J Am Coll Cardiol 1995;26:1340. [PubMed: 7594052]

Hansen BW. High-speed photographic studies of droplet formation at 20 kHz ultrasonic atomization of oil. Ultrasonics 1970;8:97.

Harpaz D, Chen X, Francis CW, et al. Ultrasound enhancement of thrombolysis and reperfusion *in vitro*, J Am Coll Cardiol 1993;21:1507. [PubMed: 8473663]

Harrison GH, Balcer-Kubiczek EK, Eddy HA. Potentiation of chemotherapy by low-level ultrasound. Int J Radiat Biol 1991;59:1453. [PubMed: 1677389]

Harrison GH, Eddy HA, Wang JP, et al. Microscopic lung alterations and reduction of respiration rate in insonated anesthetized swine. Ultrasound Med Biol 1995;21:981. [PubMed: 7491752]

Hartman C, Child SZ, Mayer R, et al. Lung damage from exposure to the fields of an electrohydraulic lithotripter. Ultrasound Med Biol 1990;16:675. [PubMed: 2281556]

Harvey EN, Barnes DK, McElroy WD, et al. Bubble formation in animals I: Physical factors. J Cell Comp Physiol 1944;24:1.

Harvey EN, Loomis L. High frequency sound waves of small intensity and their biological effects. Nature 1928;121:622.

Harvey, W.; Dyson, M.; Pond, JB., et al. The *in vitro* stimulation of protein synthesis in human fibroblasts by therapeutic levels of ultrasound. In: Kazner, E.; de Vlieger, M.; Muller, HR.; McCready, VE., editors. Proceedings of the Second European Congress on Ultrasonics in Medicine. Excerpta Medica International Congress series no. 363; Amsterdam, Excerpta Medica Foundation. 1982. p. 10-21.

Hawgood S, Shiffer K. Structures and properties of the surfactant-associated proteins. Annu Rev Physiol 1991;53:375. [PubMed: 2042965]

Heckman JD, Ryaby JP, McCabe J, et al. Acceleration of tibial fracture-healing by non-invasive, low-intensity pulsed ultrasound. J Bone Joint Surg [Am] 1994;76:26.

Henglein A. Sonochemistry: Historical developments and modern aspects. Ultrasonics 1987;25:6.

Henglein A, Kormann C. Scavenging of OH radicals produced in the sonolysis of water. Int J Radiat Biol 1985;48:251.

Herbertz J. Spontaneous cavitation in liquids free of nuclei. Fortschritte der Akustik DAGA 1988;14:439.

Hildebrandt, J.; Young, AC. Anatomy and physics of respiration. In: Ruch, TC.; Patton, HD., editors. Physiology and Biophysics. 19. Philadelphia, PA: W.B. Saunders; 1966. p. 733

Hislop A, Howard S, Fairweather DV. Morphometric studies on the structural development of the lung in Macaca fasicularis during fetal and postnatal life. J Anat 1984;138:95. [PubMed: 6706842]

Holland CK, Apfel RE. An improved theory for the prediction of microcavitation thresholds. IEEE Trans Ultrasonics, Ferroelectrics, and Frequency Control 1989;36:204.

Holland CK, Apfel RE. Thresholds for transient cavitation in a controlled nuclei environment. J Acoust Soc Am 1990;88:2059. [PubMed: 2269722]

Holland CK, Deng CX, Apfel RE, et al. Direct evidence of cavitation *in vivo* from diagnostic ultrasound. Ultrasound Med Biol 1996;22:917. [PubMed: 8923710]

Holland CK, Roy RA, Apfel RE, et al. *In vitro* detection of cavitation induced by a diagnostic ultrasound system. IEEE Trans Ultrasonics, Ferroelectrics, and Frequency Control 1992;39:95.

Holland CK, Sandstrom K, Zheng X, et al. The acoustic field of a pulsed Doppler diagnostic ultrasound system near a pressure-release surface. J Acoust Soc Am 1994;95:2855.

Hong AS, Chae JS, Dublin SB, et al. Ultrasonic clot dissolution: An *in vitro* study. Am Heart J 1990;2:418. [PubMed: 2382618]

Hoshi S, Orikasa S, Kuwahara M-A, et al. High energy shock wave treatment on implanted urinary bladder cancer in rabbits. J Urol 1991;146:439. [PubMed: 1649927]

Howard D, Sturtevant B. *In vitro* study of the mechanical effects of shock-wave lithotripsy. Ultrasound Med Biol 1997;23:1107. [PubMed: 9330454]

Huber P, Debus P, Peschke P, et al. *In vivo* detection of ultrasonically induced cavitation by a fibre-optic technique. Ultrasound Med Biol 1994;20:811. [PubMed: 7863570]

Hug O, Pape R. Nachweis der Ultraschallkavitation in Gewebe. Strahlentherapies 1954;94:79.

Hynynen K. The threshold for thermally significant cavitation in dog's thigh muscle *in vivo*. Ultrasound Med Biol 1991;17:157. [PubMed: 2053212]

Hynynen K, Chung AH, Colucci V, et al. Potential adverse effects of high-intensity ultrasound exposure on blood vessels *in vivo*. Ultrasound Med Biol 1996;22:193. [PubMed: 8735529]

Inoue M, Church CC, Brayman AA, et al. Confirmation of the protective effect of cysteamine in *in vitro* ultrasound exposure. Ultrasonics 1989;27:362. [PubMed: 2815407]

Inoue M, Miller MW, Church CC. An alternative explanation for a postulated non-thermal non-cavitational ultrasound mechanism of action on *in vitro* cells at hyperthermic temperature. Ultrasonics 1990;28:185.

Ishimaru, A. Wave Propagation and Scattering in Random Media. New York, NY: Academic Press; 1978.

Ito H, Tomooka T, Sakai N, et al. Lack of myocardial perfusion immediately after successful thrombolysis: A predictor of poor recovery of left ventricular function in anterior myocardial infarction. Circulation 1992;85:1699. [PubMed: 1572028]

Ivey JA, Gardner EA, Fowlkes JB, et al. Acoustic generation of intra-arterial contrast boluses. Ultrasound Med Biol 1995;21:757. [PubMed: 8571464]

Jakobsen JÅ, Egge TS, Abildgaard A, et al. Infusion in vascular and renal sonography. Acad Radiol 1996;3:S322. [PubMed: 8796593]

Jayaweera A, Edwards N, Glasheen WP, et al. *In vivo* myocardial kinetics of air-filled albumin microbubbles during myocardial contrast echocardiography. Comparison with radiolabeled red blood cells. Circ Res 1994;74:1157. [PubMed: 8187282]

Jeffers RJ, Feng RQ, Fowlkes JB, et al. Dimethyl-foramide as an enhancer of cavitation-induced cell lysis *in vitro*, J Acoust Soc Am 1995;97:669. [PubMed: 7860841]

Jones, HW.; Hoerr, NL.; Osol, A., editors. Blakiston's New Gould Medical Dictionary. 3. NY, New York: McGraw Hill; 1972.

Jones, JH.; Longworth, KE. Gas exchange at rest and during exercise in mammals. In: Parent, RA., editor. Comparative Biology of the Normal Lung. Boca Raton, FL: CRC Press; 1992. p. 271-308.

Kaps M, Schaffer P, Beller KD, et al. Phase I: Transcranial echo contrast studies in healthy volunteers. Stroke 1995;26:2048. [PubMed: 7482648]

Kaufman GE. Mutagenicity of ultrasound in cultured mammalian cells. Ultrasound Med Biol 1985;11:497. [PubMed: 4049568]

Kaufman GE, Miller MW, Griffiths TD, et al. Lysis and viability of cultured mammalian ceils exposed to 1 MHz ultrasound. Ultrasound Med Biol 1977;3:21. [PubMed: 919085]

Kaufman GE, Miller MW. Growth retardation in Chinese hamster V-79 cells exposed to 1 MHz ultrasound. Ultrasound Med Biol 1978;4:139. [PubMed: 734793]

Kaul S, Pandian N, Okada RD, et al. Contrast echocardiography in acute myocardial ischemia: I. *In vivo* determination of total left ventricular: Area at risk. J Am Coil Cardiol 1984;4:1272.

Kay, JM. Blood vessels of the lung. In: Parent, RA., editor. Comparative Biology of the Normal Lung. Boca Raton, FL: CRC Press; 1992. p. 163-174.

Kedar RP, Cosgrove D, McCready VR, et al. Microbubble contrast agent for color Doppler US: Effect on breast masses. Work in progress Radiology 1996;198:679.

Keller MW, Feinstein SB, Briller RA, et al. Automated production and analysis of echo contrast agents. J Ultrasound Med 1986;5:493. [PubMed: 3761412]

Keller MW, Feinstein SB, Watson DD. Successful left ventricular opacification following peripheral venous injection of sonicated contrast agent: An experimental evaluation. Am Heart J 1987;114:570. [PubMed: 3307360]

Kessel D, Jeffers RJ, Fowlkes JB, et al. Porphyrin-induced enhancement of ultrasound cytotoxicity. Int J Radiat Biol 1994;66:221. [PubMed: 8089632]

Killam AL, Greener Y, McFerran BA, et al. Lack of bio-effects of ultrasound energy after intravenous administration of FS069 (Optison™) in the anesthetized rabbit. J Ultrasound Med 1998;17:349. [PubMed: 9623471]

Kim HJ, Greenleaf JF, Kinnick RR, et al. Ultrasound-mediated transfection of mammalian cells. Hum Gene Ther 1996;7:1339. [PubMed: 8818721]

Kirton OC, DeHaven CB, Morgan JP, et al. Elevated imposed work of breathing masquerading as ventilator weaning intolerance. Chest 1995;108:1021. [PubMed: 7555113]

Klibanov AL, Ferrara KW, Hughes MS, et al. Direct video microscopic observation of the dynamic effects of medical ultrasound on ultrasound contrast microspheres. Investigative Radiology 1998;33:863. [PubMed: 9851820]

Kodama T, Takayama K. Dynamic behavior of bubbles during extracorporeal shock-wave lithotripsy. Ultrasound Med Biol 1998;24:723. [PubMed: 9695276]

Kondo T, Gamson J, Mitchell JB, et al. Free radical formation and cell lysis induced by ultrasound in the presence of different rare gases. Int J Radiat Biol 1988a;54:955. [PubMed: 2903892]

Kondo T, Kano E. Effect of free radicals induced by ultrasonic cavitation on cell killing. Int J Radiat Biol 1988b;54:475. [PubMed: 2900867]

Kondo T, Kano E. Enhancement of hyperthermic cell killing by non-thermal effect of ultrasound. Int J Radiat Biol 1987;51:157.

Kondo T, Lodaira T, Kano E. Free radical formation induced by ultrasound and its effects on strand breakage in DNA of cultured FM3A cells. Free Radic Res Common 1993;19:S193.

Kornowski R, Meltzer RS, Chernine A, et al. Does external ultrasound accelerate thrombolysis? Results from a rabbit model. Circulation 1994;89:339. [PubMed: 8281667]

Kremkau FW. Mechanical index rationale (Abstract). J Ultrasound Med 1991;10:S32.

Krishna PD, Newhouse VL. Second harmonic characteristics of the ultrasound contrast agents Albunex® and FS069. Ultrasound Med Biol 1997;23:453. [PubMed: 9160913]

Kristiansen TK. The effect of low power specifically programmed ultrasound on the healing time of fresh fractures using a Colles' model. J Orthop Trauma 1990;4:227.

Kudo S, Kinoshita H, Hirohashi K, et al. Preoperative localization of hepatomas by sonography with microbubbles of carbon dioxide. Am J Roentgenol 1994;163:1405. [PubMed: 7992737]

Kudo M, Tomita S, Tochio H, et al. Small hepatocellular carcinoma: Diagnosis with US angiography with intraarterial CO_2 microbubbles. Radiology 1992a;182:155. [PubMed: 1309216]

Kudo M, Tomita S, Tochio H, et al. Sonography with intraarterial infusion of carbon dioxide microbubbles (sonographic angiography): Value in differential diagnosis of hepatic tumors. Am J Roentgenol 1992b;158:65. [PubMed: 1309220]

Kuwahara M, Ioritani N, Kanube K, et al. Hyperechoic region induced by focused shock waves *in vitro* and *in vivo*: Possibility of acoustic cavitation bubbles. J Lithotr Stone Dis 1989;1:282.

Kwak HY, Panton RL. Tensile-strength of simple liquids predicted by a model of molecular-interactions. J Phys D Appl Phys 1985;18:647.

Lafay V, Boussuges A, Ambrosi P, et al. Doppler-echocardiography study of cardiac function during a 36 arm (3,650 kPa) human dive. Undersea Hyperb Med 1997;24:67. [PubMed: 9171465]

Lanza GM, Wallace KD, Scott MJ, et al. Thrombi/arteries: A novel site-targeted ultrasonic contrast agent with broad biomedical application. Circulation 1996;94:3334. [PubMed: 8989148]

Lauer CG, Burge R, Tang DB, et al. Effect of ultrasound on tissue-type plasminogen activator-induced thrombolysis. Circulation 1992;86:1257. [PubMed: 1394932]

Lee CS, Frizzell LA. Exposure levels for ultrasonic cavitation in the mouse neonate. Ultrasound Med Biol 1988;14:735. [PubMed: 3212840]

Lehmann JF, Herrick JF. Biologic reactions to cavitation, a consideration for ultrasonic therapy. Arch Phys Med Rehabil 1953;34:86. [PubMed: 13017801]

Liebeskind D, Bases R, Elequin F, et al. Diagnostic ultrasound: Effects on the DNA and growth patterns of animal cells. Radiology 1979a;131:177. [PubMed: 424580]

Liebeskind D, Bases R, Mendez F, et al. Sister chromatid exchanges in human lymphocytes after exposure to diagnostic ultrasound. Science 1979b;205:1273. [PubMed: 472742]

Liebeskind D, Padawer J, Wolley, et al. Diagnostic ultrasound time-lapse and transmission electron microscopic studies of cells insonated *in vitro*. Br J Cancer Suppl 1982;45:176. [PubMed: 6950757]

Litscher, G.; Schwarz, G.; Lenhard, H., et al. Biomed Tech (Berl). 42. 1997. Embolism detection in transcranial Doppler ultrasound-Most recent technical developments; p. 515

Loverock P, ter Haar G, Omerod MG, et al. The effect of ultrasound on the cytotoxicity of adriamycin. Br J Radiol 1990;63:542. [PubMed: 2390688]

Luo H, Steffen W, Cercek B, et al. Enhancement of thrombolysis by external ultrasound. Am Heart J 1993;125:1564. [PubMed: 8498294]

Macdonald, M.; Madsen, E. Nonlinear propagation in a liquid tissue-mimicking medium. In: Edmonds, P., editor. American Institute of Ultrasound in Medicine Workshop on Effects of Nonlinear Propagation on Output Display Indices (TI and MI), Abstracts and Handouts, Boston, March 20, 1998. Laurel, MD: American Institute of Ultrasound in Medicine; 1998. Chair

MacRobbie AG, Raeman CH, Child SZ, et al. Thresholds for premature contractions in murine hearts exposed to pulsed ultrasound. Ultrasound Med Biol 1997;23:761. [PubMed: 9253824]

Madanshetty SI, Roy RA, Apfel RE. Acoustic microcavitation: Its active and passive acoustic detection. J Acoust Soc Am 1991;90:1515. [PubMed: 1939908]

Makin IRS, Everbach EC, Porter T, et al. Comparison of cavitational activity of echocontrast agents filled with different gases. Circulation 1995;92 (Suppl I):1. [PubMed: 7788902]

Markus H. Transcranial Doppler detection of circulating cerebral emboli. A Review Stroke 1993;24:1246.

Maroulis GB, Parsons AK, Yeko TR. Hydrogynecography: A new technique enables vaginal sonography to visualize pelvic adhesions and other pelvic structures. Fertil Steril 1992;58:1073. [PubMed: 1426364]

Marsh JN, Hall CS, Hughes MS, et al. Broadband through transmission signal loss measurements of Albunex® at concentrations approaching *in vivo* doses. J Acoust Soc Am 1997;101:1155.

Mayer R, Schenk E, Child SZ, et al. Pressure threshold for shock wave induced renal hemorrhage. J Urol 1990;144:1505. [PubMed: 2231957]

Medwin H. Counting bubbles acoustically: A review. Ultrasonics 1977;15:7.

Meerbaum, S.; Meltzer, RS., editors. Echocardiography. Boston, MA: Kluwer/Martinus Nijhoff; 1989. Myocardial Contrast Two-Dimensional.

Meltzer, RS.; Roelandt, J., editors. Contrast Echocardiography. The Hague, The Netherlands: Martinus Nijhoff; 1982a.

Meltzer RS, Adsumelli R, Risher W, et al. Lack of lung hemorrhage in humans after intraoperative trans-esophageal echocardiography with ultrasound conditions similar to those causing lung hemorrhage in laboratory animals. J Am Soc Echocardiogr 1998;11:57. [PubMed: 9487470]

Meltzer, RS.; Porder, JB.; Porder, K. Ultrasound bioeffects, mechanisms, and safety. In: Siegel, R., editor. Ultrasound Angioplasty. Boston, MA: Kluwer Academic Publishers; 1986.

Meltzer RS, Schwarz KQ, Mottley JG, et al. Therapeutic cardiac ultrasound. Am J Cardiol 1991;67:422. [PubMed: 1825260]

Meltzer RS, Vermeulen HWJ, Valk NK, et al. New echocardiographic contrast agents: Transmission through the lungs and myocardial perfusion imaging. J Cardiovasc Ultrasonogr 1982b;1:277.

Mercer, RR.; Crapo, JP. Architecture of the acinus. In: Parent, RA., editor. Comparative Biology of the Normal Lung. Boca Raton, FL: CRC Press; 1992. p. 109-119.

Metzger-Rose C, Wright WH, Baker MR, et al. Effects of phospholipid-coated microbubbles (MRX-115) on the detection of testicular ischemia in dogs. Acad Radiol 1996;3:S314.

Meza M, Greener Y, Hunt R, et al. Myocardial contrast echocardiography: Reliable, safe, and efficacious myocardial perfusion assessment after intravenous injections of a new echocardiographic contrast agent. Am Heart J 1996;132:871. [PubMed: 8831379]

Mihran RT, Barnes FS, Wachtel H. Temporally specific modification of myelinated axon excitability *in vitro* following a single ultrasound pulse. Ultrasound Med Biol 1990;16:297. [PubMed: 2363236]

Miller DL. The influence of hematocrit on hemolysis by ultrasonically activated gas-filled micropores. Ultrasound Med Biol 1988;14:293. [PubMed: 3413902]

Miller DL, Bao S. The relationship of scattered subharmonic, 3.3 MHz fundamental and second harmonic signals to damage of monolayer cells by ultrasonically activated Albunex®. J Acoust Soc Am 1998a;103:1183. [PubMed: 9479770]

Miller DL, Geis RA. Enhancement of ultrasonically induced hemolysis by perfluorocarbon-based compared to air-based echo contrast agents. Ultrasound Med Biol 1998b;24:285. [PubMed: 9550187]

Miller DL, Geis RA. Gas-body-based contrast agent enhances vascular bioeffects of 1.09 MHz ultrasound on mouse intestine. Ultrasound Med Biol 1998c;24:1201. [PubMed: 9833589]

Miller DL, Geis RA. The interaction of ultrasonic heating and cavitation in vascular bioeffects on mouse intestine. Ultrasound Med Biol 1998d;24:123. [PubMed: 9483779]

Miller DL, Geis RA, Chrisler WB. Ultrasonicaliy induced hemolysis at high cell and gas body concentrations in a thin-disc exposure chamber. Ultrasound Med Biol 1997;23:625. [PubMed: 9232772]

Miller DL, Reese JA, Frazier ME. Single strand DNA breaks in human lymphocytes induced by ultrasound *in vitro*. Ultrasound Med Biol 1989;15:765. [PubMed: 2617724]

Miller DL, Thomas RM. Contrast agent gas-bodies enhance hemolysis induced by lithotripter shockwaves and high-intensity focused ultrasound in whole blood. Ultrasound Med Biol 1996a; 22:1089. [PubMed: 9004433]

Miller DL, Thomas RM. Frequency dependence of cavitation activity in a rotating tube exposure system compared to the Mechanical Index. J Acoust Soc 1993;93:3475.

Miller DL, Thomas RM. Heating as a mechanism for ultrasonically induced petechial hemorrhages in mouse intestine. Ultrasound Med Biol 1994;20:493. [PubMed: 7941106]

Miller DL, Thomas RM. Thresholds for hemorrhages in mouse skin and in intestine induced by lithotripter shock waves. Ultrasound Med Biol 1995a;21:249. [PubMed: 7571133]

Miller DL, Thomas RM. The role of cavitation in the induction of cellular DNA damage by ultrasound and lithotripter Shockwaves *in vitro*. Ultrasound Med Biol 1996b;22:681. [PubMed: 8865563]

Miller DL, Thomas RM. Ultrasound contrast agents nucleate inertial cavitation *in vitro*. Ultrasound Med Biol 1995b;21:1059. [PubMed: 8553500]

Miller DL, Thomas RM, Buschbom RL. Comet assay reveals DNA strand breaks induced by ultrasonic cavitation *in vitro*. Ultrasound Med Biol 1995c;21:841. [PubMed: 8571472]

Miller DL, Thomas RM, Frazier ME. Single strand breaks in CHO cell DNA induced by ultrasonic cavitation *In vitro*. Ultrasound Med Biol 1991b;17:401. [PubMed: 1949351]

Miller DL, Thomas RM, Frazier ME. Ultrasonic cavitation indirectly induces single strand breaks in DNA of viable cells *in vitro* by the action of residual hydrogen peroxide. Ultrasound Med Biol 1991 c;17:729. [PubMed: 1781077]

Miller DL, Thomas RM, Williams AR. Mechanisms for hemolysis by ultrasonic cavitation in the rotating exposure system. Ultrasound Med Biol 1991a;17:171. [PubMed: 2053213]

Miller DL, Williams AR. Bubble cycling as the explanation of the promotion of ultrasonic cavitation in a rotating tube exposure system. Ultrasound Med Biol 1989;15:641. [PubMed: 2815408]

Miller MW. Does ultrasound induce sister chromatid exchanges? Ultrasound Med Biol 1985;11:561. [PubMed: 3901464]

Miller MW, Azadniv M, Cox C, et al. Lack of induced increase in sister chromatid exchanges in human lymphocytes exposed to *in vivo* therapeutic ultrasound. Ultrasound Med Biol 1991;17:81. [PubMed: 2021016]

Miller MW, Azadniv M, Doida Y, et al. Effect of a stabilized microbubble contrast agent on CW ultrasound-induced red blood cell lysis *in vitro*. Echocardiography 1995;12:1.

Miller MW, Azadniv M, Petit SE, et al. Sister chromatid exchanges in Chinese hamster ovary cells exposed to high intensity pulsed ultrasound: Inability to confirm previous positive results. Ultrasound Med Biol 1989;15:255. [PubMed: 2741252]

Miller MW, Brayman AA. Comparative sensitivity of human erythrocytes and lymphocytes to sonolysis by 1 MHz ultrasound. Ultrasound Med Biol 1997;23:635. [PubMed: 9232773]

Miller MW, Church CC, Ciaravino V. Time lapse and microscopic examinations of insonated *in vitro* cells. Ultrasound Med Biol 1990;16:73. [PubMed: 2321316]

Miller MW, Miller DL, Brayman AA. A review of *in vitro* bioeffects of inertial ultrasonic cavitation from a mechanistic perspective. Ultrasound Med Biol 1996;22:1131. [PubMed: 9123638]

Mitri FF, Andronikov AD, Perpinyal S, et al. A clinical comparison of sonographic hydrotubation and hysterosalpingography. Br J Obstet Gynaecol 1991;98:1031. [PubMed: 1751435]

Miyoshi N, Misík V, Reisz P. Sonodynamic toxicity of gallium-porphyrin analogue ATX-70 in human leukemia cells. Radiat Res 1997;148:43. [PubMed: 9216617]

Mobley J, Marsh JN, Hall CS, et al. Broadband measurements of phase velocity in Albunex® suspensions. J Acoust Soc Am 1998;103:2145. [PubMed: 9566335]

Mor-Avi V, Robinson K, Shroff S, et al. Stability of Albunex® microspheres under ultrasonic irradiation: An *in vitro* study. J Am Soc Echocardiogr 1994;7:S29.

Morgan TR, Laudone VP, Heston WD, et al. Free radical production by high energy shock waves—Comparison with ionizing irradiation. J Urol 1988;139:186. [PubMed: 3275798]

Mulvagh SL, Foley DA, Aeschbacher BC, et al. Second harmonic imaging of an intravenously administered echocardiographic contrast agent: Visualization of coronary arteries and measurement to coronary blood flow. J Am Coll Cardiol 1996;27:1519. [PubMed: 8626968]

Nada T, Moriyasu F, Fujimoto M, et al. Gray scale enhancement of liver tumors using proteinacious microspheres (FS069). J Ultrasound Med 1995;14:S7.

National Council on Radiation Protection and Measurement. Biological Effects of Ultrasound: Mechanisms and Clinical Implications. Report No. 74. Bethesda, MD: National Council on Radiation Protection and Measurement; 1983.

Nilsson A-M, Odselius R, Roijer A. Pro- and antifibrinolytic effects of ultrasound on streptokinase-induced thrombolysis. Ultrasound Med Biol 1995;21:833. [PubMed: 8571471]

Nishioka T, Luo H, Fishbein MC, et al. Dissolution of thrombotic arterial occlusion by high intensity, low frequency ultrasound and dodecafluoropentane emulsion: An *in vitro* and *in vivo* study. J Am Coll Cardiol 1997;30:561. [PubMed: 9247533]

Nomura Y, Matsuda Y, Yabuuchi I, et al. Hepatocellular carcinoma in adenomatous hyperplasia: Detection with contrast-enhanced US with carbon dioxide microbubbles. Radiology 1993;187:353. [PubMed: 8386389]

Nyborg, WL. Acoustic streaming. In: Hamilton, MF.; Blackstock, DT., editors. Nonlinear Acoustics. San Diego, CA: Academic Press; 1997.

Nyborg, WL. Acoustic streaming. In: Mason, WP., editor. Physical Acoustics (Volume 1B). New York, NY: Academic Press; 1965. p. 265

Nyborg, WL. Physical principles of ultrasound. In: Fry, FJ., editor. Ultrasound: Its Application in Medicine and Biology. New York, NY: Elsevier; 1978.

O'Brien WD Jr, Zachary JF. Comparison of mouse and rabbit lung damage exposure to 30 kHz ultrasound. Ultrasound Med Biol 1994a;20:299.

O'Brien WD Jr, Zachary JF. Lung damage assessment from exposure to pulsed-wave ultrasound in the rabbit, mouse, and pig. IEEE Trans Ultrasonics, Ferroelectrics, and Frequency Control 1997;44:473.

O'Brien WD Jr, Zachary JF. Mouse lung damage from exposure to 30 kHz ultrasound. Ultrasound Med Biol 1994b;20:287.

O'Brien WD Jr, Zachary JF. Rabbit and pig lung damage from exposure to CW 30-kHz ultrasound. Ultrasound Med Biol 1996;22:345. [PubMed: 8783467]

Okura H, Yoshikawa J, Yoshida K, et al. Quantitation of left-to-right shunts in secundum atrial septal defect by two-dimensional contrast echocardiography with use of Albunex®. Am J Cardiol 1995;75:639. [PubMed: 7887400]

Olsson SB, Johansson B, Nilsson A-M, et al. Enhancement of thrombolysis by ultrasound. Ultrasound Med Biol 1994;20:375. [PubMed: 8085294]

Oosterhof GON, Cornel EB, Smits GAHJ, et al. The influence of high energy shock waves on the development of metastases. Ultrasound Med Biol 1996;22:339. [PubMed: 8783466]

Oosterhof GON, Smits GAHJ, de Ruyter AE, et al. *In vivo* effects of high energy shock waves on urological tumors: An evaluation of treatment modalities. J Urol 1990;144:785. [PubMed: 2388350]

Ophir J, Parker KJ. Contrast agents in diagnostic ultrasound. Ultrasound Med Biol 1989;15:319. [PubMed: 2669297]

Panigel, M.; Abramowicz, JS.; Miller, RK. Techniques: Biophysical methods for assessment of placental function. In: Rama Sastry, BV., editor. Placental Pharmacology. Boca Raton: Florida, CRC Press; 1996.

Parsons, AK.; Cullinan, JA.; Goldstein, SR., et al. Sonohysterography, sonosalpingography, and sonohysterosalpingography. A text-atlas of normal and abnormal findings. In: Fleischer, AC.; Manning, FA.; Jeanty, P., et al., editors. Sonography in Obstetrics and Gynecology. Principles and Practice. Stamford, CT: Appleton and Lange; 1996.

Parsons AK, Lense JJ. Sonohysterography for endormetrial abnormalities: Preliminary results. J Clin Ultrasound 1993;21:87. [PubMed: 8381140]

Patton CA, Harris GR, Phillips RA. Output levels and bioeffect indices from diagnostic ultrasound exposure data reported to the FDA. IEEE Trans Ultrasonics, Ferroelectrics, and Frequency Control 1994;41:353.

Penney DP, Schenk EA, Maltby K, et al. Morphologic effects of pulsed ultrasound in the lung. Ultrasound Med Biol 1993;19:127. [PubMed: 8516959]

Peters AJ, Coulam CB. Hysterosalpingography with color Doppler ultrasonography. Am J Obstet Gynecol 1991;164:1530. [PubMed: 2048599]

Pilla AA, Mont MA, Nusser PR. Non-invasive low-intensity pulsed ultrasound accelerates bone healing in the rabbit. J Orthop Trauma 1990;4:246. [PubMed: 2231120]

Pilmanis AA, Meissner FW, Olson RM. Left ventricular gas emboli in six cases of altitude-induced decompression sickness. Aviat Space Environ Med 1996;67:1092. [PubMed: 8908349]

Pinamonti S, Caruso A, Mazzeo V, et al. DNA damage from pulsed sonications of human leucocytes *in vitro*. IEEE Trans Ultrasonics, Ferroelectrics, and Frequency Control 1986;33:179.

Pinkerton, KE.; Gehr, P.; Crapo, JD. Architecture and cellular composition of the air-blood barrier. In: Parent, RA., editor. Comparative Biology of the Normal Lung. Boca Raton, FL: CRC Press; 1992. p. 121-128.

Plopper, CG.; Pinkerton, KE. Structural and cellular diversity of the mammalian respiratory system. In: Parent, RA., editor. Comparative Biology of the Normal Lung. Boca Raton, FL: CRC Press; 1992. p. 1-5.

Pohl EE, Rosenfeld EH, Pohl P. Effects of ultrasound on agglutination and aggregation of human erythrocytes *in vitro*. Ultrasound Med Biol 1995;21:711. [PubMed: 8525562]

Pohlhammer J, O'Brien WD Jr. Dependence of the ultrasonic scatter coefficient on collagen concentration in mammalian tissues. J Acoust Soc Am 1981;69:283. [PubMed: 7217526]

Porter TR, Iversen PL, Li S, et al. Interaction of diagnostic ultrasound with synthetic oligonucieotide-labeled perfluorocarbon-exposed sonicated dextrose albumin microbubbles. J Ultrasound Med 1996a;15:577. [PubMed: 8839405]

Porter TR, Kricsfeld A, Cheatham S, et al. The effect of ultrasound frame rate on perfluorocarbon-exposed sonicated dextrose albumin microbubble size and concentration when insonifying at different flow rates, transducer frequencies, and acoustic outputs. J Am Soc Echocardiogr 1997;10:593. [PubMed: 9282348]

Porter TR, LaVeen RF, Fox R, et al. Thrombolytic enhancement with perfluorocarbon-exposed sonicated dextrose albumin microbubbles. Am Heart J 1996b;132:964. [PubMed: 8892768]

Porter TR, Li S, Everbach EC. Direct *in vivo* recordings of cavitational activity within the anterior myocardium during intermittent and conventional harmonic imaging following intravenous ultrasound contrast (Abstract). J Am Coll Cardiol 1998a;31 (Suppl A):400A.

Porter TR, Li S, Hiser W, et al. Simultaneous assessment of wall motion and myocardial perfusion using a rapid acquisition intermittent harmonic imaging pulsing interval of 5–15 Hz following acute myocardial infarction and during stress echocardiography (Abstract). J Am Coll Cardiol 1998b;31 (Suppl A):123A.

Porter TR, Xie F. Visually discernible myocardial echocardiographic contrast after intravenous injection of sonicated dextrose albumin microbubbles containing high molecular weight, less soluble gases. J Am Coll Cardiol 1995a;25:509. [PubMed: 7829807]

Porter TP, Xie F, Kilzer K. A non-invasive method of visually assessing renal perfusion using a newly developed intravenous ultrasound contrast. J Am Coll Cardiol 1995b;26:246A.

Porter TR, Xie F, Kricsfeld A. Myocardial ultrasound contrast with intravenous perfluoropropane-enhanced sonicated dextrose albumin: Initial clinical experience in humans. J Am Coll Cardiol (Special Issue) 1995c;26:39A.

Porter TR, Xie F, Kricsfeld A, et al. Noninvasive identification of acute myocardial ischemia and reperfusion with contrast ultrasound using intravenous perfluoropropane-exposed sonicated dextrose albumin. J Am Coll Cardiol 1995d;26:33. [PubMed: 7797773]

Porter TR, Xie F, Li S, et al. Increased ultrasound contrast and decreased microbubble destruction rates using triggered ultrasound imaging. J Am Soc Echocardiogr 1996c;9:599. [PubMed: 8887861]

Prat F, Chapelon J-Y, el Fadil FA, et al. *In vivo* effects of cavitation alone or in combination with chemotherapy in a peritoneal carcinomatosis in the rat. Br J Cancer 1991;68:13. [PubMed: 8318402]

Prat F, Ponchon T, Berger F, et al. Hepatic lesions in the rabbit induced by acoustic cavitation. Gastroenterology 1991;100:1345. [PubMed: 2013379]

Prat F, Sibille A, Luccioni C, et al. Increased chemo-cytotoxicity to colon cancer cells by shock wave-induced cavitation. Gastroenterology 1994;106:937. [PubMed: 8143998]

Prentice D, Ahrens T. Pulmonary complications of trauma. Crit Care Nurs Q 1994;17:24. [PubMed: 8055358]

Quay SA. Ultrasound contrast agent development: Phase shift colloids. J Ultrasound Med 1994;13:S9.

Raeman CH, Child SZ, Carstensen EL. Timing of exposures in ultrasonic hemorrhage of murine lung. Ultrasound Med Biol 1993;19:507. [PubMed: 8236592]

Raeman CH, Child SZ, Dalecki D, et al. Damage to murine kidney and intestine from exposure to the fields of a piezoelectric lithotripter. Ultrasound Med Biol 1994;20:589. [PubMed: 7998379]

Raeman CH, Child SZ, Dalecki D, et al. Exposure-time dependence of the threshold for ultrasonically induced murine lung hemorrhage. Ultrasound Med Biol 1996;22:139. [PubMed: 8928311]

Raeman CH, Dalecki D, Child SZ, Meltzer RS, et al. Albunex® does not increase the sensitivity of the lung to pulsed ultrasound. Echocardiography 1997;14:553. [PubMed: 11174994]

Ramnarine KV, Nassiri DK, McCarthy A, et al. Effects of pulse ultrasound on embryonic development: An *in vitro* study. Ultrasound Med Biol 1998;24:575. [PubMed: 9651967]

Ramnarine KV, Nassiri DK, Pearce JM, et al. Estimation of *in situ* ultrasound exposure during obstetric examinations. Ultrasound Med Biol 1993;19:319. [PubMed: 8346606]

Reher P, Elbeshir el-NI, Harvey W, et al. The stimulation of bone formation *in vitro* by therapeutic ultrasound. Ultrasound Med Biol 1997;23:1251. [PubMed: 9372573]

Richman TS, Viscomi EN, deCherney A. Fallopian tubal patency assessed by ultrasound following fluid injection. Radiology 1984;152:507. [PubMed: 6539931]

Riesz P, Kondo T. Free radical formation induced by ultrasound and its biological implications. J Free Radic Biol Med 1992;13:247.

Roach GW, Kanchuger M, Mangano CM, et al. Adverse cerebral outcomes after coronary bypass surgery. N Engl J Med 1996;335:1857. [PubMed: 8948560]

Rovai D, Lubrano V, Paterni M, et al. Left ventricular and myocardial opacification after intravenous injection of a novel ultrasound contrast agent: BR1. Eur Heart J 1995;16(S):91.

Roy RA, Atchley AA, Crurn LA, et al. A precise technique for the measurement of acoustic cavitation thresholds, and some preliminary results. J Acoust Soc Am 1985;78:1799. [PubMed: 4067082]

Roy RA, Madanshetty SI, Apfel RE. An acoustic backscattering technique for the detection of transient cavitation produced by microsecond pulses of ultrasound. J Acoust Soc Am 1990;87:2451. [PubMed: 2373791]

Saad, AH. PhD thesis. Manchester, England: University of Manchester; 1983. Some Biological Effects of Ultrasound.

Saad AH, Hahn GM. Ultrasound-enhanced drug toxicity on Chinese hamster ovary cells *in vitro*. Cancer Res 1989;49:5931. [PubMed: 2790808]

Saad AH, Hahn GM. Ultrasound-enhanced effects of Adriamycin against murine tumors. Ultrasound Med Biol 1992;18:715. [PubMed: 1440992]

Sabia PJ, Powers ER, Jayaweera AR, et al. Functional significance of collateral blood flow in patients with recent acute myocardial infarction: A study using myocardial contrast echocardiography. Circulation 1992a;85:2080. [PubMed: 1591827]

Sabia PJ, Powers ER, Ragosta M, et al. An association between collateral blood flow and myocardial viability in patients with recent myocardial infarction. N Engl J Med 1992b;327:1825. [PubMed: 1448120]

Sacks PG, Miller MW, Sutherland RM. Response of multicell spheroids to 1 MHz ultrasonic irradiation: Cavitation related damage. Radiat Res 1983;93:545. [PubMed: 6856756]

Sahebjami, H. Aging of the normal lung. In: Parent, RA., editor. Comparative Biology of the Normal Lung. Boca Raton, FL: CRC Press; 1992. p. 351-366.

Sandstrom, K. Challenges associated with characterizing and predicting acoustic fields in water. In: Edmonds, P., editor. American Institute of Ultrasound in Medicine Workshop on Effects of Nonlinear Propagation on Output Display Indices (TI and MI), Abstracts and Handouts, Boston, March 20, 1998. Laurel, MD: American Institute of Ultrasound in Medicine; 1998. Chair

Santoso T, Roelandt J, Mansyoer H, et al. Myocardial perfusion imaging in humans by contrast echocardiography using polygelin colloid solution. J Am Coll Cardiol 1985;6:612. [PubMed: 4031272]

Schaer GN, Koechli OR, Schuessler B, et al. Improvement in perineal sonographic bladder neck imaging with ultrasound contrast medium. Obstet Gynecol 1995;86:950. [PubMed: 7501346]

Schlief R, Schurman R, Niendorf HP. Basic properties and results of clinical trials of ultrasound contrast agents based on galactose. Ann Acad Med Singapore 1993;22:762. [PubMed: 8267359]

Schlief R, Staks T, Mahler M, et al. Successful opacification of the left heart chambers on echocardiographic examination after intravenous injection of a new saccharide based contrast agent. Echocardiography 1990;7:61. [PubMed: 10149193]

Schneider M, Arditi M, Barrau MB, et al. BR1: A new ultrasonographic contrast agent based on sulfur hexafluoride-filled microbubbles. Invest Radiol 1995;30:451. [PubMed: 8557510]

Schneider M, Broillet A, Arditi M, et al. Doppler intensitometry with BR1, a sonographic contrast agent. Acad Radiol 1996;3:S308. [PubMed: 8796588]

Schneider M, Bussat P, Barrau MB, et al. Polymeric microballoons as ultrasound contrast agents. Physical and ultrasonic properties compared with sonicated albumin. Invest Radiol 1992;27:134. [PubMed: 1376304]

Schrope BA, Newhouse VL. Second harmonic ultrasound blood perfusion measurement. Ultrasound Med Biol 1993;19:567. [PubMed: 8310553]

Schrope BA, Newhouse VL, Uhlendorf V. Simulated capillary blood flow measurement using a nonlinear ultrasonic contrast agent. Ultrason Imaging 1992;14:134. [PubMed: 1604755]

Schurmann R, Schlief R. Saccharide-based contrast agents. Characteristics and diagnostic potential. Radiol Med (Torino) 1994;87(5 Suppl 1):15. [PubMed: 8209013]

Schwarz KO, Becher H, Schimpfky C, et al. Doppler enhancement with SH U 508A in multiple vascular regions. Radiology 1994;193:195. [PubMed: 7916468]

Sehgal CM, Arger PH, Pugh CR. Sonographic enhancement of the renal cortex by contrast media. J Ultrasound Med 1995;14:741. [PubMed: 8544240]

Sehgal CM, LaVeen RF, Shalansky-Goldberg RD. Ultrasound-assisted thrombolysis. Invest Radiol 1993;28:939. [PubMed: 8262749]

Shastri KA, Logue GL, Lundgren CE, et al. Diving decompression fails to activate complement. Undersea Hyperb Med 1997;24:51. [PubMed: 9171463]

Shaw PJ, Bates D, Cartilidge NEF, et al. Neurologic and neuropsychological morbidity following major surgery: Comparison of coronary artery bypass and peripheral vascular surgery. Stroke 1987;18:700. [PubMed: 3496690]

Shung KK, Flenniken RR. Time-domain ultrasonic contrast blood flowmetry. Ultrasound Med Biol 1995;21:71. [PubMed: 7754580]

Shung, KK.; Smith, MB.; Tsui, BMW. Principles of Medical Imaging. San Diego, CA: Academic Press; 1992.

Shung, KK.; Thieme, GA. Ultrasonic Scattering in Biological Tissue. Boca Raton, FL: CRC Press; 1993.

Shung KK, Zipparo M. Ultrasonic transducers and arrays. IEEE Eng Med Biol Mag 1996;15:20.

Siddiqi TA, O'Brien WD Jr, Meyer RA, et al. *In situ* exposimetry: The ovarian ultrasound examination. Ultrasound Med Biol 1991;17:257. [PubMed: 1887511]

Simon, RH. The biology and biochemistry of pulmonary epithelial cells. In: Parent, RA., editor. Comparative Biology of the Normal Lung. Boca Raton, FL: CRC Press; 1992a. p. 545-564.

Simon RH, Ho SY, Lange SC, et al. Applications of lipid-coated microbubble contrast to tumor therapy. Ultrasound Med Biol 1993;19:123. [PubMed: 8516958]

Simon RH, Ho SY, Perkins CR, et al. Quantitative assessment of tumor enhancement by ultrastable lipid-coated microbubbles as a sonographic contrast agent. Invest Radiol 1992b;27:29. [PubMed: 1733877]

Singh, C.; Katyal, SL. Secretory proteins of clara cells and type ii cells. In: Parent, RA., editor. Comparative Biology of the Normal Lung. Boca Raton, FL: CRC Press; 1992. p. 93-108.

Skyba DM, Price RJ, Linka AZ, et al. Microbubble destruction by ultrasound results in capillary rupture: Adverse bioeffects or a possible mechanism for *in vivo* drug delivery? J Am Soc Echocardiogr 1998;11:497.

Smith MD, Elion JL, McClure RR, et al. Left heart opacification with peripheral venous injection of a new saccharide echo contrast agent in dogs. J Am Coll Cardiol 1989;13:1622. [PubMed: 2723275]

Smith MD, Kwan OL, Reiser J, et al. Superior intensity and reproducibility of SHU-454, a new right' heart contrast agent. J Am Coll Cardiol 1984;3:992. [PubMed: 6546768]

Smith, NB.; Vorhees, CV.; Meyer, A. Proceedings of the 1990 IEEE Ultrasonics Symposium. 1990. An automated ultrasonic exposure system to assess the effects of *in utero* diagnostic ultrasound; p. 1385-1388.

Smith PL, Treasure T, Newman SP, et al. Cerebral consequences of cardiopulmonary by pass. Lancet 1986;1:823. [PubMed: 2870314]

Solleder P, Beller KD, Linder R. BY963: A sonographic contrast medium. Acad Radiol 1996;3:S194. [PubMed: 8796560]

Sonne HS, Christensen PD, Muan B, et al. Left ventricular opacification after intravenous injection of Albunex®: The effect of different administration procedures. Int J Cardiac Imaging 1995;11:47.

Sotaniemi KA, Mononen H, Hokkanen TE. Long-term cerebral outcome after open-heart surgery. A five-year neuropsychological follow-up study. Stroke 1986;17:410. [PubMed: 3715937]

Starritt HC, Duck FA. Quantification of acoustic shock in routine exposure measurement. Ultrasound Med Biol 1992;18:513. [PubMed: 1509625]

Starritt HC, Duck FA, Humphrey VF. An experimental investigation of streaming in pulsed diagnostic ultrasound beams. Ultrasound Med Biol 1989;15:363. [PubMed: 2527429]

Stella M, Trevison L, Montaldi A, et al. Induction of sister-chromatid exchanges in human lymphocytes exposed *in vitro* and *in vivo* to therapeutic ultrasound. Mutat Res 1984;138:75. [PubMed: 6387479]

Stevenson D, Walther F, Long W, et al. Controlled trial of a single dose of synthetic surfactant at birth in premature infants weighting 500 to 699 grams. J Pediatr 1992;120:S3. [PubMed: 1735849]

Stonehill MA, Williams JC Jr, Bailey MR, et al. An acoustically matched high pressure chamber for control of cavitation in shock wave lithotripsy: Mechanisms of shock wave damage *in vitro*. Methods Cell Science 1998;19:303.

Suhr D, Brummer F, Irmer U, et al. Disturbance of cellular calcium homeostasis by *in vitro* application of shock waves. Ultrasound Med Biol 1996;22:671. [PubMed: 8865562]

Suhr D, Brummer F, Irmer U, et al. Reduced cavitation-induced cellular damage by the antioxidative effect of vitamin E. Ultrasonics 1994;32:301. [PubMed: 7517598]

Suneetha N, Kumar RP. Ultrasound-induced enhancement of ACH, ACHE and GABA in fetal brain tissue of mouse. Ultrasound Med Biol 1993;19:411. [PubMed: 8356785]

Suren A, Osmers R, Kulenkampff D, et al. Visualization of blood flow in small ovarian tumor vessel by transvaginal color Doppler sonography after echo enhancement with injection of Levovist. Gynecol Obstet Invest 1994;38:210. [PubMed: 8001878]

Szabo, T.; Grossman, C.; Clougherty, F. Tissue loss effects on acoustic output parameters. In: Edmonds, P., editor. American Institute of Ultrasound in Medicine Workshop on Effects of Nonlinear Propagation on Output Display Indices (TI and MI), Abstracts and Handouts, Boston, March 20, 1998. Laurel, MD: American Institute of Ultrasound in Medicine; 1998. Chair

Tachibana K. Enhancement of fibrinolysis with ultrasound energy. J Vasc Interv Radiol 1992;3:299. [PubMed: 1627877]

Tachibana K, Tachibana S. Albumin microbubble echo-contrast material as an enhancer for ultrasound accelerated thrombolysis. Circulation 1995;92:1148. [PubMed: 7648659]

Tachibana K, Tachibana S. Prototype therapeutic ultrasound emitting catheter for accelerating thrombolysis. J Ultrasound Med 1997;16:529. [PubMed: 9315208]

Tarantal AF, Canfield DR. Ultrasound-induced lung hemorrhage in the monkey. Ultrasound Med Biol 1994;20:65. [PubMed: 8197628]

Taylor GA, Ecklund K, Dunning PS. Renal cortical perfusion in rabbits: Visualization with color amplitude imaging and an experimental microbubble-based US contrast agent. Radiology 1996;210:125. [PubMed: 8816532]

Tei C, Sakamaki T, Shah P, et al. Myocardial contrast echocardiography: A reproducible technique of myocardial opacification for identifying regional perfusion deficits. Circulation 1983;67:585. [PubMed: 6821901]

Tenney SM, Remmers JE. Comparative quantitative morphology of the mammalian lung: Diffusing area. Nature 1963;197:54. [PubMed: 13980583]

ter Haar G, Daniels S. Evidence for ultrasonically induced cavitation *in vivo*. Phys Med Biol 1981;26:1145. [PubMed: 7323152]

Thorsen E, Risberg J, Segabdal K, et al. Effects of venous gas microemboli on pulmonary gas transfer function. Undersea Hyperb Med 1995;22:347. [PubMed: 8574122]

Trenchard PM. Ultrasound-induced orientation of discoid platelets and simultaneous changes in light transmission: Preliminary characterization of the phenomenon. Ultrasound Med Biol 1987;13:183. [PubMed: 3590365]

Tsirulnikov EM, Vartanyan IA, Gersurd GV, et al. Use of amplitude-modulated focused ultrasound for diagnosis of hearing disorders. Ultrasound Med Biol 1988;14:277. [PubMed: 3046092]

Tufecki EC, Girit S, Bayirli E. Evaluation of tubal patency by transvaginal sonosalpingography. Fertil Steril 1992;57:336. [PubMed: 1735485]

Tyler, WS.; Julian, MD. Gross and subgross anatomy of lungs, pleura, connective tissue septa, distal airways, and structural units. In: Parent, RA., editor. Comparative Biology of the Normal Lung. Boca Raton, FL: CRC Press; 1992. p. 37-47.

Uhlendorf V, Hoffmann C. Nonlinear acoustical response of coated microbubbles in diagnostic ultrasound. Cannes, France, IEEE Ultrasonics Symposium Proceedings 1994;3:1559.

Uhlendorf V, Scholle F-D. Imaging of spatial distribution and flow of microbubbles using nonlinear acoustic properties. Acoustic Imaging 1996;22:233.

Umemura, S.; Kawabata, K. 1993 IEEE Ultrasonics Symposium Proceedings; Enhancement of sonochemical reactions by second-harmonic superimposition; New York, NY. 1993. p. 917

Umemura S, Kawabata K, Sasaki K. *In vitro* and *in vivo* enhancement of sonodynamically active cavitation by second-harmonic superimposition. J Acoust Soc Am 1997;101:569. [PubMed: 9000745]

Umemura S, Yumita N, Nishigaki R, et al. Mechanism of cell damage by ultrasound in combination with hematoporphyrin. Jpn J Cancer Res 1990;81:962. [PubMed: 2172198]

Unger, E. Liposomes as myocardial imaging ultrasound contrast agents. Atlantic City, NJ. The Leading Edge in Diagnostic Ultrasound 1995 Conference, First Annual International Symposium of Contrast Agents in Diagnostic Ultrasound, sponsored by the Thomas Jefferson University and Jefferson Medical College; 1995a.

Unger, E. MRX-115 Aerosomes as ultrasound contrast agents for diagnostic radiology. Chicago, IL: Advances in Echocardiography Symposium; 1995b.

Unger EC, Lund PJ, Shen DK, et al. Nitrogen-filled liposomes as a vascular US contrast agent: Preliminary evaluation. Radiology 1992;185:453. [PubMed: 1410353]

Vakil N, Everbach EC. Transient acoustic cavitation in gallstone fragmentation: A study of gallstones fragmented *in vivo*. Ultrasound Med Biol 1993;19:331. [PubMed: 8346607]

Van Liew HD, Burkard ME. Behavior of bubbles of slowly permeating gas used for ultrasonic imaging contrast. Invest Radiol 1995a;30:315. [PubMed: 7558737]

Van Liew HD, Burkard ME. Bubbles in circulating blood: Stabilization and simulations of cyclic changes of size and content. J Appl Physiol 1995b;74:1379.

Van Roessel J, Wamsteker K, Exalto N. Sonographic investigation of the uterus during artificial uterine cavity distention. J Clin Ultrasound 1987;15:439. [PubMed: 2455739]

Vandenberg BF, Melton HG. Acoustic lability of albumin microspheres. J Am Soc Echocardiogr 1994;7:582. [PubMed: 7840985]

Veltri A, Capello S, Faissola B, et al. Dynamic contrast-enhanced ultrasound with carbon dioxide microbubbles as adjunct to arteriography of liver tumors. Cardiovasc Intervent Radiol 1994;17:133. [PubMed: 8087828]

Venezia R, Zangara C. Echohysterosalpingography: New diagnostic possibilities with SHU 450 Echovist. Acta Eur Fertil 1991;22:279. [PubMed: 1845751]

Veress E, Vincze J. The haemolysing action of ultrasound on erythrocytes. Acustica 1977;36:100.

Verrall, RE.; Seghal, CM. Sonoluminescence. In: Suslick, KS., editor. Ultrasound: Its Chemical, Physical and Biological Effects. New York, NY: VCH Publishers; 1988. p. 227

Villanueva F, Glasheen WP, Sklenar J, et al. Assessment of risk area coronary occlusion and infarct size after reperfusion with myocardial contrast echocardiography using left and right atrial injections of contrast. Circulation 1993;88:596. [PubMed: 8339423]

Villanueva F, Glasheen WP, Sklenar J, et al. Successful and reproducible myocardial opacification during two-dimensional echocardiography from right heart injection of contrast. Circulation 1992;85:1557. [PubMed: 1555293]

Vivino AA, Boraker DK, Miller D, et al. Stable cavitation at low ultrasonic intensities induces cell death and inhibits 3H-TdR incorporation by Con-A-stimulated murine lymphocytes *in vitro*. Ultrasound Med Biol 1985;11:751. [PubMed: 3877358]

Vladimirtseva AL, Manzhos PI. Effect of low-frequency ultrasound on the pleura and adjoining lung tissue. (Russian) Biull Eksp Biol Med 1986;102:102.

Voelkel, NF. Lung endothelial cell biology. In: Parent, RA., editor. Comparative Biology of the Normal Lung. Boca Raton, FL: CRC Press; 1992. p. 565-571.

Vogel J, Hopf C, Eysel P, et al. Application of extracorporeal shock-waves in the treatment of pseudarthrosis of the lower extremity. Preliminary results. Arch Orthop Trauma Surg 1997;116:480. [PubMed: 9352042]

Vorhees CV, Acuff-Smith KD, Schilling MA, et al. Behavior teratologic effects of prenatal exposure to continuous-wave ultrasound in unanesthetized rats. Teratology 1994;50:238. [PubMed: 7871488]

Vorhees CV, Acuff-Smith KD, Weisenburger WP, et al. A teratologic evaluation of continuous-wave, daily ultrasound exposure in unanesthetized rats. Teratology 1991;44:667. [PubMed: 1805437]

Wang S-J, Lewallen DG, Bolander ME, et al. Low intensity ultrasound treatment increases strength in a rat femoral fracture model. J Orthop Res 1994;12:40. [PubMed: 8113941]

Ward B, Baker AC, Humphrey VF. Nonlinear propagation applied to the improvement of resolution in diagnostic medical ultrasound. J Acoust Soc Am 1997;101:143. [PubMed: 9000731]

Watson, JW. Elastic, resistive, and inertial properties of the lung. In: Parent, RA., editor. Comparative Biology of the Normal Lung. Boca Raton, FL: CRC Press; 1992. p. 175-216.

Weaver LK, Morris A. Venous and arterial gas embolism associated with positive pressure ventilation. Chest 1998;113:1132. [PubMed: 9554661]

Weber C, Moran ME, Braun EJ, et al. Injury of rat renal vessels following extracorporeal shock wave treatment. J Urol 1992;147:476. [PubMed: 1732627]

Weibel, ER. Dimensions of the tracheobronchial tree and alveoli. In: Altman, PL.; Dittmer, DS., editors. Biological Handbooks: Respiration arid Circulation. Bethesda, MD: Federation of American Societies for Experimental Biology; 1971. p. 105

West, JB. Respiratory Physiology—The Essentials. 4. Baltimore, MD: Williams and Wilkins; 1990. p. 1

WFUMB (World Federation of Ultrasound in Medicine and Biology). WFUMB Symposium on Safety and Standardization in Medical Ultrasound. Conclusions and Recommendations Regarding Nonthermal Mechanisms for Biological Effects of Ultrasound. Ultrasound Med Biol 1998;24(Suppl 1)

Williams AR. Absence of meaningful thresholds for bioeffect studies on cell suspensions *in vitro*. Br J Cancer 1982;45:192.

Williams, AR. Ultrasound: Biological Effects and Potential Hazards. New York, NY: Academic Press; 1983.

Williams AR, Delius M, Miller DL, et al. Investigation of cavitation in flowing media by lithotripter shock waves both *in vitro* and *in vivo*. Ultrasound Med Biol 1989;15:53. [PubMed: 2922881]

Williams AR, Kubowicz G, Cramer E, et al. The effects of the microbubble suspension SH U 454 (Echovist®) on ultrasonically induced cell lysis in a rotating tube exposure system. Echocardiography 1991;8:423. [PubMed: 10149264]

Williams AR, Miller DL. The role of non-acoustic factors in the induction and proliferation of cavitational activity *in vitro*. Phys Med Biol 1989;34:1561. [PubMed: 2587627]

Wiison WL, Wiercinski FL, Nyborg WL, et al. Deformation and motion produced in isolated living cells by localized ultrasonic vibration. J Acoust Soc Am 1966;40:1363. [PubMed: 5975573]

Winkelmann JW, Kenner MD, Dave R, et al. Contrast echocardiography. Ultrasound Med Biol 1994;20:507. [PubMed: 7998371]

Wray RA, Zoghbi WA, Quinones MA, et al. Contrast echocardiography: Relation of acoustic power and time gain compensation to contrast intensity duration. J Am Soc Echocardiog 1992;4:286.

Wu J, Tong J. Experimental study of stability of contrast agents in an ultrasound field. Ultrasound Med Biol 1998a;24:257. [PubMed: 9550184]

Wu J, Tong J. Measurements of nonlinearity parameter B/A of contrast agents. Ultrasound Med Biol 1998b;24:153. [PubMed: 9483783]

Wu J, Zhu Z, Du G. Nonlinear behavior of a liquid containing uniform bubbles: Comparison between theory arid experiments. Ultrasound Med Biol 1995;21:545. [PubMed: 7571147]

Xavier, CAM.; Duarte, LR. Treatment of nonunions by ultrasound stimulation: First clinical applications. San Francisco, CA. Annual Meeting of the American Academy of Orthopaedic Surgeons; January 25, 1987;

Yang KH, Parvizi J, Wang SJ, et al. Exposure to low-intensity ultrasound increases aggrecan gene expression in a rat femur fracture model. J Orthopaed Res 1996;14:802.

Yarali H, Gurgan T, Erden A, et al. Color Doppler hys terosalpingosonography: A single and potentially useful method to evaluate fallopian tubal patency. Hum Reprod 1994;9:64. [PubMed: 8195353]

Yount DE. On the evolution, generation, and regeneration of gas cavitation nuclei. J Acoust Soc Am 1982;71:1473.

Yumita N, Nishigaki R, Umemura K, et al. Hematoporphyrin as a sensitizer of cell-damaging effect of ultrasound. Jpn J Cancer Res 1989;80:219. [PubMed: 2470713]

Yumita N, Nishigaki R, Umemura K, et al. Synergistic effect of ultrasound and hematoporphyrin on Sarcoma 180. Jpn J Cancer Res 1990;81:304. [PubMed: 2112531]

Yumita N, Sasaki K, Umemura S, et al. Sono-dynamically induced antitumor effect of gallium-porphyrin complex by focused ultrasound on experimental kidney tumor. Cancer Lett 1997;112:79. [PubMed: 9029172]

Zachary JF, O'Brien WD Jr. Lung lesion induced by continuous- and pulsed-wave (diagnostic) ultrasound in mice, rabbits, and pigs. Vet Pathol 1995;32:43. [PubMed: 7725597]

Zagzebski, JA. Essentials of Ultrasound Physics. St Louis, MO: CV Mosby; 1996.

Zhong P. Effects of tissue constraining on shock wave-induced bubble oscillation *in vivo*. J Acoust Soc Am 1998;103:3038.

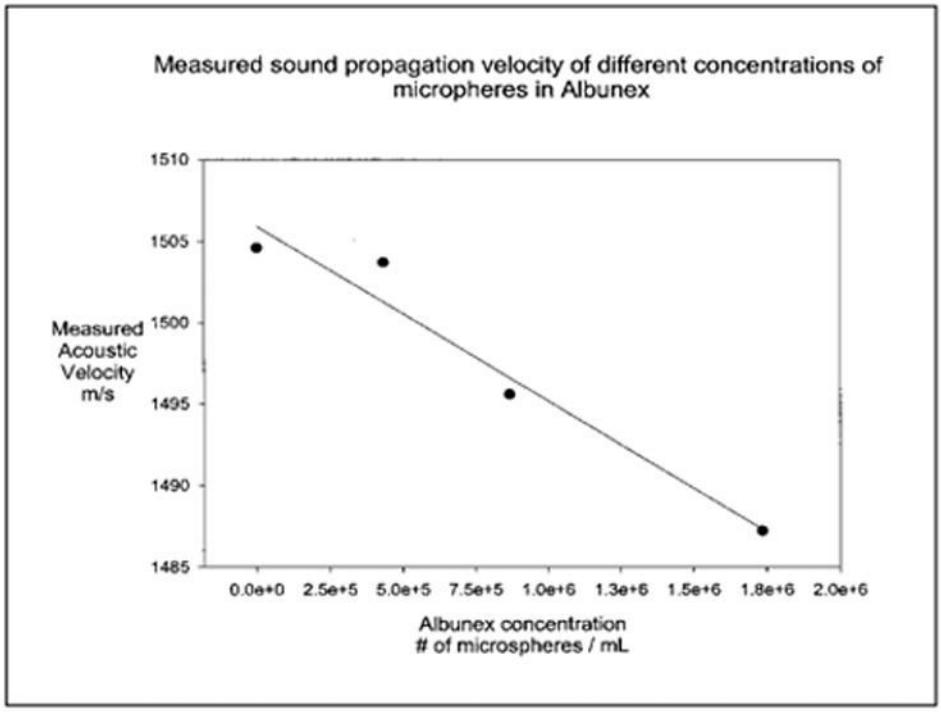

Figure 6-1.
Sound velocity in an Albunex suspension as a function of concentration. The solid circles and the line represent the data points and the least squares regressions line, respectively.

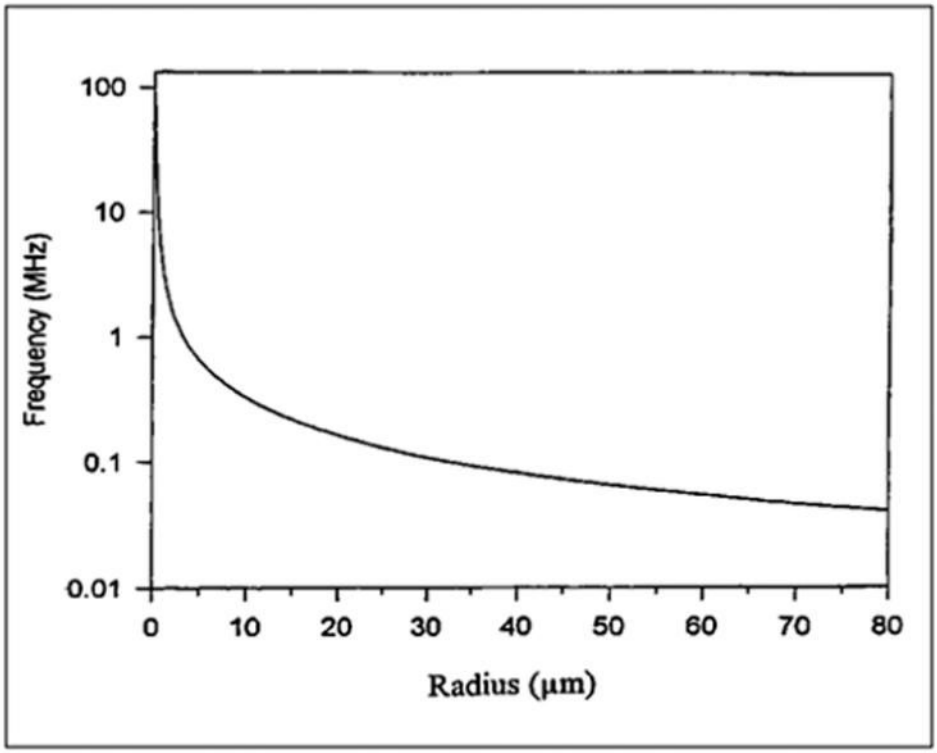

Figure 6-2.
Computed resonance frequency versus the radius of a bubble.

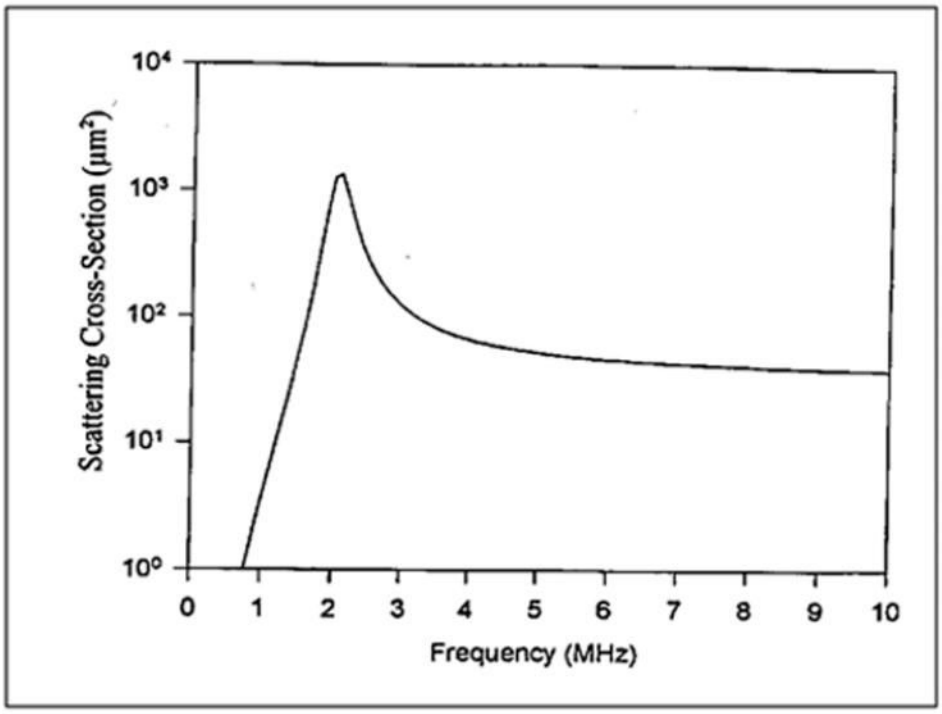

Figure 6-3.
Computed scattering cross section of a bubble of 1.7 μm radius.

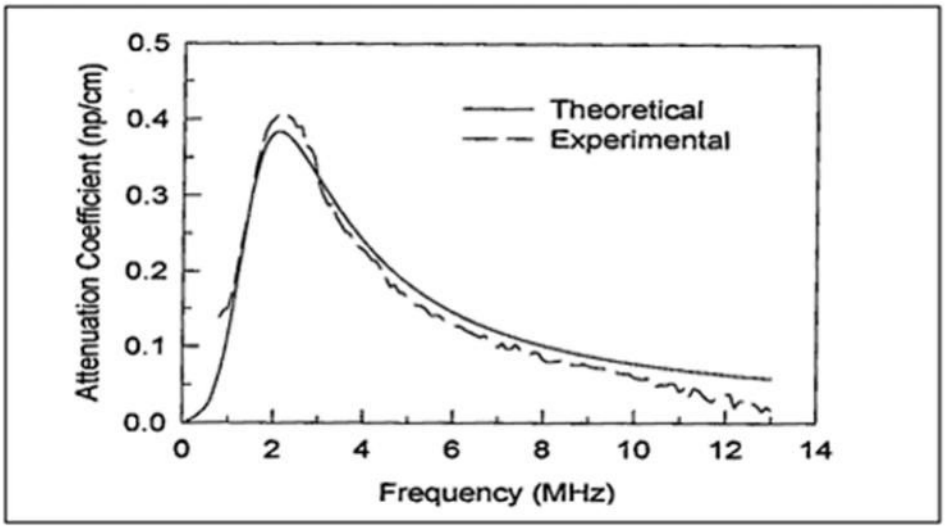

Figure 6-4.
Experimental and theoretical results of attenuation coefficient of an Albunex suspension as a function of frequency. Mean diameter of Albunex = 3.15 μm.

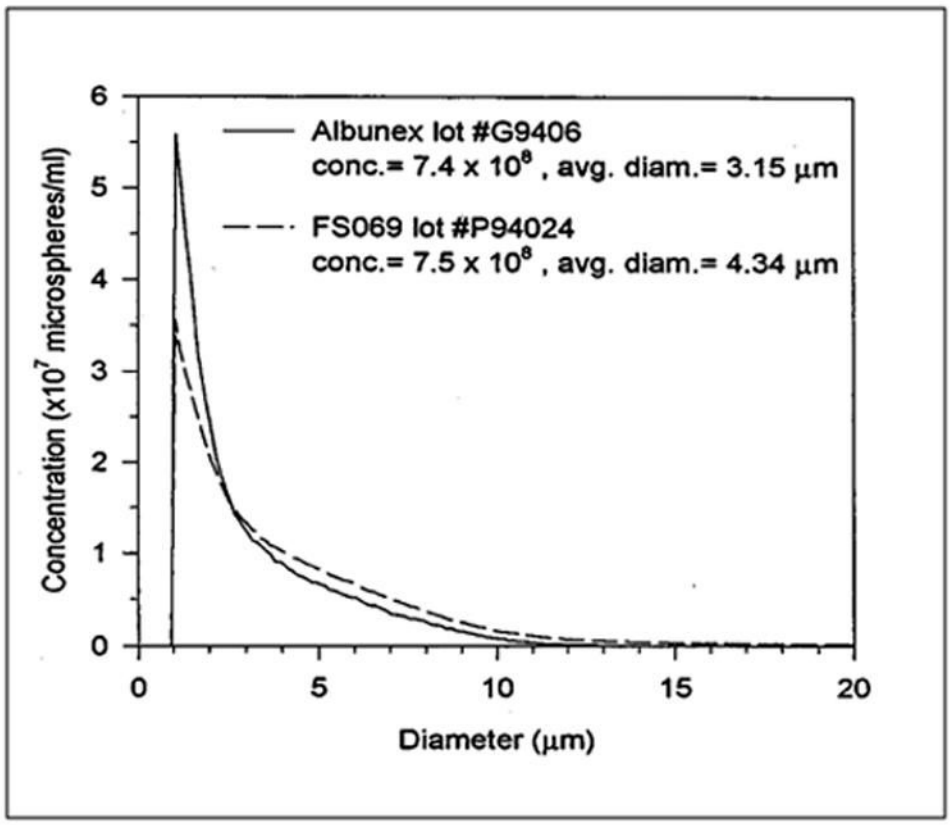

Figure 6-5.
Size distributions of Albunex and FS069.

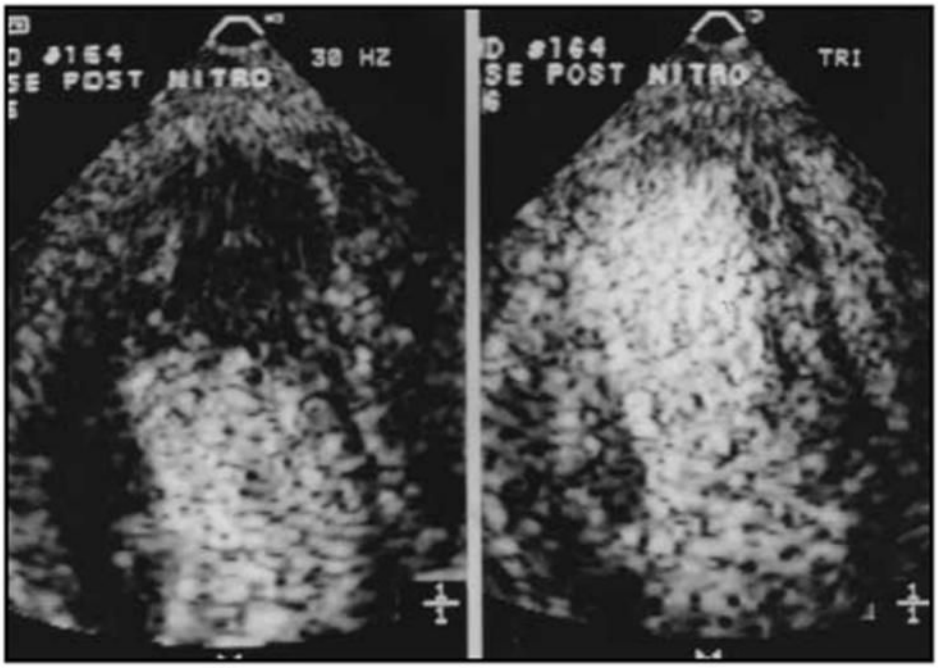

Figure 6-6.
An example of the increase in myocardial contrast observed during continuous infusion of PESDA microbubbles when using a low frame rate (right panel) as opposed to conventional frame rates (left panel); the latter are usually > 30 Hz.

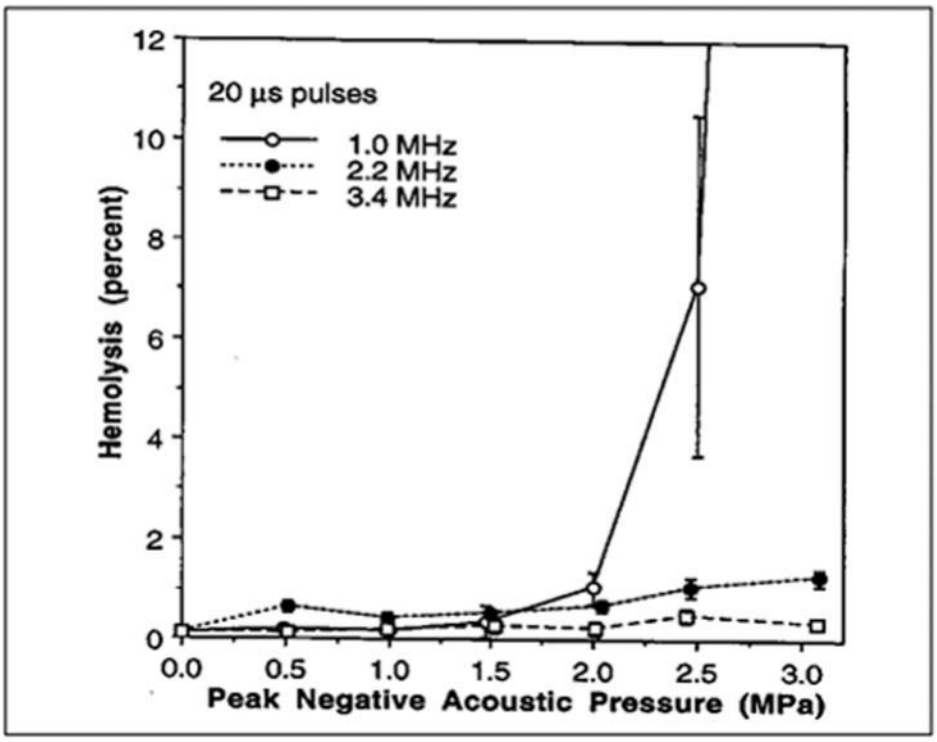

Figure 6-7.
Hemolysis of whole human blood containing 3.6 V % Albunex and exposed with sample rotation to 20 µs pulses of 1.0, 2.2, or 3.4 MHz ultrasound. The duty factor was 0.01 and the total exposure duration 60 s. (Data from and reprinted by permission of Elsevier Science, from Brayman AA, et al: Hemolysis of 40% hematocrit, Albunex-supplemented human erythrocyte suspensions by intense pulsed ultrasound: Frequency, duty factor, pulse length and sample rotation dependence. *Ultrasound Med Biol* 23:1237, 1997b.)

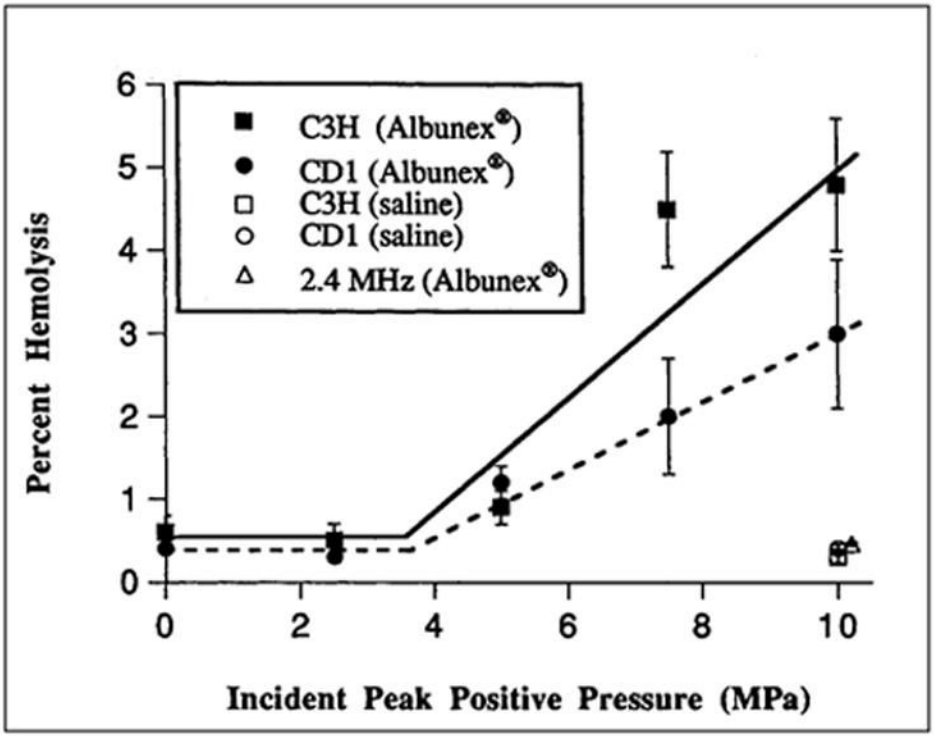

Figure 6-8.

Hemolysis *in vivo* in mice exposed to pulsed ultrasound. Percent hemolysis is plotted as a function of peak positive pressure at the surface of the animal. Solid squares and circles are data for C3H and CD1 strains of mice, respectively, exposed to 1.2 MHz ultrasound and injected with Albunex. Open squares and circles are data for C3H and CD1 mice, respectively, exposed to 1.2 MHz ultrasound and injected with saline. Open triangle is datum for CD1 mice exposed to 2.4 MHz ultrasound and injected with Albunex. (Figure adapted from and reprinted by permission of Elsevier Science, from Dalecki D, et al: Remnants of Albunex nucleate acoustic cavitation. *Ultrasound Med Biol* 23:1405, 1997e). Data are presented as the mean percentage of hemolysis; error bars represent the standard error of the mean.